

Mudstone-rich fluvial systems as reservoirs: The Brushy
Basin Member of the Morrison Formation, Eastern
Utah

Master in Petroleum Geology

Aasmund Olav Løvestad



Department of Earth Science
University of Bergen
September 2018

Abstract

Mudstone-rich fluvial systems are common in the sedimentary record, such as the Triassic of the Barents Sea, but have received little scientific attention compared to their sandstone-rich counterparts. However, mudstone-rich fluvial systems often have large river channels which are easily imaged on seismic data, and thus make good exploration targets. The late stages of the Jurassic sedimentary succession of Utah, USA, comprise of a collection of low-gradient, mudstone-rich fluvial continental deposits known as the Brushy Basin Member of the Morrison Formation. This thesis investigates the Jurassic Brushy Basin Member as an analogue to mudstone-rich fluvial reservoirs and offers new insight into distributary fluvial systems.

Fieldwork was done on a 2x2 km, v-shaped outcrop which offers a high degree of three-dimensionality. Data acquisition was done through combining traditional fieldwork techniques with modern digital acquisition techniques and a virtual model of the outcrop was constructed. Through interpreting and correlating logs with the virtual-outcrop, facies associations and their spatial organization was identified and understood. A conceptual geological model was constructed which schematically captures the upwards changes in the fluvial system. A reservoir model based on the geological model was then built with the goal of flow-simulating oil production from the reservoir model.

The results from studying the Brushy Basin Member implies a retrograding distributary fluvial system, with an upwards decrease in channel-belt width, thickness, amalgamation and interconnection. This interpretation has not been described in previous work.

Production results from flow simulating the reservoir model shows that a mudstone-rich fluvial system highly depend on channel-to-channel connection which can be established through crevasse-splays. In exploration of new and poorly understood mudstone-rich fluvial systems, sub-seismic channels and crevasse-splays should be considered an upside in terms of connectivity and reservoir volumes.

Keywords: Mudstone-rich fluvial systems, Distributary fluvial systems, Brushy Basin Member, Morrison Formation, Virtual outcrop, Crevasse-splays, Colorado Plateau.

Acknowledgements

This thesis is part of my master's degree in Petroleum Geology at the Department of Earth Science: Basin and Reservoir Studies (BRS) at the University of Bergen.

First and foremost, I would like to direct my utmost gratitude to my supervisor Dr. Christian Haug Eide for his superb guidance both during fieldwork and in the process of writing this thesis. Thank you for great discussion, constructive feedback and for always being available. It has been a real pleasure to work with you as your master student.

I would also like to thank Espen Friestad and my brother Torbjørn Aamelfot for their invaluable contribution during the weeks of fieldwork in Utah. I will never forget all the hours we shared logging mud in the Brushy Basin Member and drinking cold Dr.Pepper in the merciless Utah Sun.

Thanks to my fellow students and friends at the University of Bergen for 5 memorable years. Special thanks to the Goon Squad for great discussion, for creating a constructive teaching environment and for legendary field trips to Spain and USA. You all have a special place in my heart.

I want to thank my family for encouragement and for always being there.

Finally, I want to thank my girlfriend, Cecilie, for unwavering support, patience and caring. I would not have finished this degree without you.

Aasmund Olav Løvestad

18.09.2018

List of contents

1.0 Introduction.....	1
1.1 Study Area	2
2.0 Geological Background.....	5
2.1 Overall Setting	5
2.2.1 Tectonic setting	5
2.1.2 Paleogeography and climate	9
2.2. Stratigraphic background	10
2.3 Theoretical background.....	13
3.0 Methodology	17
3.1 Data acquisition.....	17
3.1.1 Fieldwork	17
3.1.2 UAV and the virtual outcrop.....	17
3.1.3 Reservoir model and flow simulation.....	19
4.0 Results	20
4.1 Facies and Facies association	21
4.1.1 Facies Association A- Channel belt.....	23
4.1.2 Facies Association B - Abandoned Channel.....	26
4.1.3 Facies Association C- Crevasse splay deposits	27
4.1.4 Facies Association D- Overbank deposits.....	28
4.1.5 Facies Association E- Volcanic ash-layers.....	30
4.2 Virtual outcrop	31
4.3 Reservoir model, Brushy Basin Member	49
4.4 Flow simulation	52
5.0 Discussion.....	59
5.1 The Brushy Basin Member distributary fluvial system.....	59
5.2 The Brushy Basin Reservoir model.....	64
5.2.1 Connectivity within the reservoir model.....	64
5.2.2 Upside in exploration of new areas.....	65
5.2.3 The reservoir model compared to the Goliat field.....	67
6.0 Summary and conclusions.....	68
7.0 List of references	71
Appendix:	79

1.0 Introduction

The late stages of the Jurassic sedimentary succession of Utah, USA, comprise of a collection of low-gradient, mudstone-rich fluvial continental deposits known as the Brushy Basin Member of the Morrison Formation (e.g. Demko et al., 2004; Hasiotis, 2004; Turner & Peterson, 2004; Galli, 2014; Owen et al., 2015). The Morrison Formation is a well-known geological formation that has been thoroughly studied due to the abundance of dinosaur fossil, but a study aimed at the Brushy Basin fluvial systems as a hydrocarbon reservoir analogue has never before been attempted. The Brushy Basin Member mudstone-rich fluvial system display channel architecture much like the potential fluvial reservoirs in the Triassic of the Barents Sea currently being explored by major oil companies (Klausen et al., 2015; Eide et al., 2017).

The Norwegian Petroleum Directorate estimates that a large proportion of the undiscovered hydrocarbon reserves left on the Norwegian Continental Shelf are situated in fluvial channels in Snadd and Kobbe formations of the Barents Sea (NPD, 2018). As many of the large oil-fields are entering tail-off stage of production, new and substantial discoveries are important to maintain production levels. Consequently, numerous studies and considerable interest has been given to the Triassic channel sandstones as potential reservoirs (e.g. Klausen et al, 2014; Klausen and Mørk, 2014; Lundschieen 2014; Martinius et al., 2014).

This project sets out to increase the understanding of mudstone-rich fluvial systems through investigating the Brushy Basin Member as an analogue to mudstone-rich fluvial reservoirs. Specifically, this thesis aims to (1) describe and understand the Brushy Basin Member fluvial system, (2) to construct and flow-simulate a reservoir model of the Brushy Basin Member, and (3) to discuss the findings in terms of the evolution of the fluvial system, and important factors for connectivity and production in the reservoir model. An essential part of this discussion will be to compare the findings with similar mud-rich fluvial systems like the Snadd Formation and Kobbe Formation of the Barents Sea.

The results of this study are significant for two reasons. Firstly, exploration in the Barents Sea has been largely based on data from seismic which gives information about large scale channel-belts, many kilometres wide and tens of meters thick (Klausen et al., 2014; Klausen

and Mørk, 2014). However, the width and spatial distribution of sub-seismic scale channel-belts could represent an upside in terms of reservoir volume and connectivity and can therefore be very valuable to investigate in a hydrocarbon exploration context. Secondly, mudstone-rich fluvial systems are common in the sedimentary record, such as the Triassic of the Barents Sea, but have received little scientific attention compared to their sandstone-rich counterparts. For that reason, investigating the Brushy Basin member could improve the understanding of low gradient, mudstone-rich fluvial systems.

1.1 Study Area

The outcrop investigated in this thesis is located in the southeaster part of Utah, USA, (Figure. 1.1.A) in the San Rafael Swell area of the Colorado Plateau in close proximity to the town Caineville (Figure. 1.1.B). The outcrop consists of Late Jurassic rocks of the Brushy Basin Member capped by the Lower Cretaceous Buckhorn Conglomerate (Galli, 2014), exposed in 95- 110-meter-tall v-shaped cliff as seen in Figure. 1.1.C. The outcrop was chosen because of the spectacular fluvial channel-sandstones (Figure. 1.2) that are exposed in the cliffs and offers a high degree of three-dimensionality within a well-documented stratigraphic framework. Alternating mudstones and sandstones from channel and overbank origin form recognisable bands of alternating light gray, green gray and red colours typical for the continental deposits of the Upper Morrison Formation.

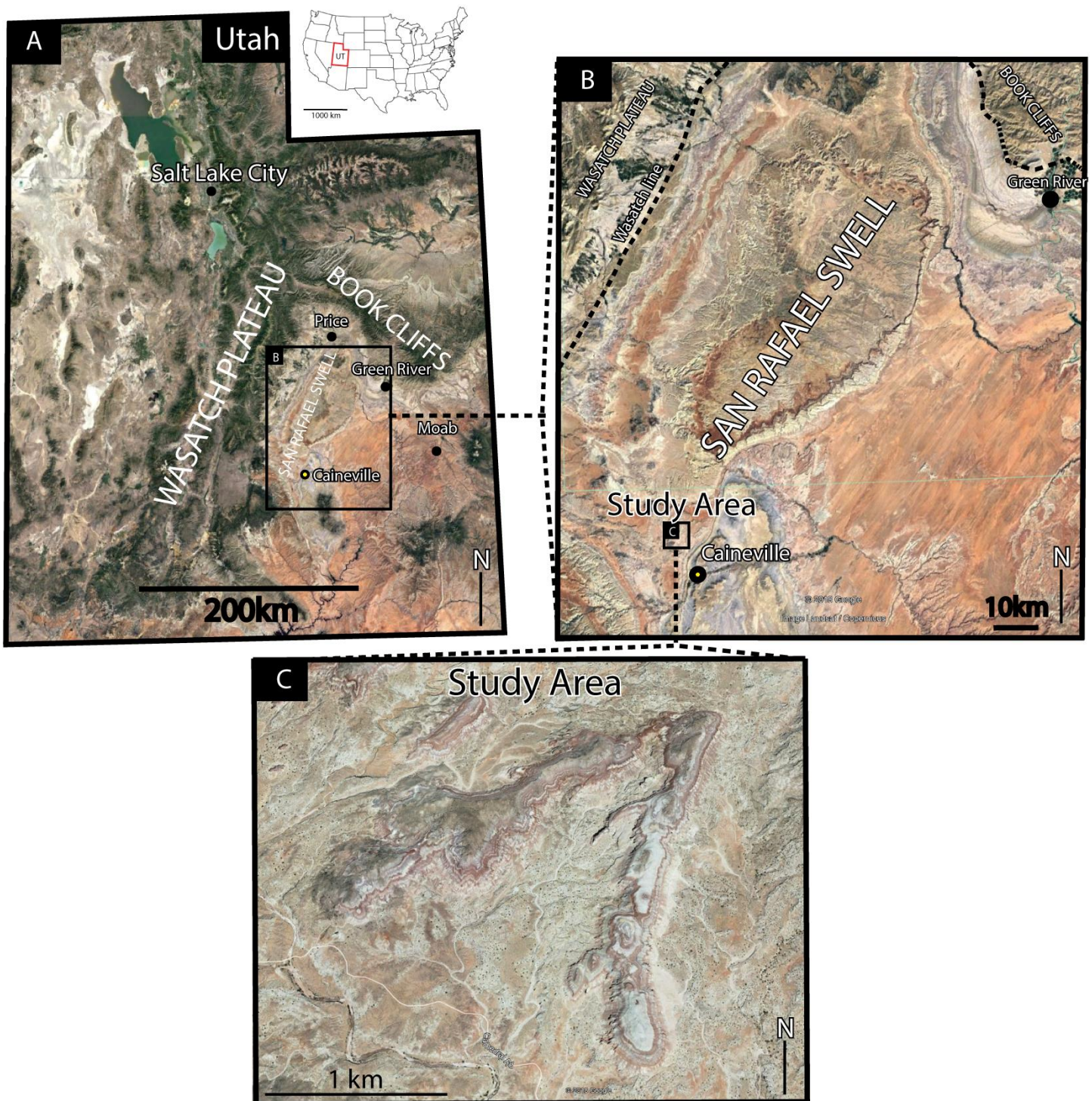


Figure 1.1: Location of the Study Area. A) Mini-map of USA and a map of Utah with key cities, towns and approximate outreach of the Colorado Plateau in Utah. B) Map of the San Rafael Swell within the Colorado Plateau with the Wasatch Line and the Wasatch plateau on the western margin and the Book cliffs on the northeastern margin. Study area right north of Caineville in the southern part of the figure. C) The V-shaped outcrop that was studied on this thesis. (Photos Google Earth)

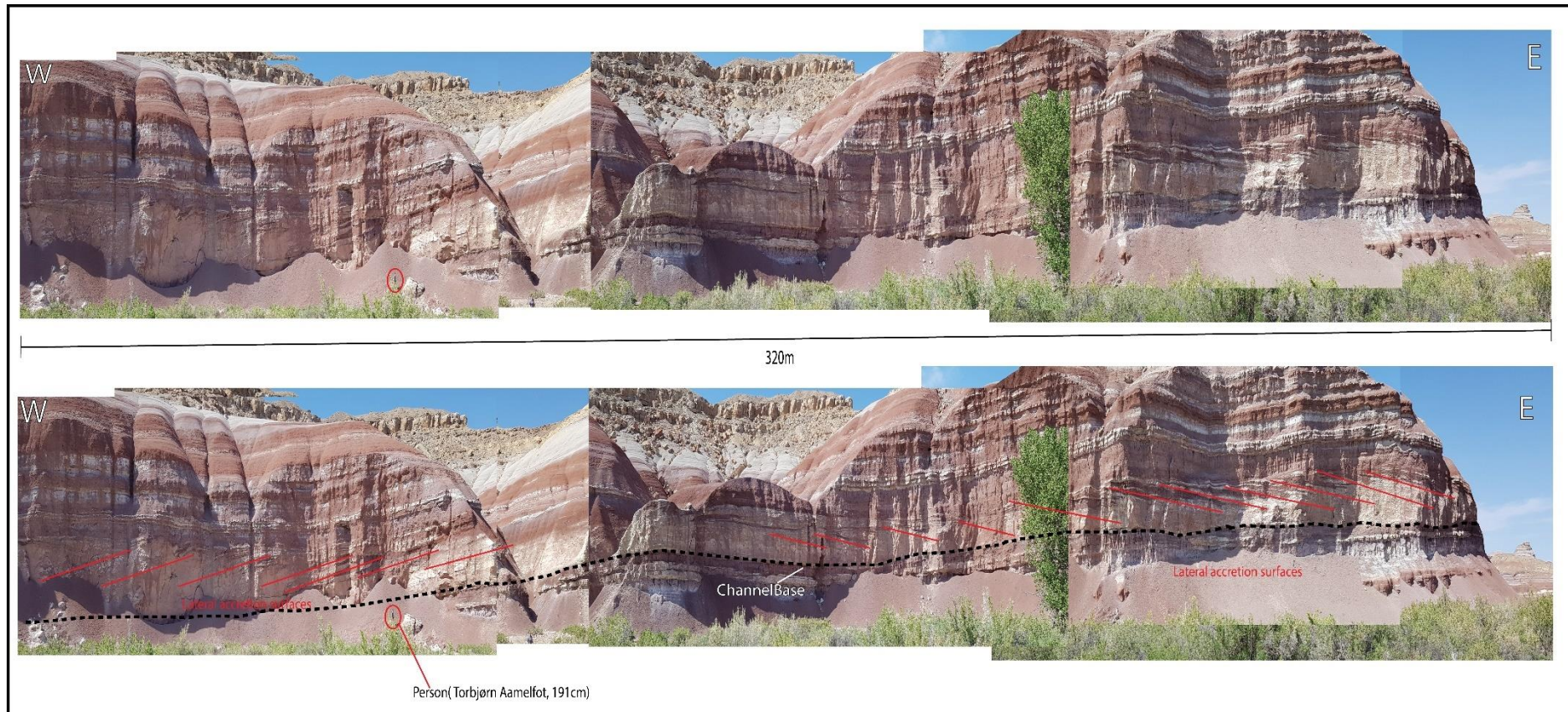


Figure 1.2: Picture-mosaic of a spectacular meandering channel in the Upper Brushy Basin Member. Person for scale. Lateral accretion surfaces indicated by red line, and channel base by dotted black line. Note that the channel belt has lateral accretion surfaces dipping in opposite directions which could indicate that the channel belt visible at the picture is a cross-section of a meander bend (Ghinassi et al., 2016). Channel belts like this is just an example of the beautiful exposure of fluvial sandstones that are visible at the studied outcrop and a clear indication of the sinuosity of the rivers in the system.

2.0 Geological Background

The purpose of this chapter is twofold: 1) to give the reader an introduction to the geological tectonic and sedimentological setting the Brushy Basin Member was deposited in, and 2) to introduce crucial terms and concepts in fluvial sedimentology that are used frequently in this thesis. This chapter is divided into three sub chapters: 1. Tectonic setting, 2. Stratigraphic background, and 3. Theoretical Background.

2.1 Overall Setting

2.2.1 Tectonic setting

Deposition of the late Jurassic Morrison Formation and the Brushy Basin Member is considered to have occurred within a back-bulge basin of a retroarc foreland basin system evident by westward onlapping onto middle Jurassic strata along large parts of central Utah, interpreted as the coeval forebulge at the time (DeCelles and Currie, 1996; DeCelles, 2004; Miall et al., 2008).

This Morrison foreland system formed as a consequence of westward continental drift of the North American continental plate subducting the Pacific Farallon plate and accreting Pacific island arc systems onto the continent in a fold-and-thrust-belt (e.g. Howell and Flint, 2003; DeCelles, 2004). This fold-and-thrust-belt accumulated toward a large retroarc mountain chain known as the North American Cordillera; a series of partly overlapping orogenies that formed during the Mesozoic Era initiated by tectonic events following the breakup of Pangaea (Saleeby and Busby-Spera, 1992; DeCelles, 2004; Hintze and Kowallis, 2009). During the Jurassic this mountain chain stretched for more than 6000 km from Canada to Southern Mexico (Ingersoll and Schweickert, 1986).

The active phase of the Cordilleran Arc during the deposition of the Brushy Basin member is called the Nevadan Orogeny, and its eastern margin is marked by the Wasatch Line; the western edge of the Colorado Plateau, in which some of North America's longest faults have been mapped (Stokes, 1986; Miall et al., 2008; Blakey and Ranney, 2018). The Nevada orogeny is evidenced by several late Jurassic granite batholiths in the Sierra Nevada and ophiolites in California (Ingersoll and Schweickert, 1986), indicating the magmatic arc was located several 100s of kilometres from the Morrison back- bulge basin.

In the Late Jurassic the area that is now the Colorado Plateau (Figure 1.1 A) lay east of the Nevadan Orogeny and subsequently was covered by the Morrison Depositional Basin (Figure 2.1). During the Nevadan phase significant uplift of the south-western margin of the Colorado Plateau, and subduction to the west and southwest, led to creation of a magmatic arc and several rift shoulders elevated by thermotectonic processes that surrounded the Plateau and the Morrison depositional basin to the west (California Nevada, area) and south (Arizona New Mexico area) (Figure 2.1) (Dickinson, 1981; Bilodeau, 1986; Lawton, 1994; Nourse, 1995; Lucas et al., 2001; Turner & Peterson, 2004). In addition, topographic highs from the ancestral Rockies to the east confined the basin and led to a drainage pattern towards the north (Turner & Peterson, 2004). This led to the formation of the succession of continental deposits known today as the Morrison Formation; Tidwell Member, Salt Wash Member, Brushy Basin Member (see Chapter 2.2).

Tectonic setting during deposition of the Brushy Basin Member, 150 Ma

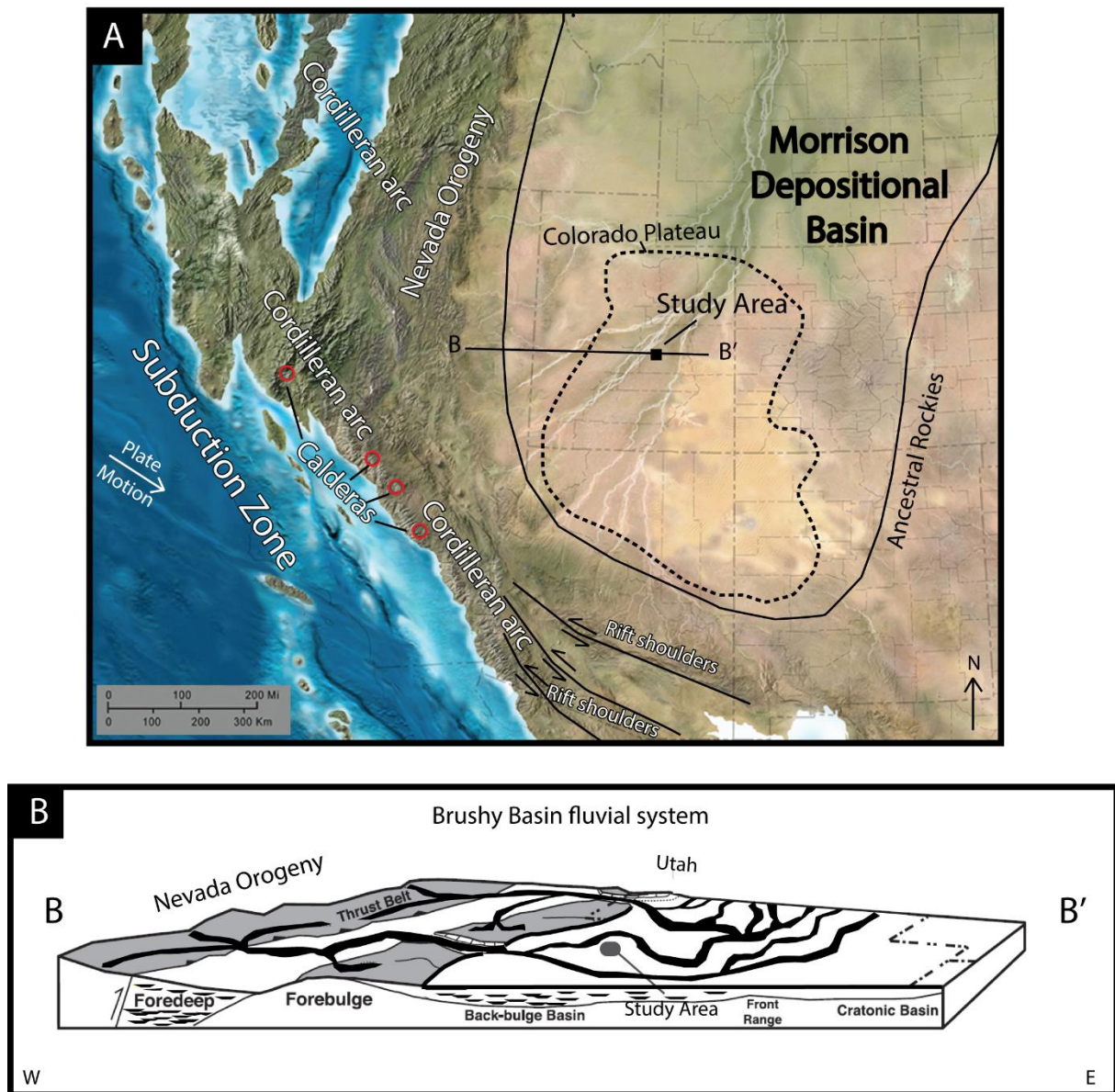


Figure 2.1: A) Tectonic setting during deposition of the Late Jurassic Brushy Basin Member. The basin is confined in a compressional regime by mountain-ranges to the west, south and elevated topography to the east. Rivers are sourced from the surrounding highlands and rift shoulders, especially from the south-west where massive calderas are perceived to have existed. B) Cross-sectional diagram across the basin showing the forebulge and the position of the preserved Brushy Basin depozone in the backbulge. Approximate location of the Study Area drawn on the cross section and the map. (modified map from Blakey (2011) and cross-section diagram modified from Demko et al., (2004).)

The prevailing winds during the Late Jurassic blew from the southwest bringing in large volumes of silicic volcanic ash and tuff layers found in the Brushy Basin Member today (Demko et al., 2004). The ash stem from the calderas in the Volcanic Arc partly surrounding the basin to the west (Demko et al., 2004). Huge eruptions from these calderas blanketed the basin on several occasions resulting in thick volcanic layers being visible in the rock record today, a testimony to the eruptiveness of the Arc (Turner & Peterson, 2004). Most of

the clastics in the depositional basin were mainly derived from the rift shoulders to the southwest called the Mogollon Highlands, although minor amount of clastic may have derived from topographic highs to the east (Ancestral Rockies) (Turner & Peterson, 2004).

The thickness of the Morrison formation, typically between 152-183 m, compared to the thousands of meters of Cretaceous strata above have led to the suggestion that plate-margin activity during deposition prevented the foredeep from subsiding (Miall et al., 2008). The main contribution to the generation for accommodation in the back-bulge depozone is assigned to dynamic subsidence on the basis of the exceedingly large geographical extent and tabular geometry of the formation (Lawton 1994; DeCelles 2004). This leads to the interpretation that the Morrison formation where it is preserved today was deposited in a back-bulge basin overlapping onto the a flexural forebulge in the central Utah (Demko et al., 2004; Galli 2014). This naturally implies the existence of a flexural foredeep in the western Utah during the Late Jurassic (Demko et al., 2004; Miall et al., 2008). However, no Upper Jurassic foredeep deposits is preserved in western Utah, structural reconstruction of the orogenic belt indicates that more than 4 km of Upper Jurassic- Lower Cretaceous sediments have been eroded away (Royse, 1993; Currie, 1997).

The deposition in the Morrison halted after 10 million years as a cessation of dynamic subsidence tied to a change in the angle of subduction along the western margin took place (Currie, 1997). This probably resulted in a decrease in accommodation in the back-bulge and the formation of an unconformity boundary between the Jurassic and Cretaceous (Currie, 1997).

Age

The age of the Morrison Formation is fairly well understood (Turner & Peterson 2004). Abundant ash layers and ashy beds in the Morrison have resulted in accurate and systematic consistent isotopic ages (Kowallis et al., 1998). They conclude that the formation was deposited from about 155 to 148 Ma, a period of 7 million years, within the late Jurassic (163-141 Ma) (Bralower et al., 1990; Kowallis et al., 1998). The Brushy Basin Member, which this thesis focuses on, was deposited within Kimmeridgian to possibly Tithonian age from 150.33 Ma to 148.1 Ma, meaning that the whole member was deposited within 2 million years (Kowallis et al., 1998). A 20 Ma hiatus at the top of Brushy Basin member makes up the

boundary between the upper Jurassic and the unconformable lower Cretaceous strata above (Kowallis et al., 1998).

2.1.2 Paleogeography and climate

During the Early and Middle Jurassic, the continent had been situated in the dry latitudes comparable to modern day Sahara and some of the largest and thickest successions of eolian sand deserts that exists in the geological record was deposited (Wingate Sandstone, Navajo Sandstone, Entrada Sandstone) (Blakey and Ranney, 2018). However, in the late Jurassic the continent moved out of the super-arid latitudes and into the subtropics leading to the climate becoming slightly more humid (Hinze and Kowallis, 2009).

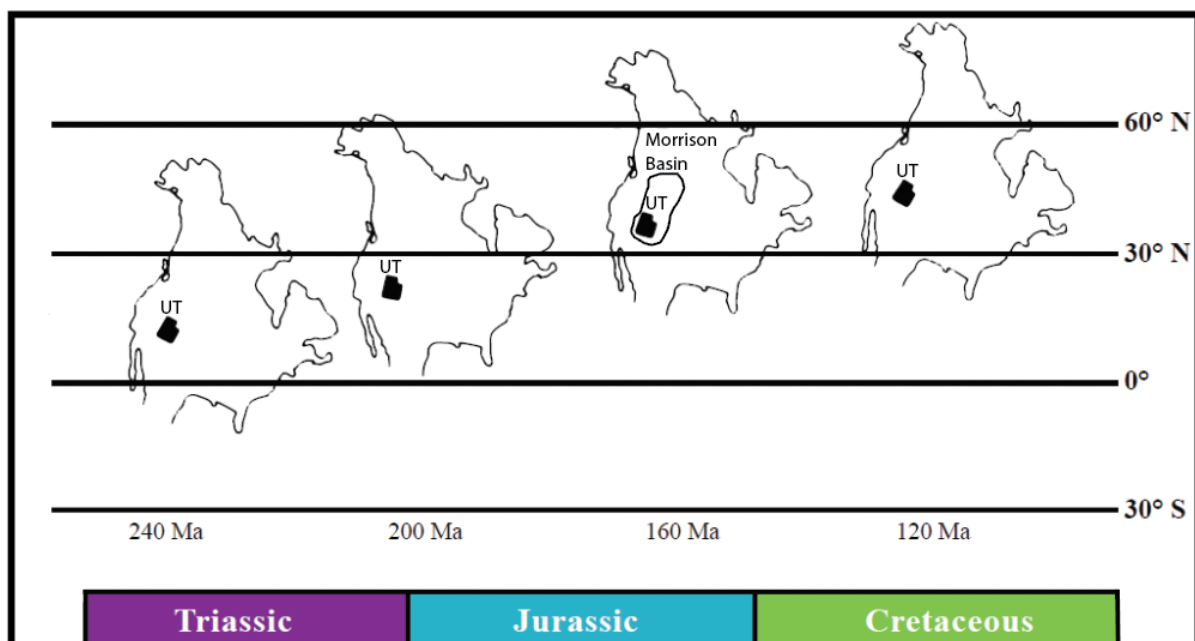


Figure 2.2: Paleogeographic reconstruction of the US during the Triassic, Jurassic and Cretaceous. Utah, and Morrison depositional basin marked on the time of deposition. Permission from Arve Sleveland, Modified from Hinze and Kowallis (2009).

Deposition of the Brushy Basin Member at the end of the Jurassic happened when the north American continent was at a paleolatitude between 30 and 45°N (**FIG 2.2**), slightly south of its current position but still dryer and warmer than today (Peterson, 1994; Currie, 1998). A subtropical high-pressure cell positioned over the eastern Paleo-Pacific Ocean dominated atmospheric circulation in the whole western American continent producing warm westerly winds that carried Pacific moisture eastward toward the Cordilleran Arc and the Nevada Orogeny (Parrish and Curtis, 1982). The moisture “rained out” as it moved inland up and above the mountain chain depleting the air mass of moisture leaving the Brushy basin

depozone seasonally dry, only the very large storms in the Paleo-Pacific led to direct meteoric precipitation (Turner & Peterson, 2004). Consequently, most of the moisture that reached the basin did so largely through ground water and surface streams from the upland surrounding the basin to the west and south (Turner & Peterson, 2004).

The degree of seasonality within the basin is fairly well documented (e.g. Demko et al., 2004; Good, 2004; Hasiotis, 2004; Turner & Peterson, 2004). In the overbank deposits the presence of carbonate horizons; indicative of drier conditions, and clay- and iron-rich horizons; indicative of wetter conditions, paired with vertic features formed by repeated swelling and wetting of mud occurs frequently and is typical for seasonality of precipitation (Retallack, 1997; Demko et al., 2004). However, especially annual growth bands in freshwater bivalves and the presence of crayfish burrows in the Brushy Basin Member are brought forward as the most conclusive evidence (Good, 2004; Hasiotis, 2004; Turner & Peterson, 2004).

The climate probably resembled today's Serengeti in Africa; with river, lakes, strong seasonality and seasonal drought (Blakey and Ranney, 2018), with an ecosystem vulnerable to extended periods of drought which account for some of the largest death assemblages of dinosaurs and other vertebrates found in the rock record (Turner & Peterson, 2004)

2.2. Stratigraphic background

The Morrison formation is described by Turner and Peterson (2004) as a complex mosaic of environments ranging from streams, riparian environments, distal floodplains, lakes and ponds. However, eolian dunes, alkaline, saline and carbonate wetlands, coal swamps and marine evaporites also existed in the basal and northernmost parts of the formation (Demko et al., 2004; Turner & Peterson, 2004). The overwhelming proportion of sediments was deposited in a fully terrestrial setting; in streams, lakes and the environments marginal to these settings which cover an area of more than 1.5 million km² of the Rocky mountain, Western Interior and the Colorado Plateau regions, all the way to Canada in the north from New Mexico in the south (Figure 2.1) (Demko et al., 2004). The stratigraphy of the formation is relatively complex due to spatial and temporal changes of facies across and because of the nomenclature changes from north to south and east to west across the massive basin (Hasiotis, 2004). This thesis therefore only focuses on the Colorado Plateau region where the

study was conducted and the depositional environment was completely terrestrial, far away from the sea.

The Morrison formation can be divided into three members; Tidwell Member, Salt Wash Member and the Brushy Basin Member, and two major depositional sequences; Lower Morrison Depositional Sequence and the upper Morrison Depositional Sequence (Figure 2.3) (Demko et al., 2004). Three regional unconformities are found in relation to the Morrison; at the base-Basal Morrison Unconformity, between the Salt Wash Member and the Brushy Basin Member-Mid Morrison Unconformity, and at the top of the Brushy Basin Member-Uppermost Morrison Unconformity (represent the end of Jurassic deposition) (Figure 2.3) (Demko et al.,2014). These unconformities consist of especially mature reddened paleosol horizons (Demko et al., 2014).

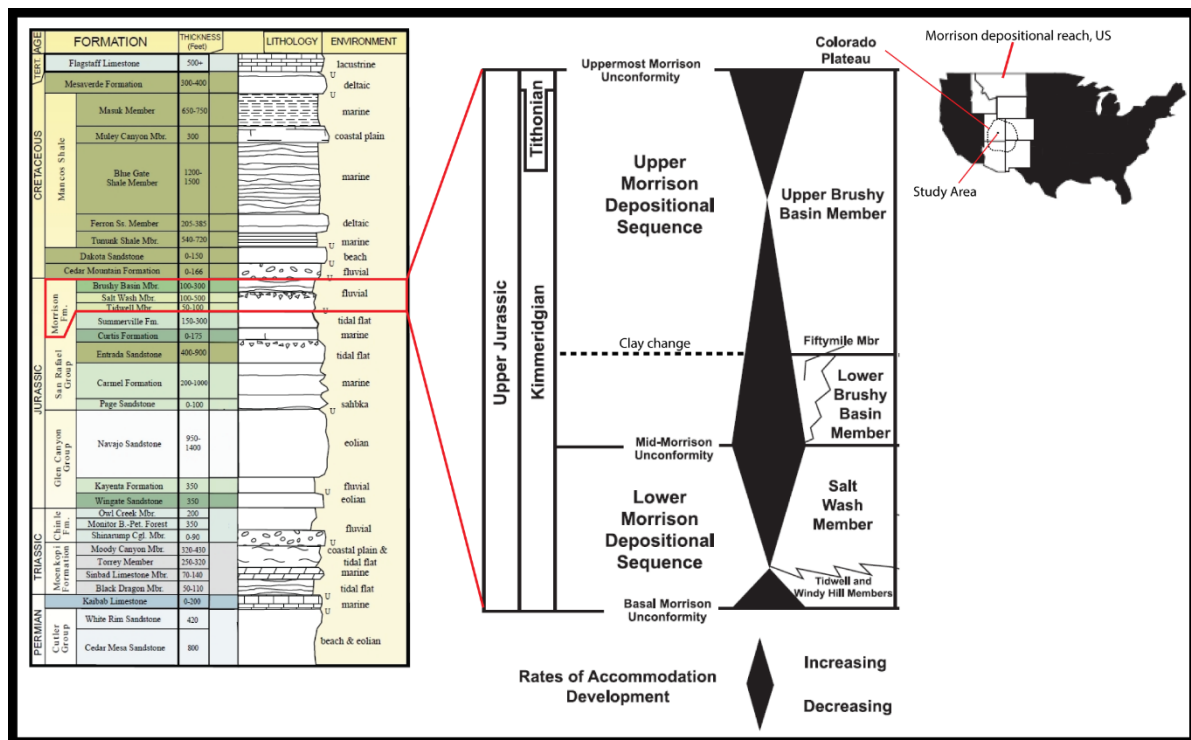


Figure 2.3: Stratigraphic column of the Colorado Plateau, the Upper Jurassic Morrison formation & depositional reach of the formation within the US. Colorado Plateau and the Study Area is marked on the US map. Two depositional sequences are identified within the succession. The Clay change visible within the Brushy Basin Member. (Modified from Demko et al., 2004 and Utah Geological Association)

The Tidwell Member was probably deposited in a dry period of the Morrison formation and the paleosols in the member display several gypsum horizons, playa deposits and minor fluvial channels that represent the distal deposition during the northward marine regression

of the Sundance Sea which occupied parts of the Colorado Plateau during the Middle Jurassic (Turner & Peterson, 2004; Owen et al., 2015).

The Salt Wash Member contains fluvial channel belt deposits that become increasingly separated by floodplain deposits downstream in a dispersive paleocurrent pattern of a typical distributary fluvial system (DFS) (Craig et al., 1995; Owen et al., 2015, 2015). The Tidwell and the Salt Wash Member, though lithostratigraphically divided, are a single depositional system where the Salt Wash Member comprises the more proximal sand dominated facies of the fluvial system that prograded over the more distal facies of the Tidwell Member (Turner & Peterson, 2004; Kjemperud et al., 2008; Weissmann et al., 2013; Owen et al., 2015). Within the sand-rich distributary fluvial system large scale amalgamated sandstone belts form sheet-like, up to 26 m thick and 10 km wide, multilateral and multistorey channel deposits. The apex of the distributary fluvial system of the Lower Morrison Depositional system was located close to the Utah-Arizona border, sourced from the southwest (Owen et al., 2015).

The Brushy Basin Member depositional sequence constitutes a much more mudstone-dominated fluvial system than that of the Salt Wash Member Depositional Sequence and is the most widespread member of the Morrison Formation (Demko et al., 2004; Galli, 2014). It is thickest close to the perceived source areas in the west, southwest and thins northward and north-eastward from 157 m to 79-138 meters (Lohman, 1965; Galli, 2014). In the study area, close to Caineville, the Brushy Basin Member is typically around 100-120 meters thick. Basin-wide the member has a lower division (Lower Brush Basin Member); containing mudstones mostly red-brown in colour, and an upper division (Upper Brushy Basin Member); characterized by variegated puffy-weathered grey ash rich mudstones (Galli, 2014). This colour change is the sole basis of the division of the two Brushy Basin lithosomes (Galli, 2014). The colour transition from Lower-to-Upper Brushy Basin Member is called the Clay change (Figure 2.3) which records the beginning of major eruptive events in the calderas in the Cordilleran Arc to the west and massive input of air-blown ash in the depozone (Turner & Peterson, 2004).

The Brushy Basin is interpreted as the deposits of fluvial systems of varying sinuosity formed under conditions of very low gradient and accommodation (Newell, 1997; Demko et al., 2004; Galli, 2014). Rivers in the system carried mud in suspension and sandy sediments as

bedload and deposited abundant and extensive overbank deposits during floods, leaving the channel sandstones commonly intercalated with stacked floodplain paleosols and crevasse-splay sandstones (Demko et al., 2004). The streams which originated from the southwest are believed to have drained out into a distal low-laying wetland area with perennial lakes located in the northern and eastern part of the basin, and in the sea at the very northern parts of the basin (Turner & Peterson, 2004). Stacked channel sandstones, especially in the upper part of the succession is believed to be limited to the southwestern parts of the basin, river deposits far into the basin are typically single-story ribbon-type fluvial channel sandstone beds (Turner & Peterson, 2004). Generally, it is believed that the lower part of the Brushy Basin Member is dominated by meandering channels, and that the streams becomes laterally stable, low sinuosity channels dominated by avulsion during the late stages (e.g. Currie 1997; Currie 1998; Galli, 2004, Turner & Peterson, 2004). Owen et al., (2015) speculate that the Brushy Basin Member as the Salt Wash Member possibly also was a distributary fluvial system, although much more mud-dominated, but states that a regional study is needed to test that hypothesis.

2.3 Theoretical background

In this subchapter terms that are used frequently in the thesis are explained. Underlying these important terms are concepts typical for meandering fluvial systems like the Brushy Basin Member, and therefore important to clarify before the results in Chapter 4.

Point bars, lateral accretion surfaces and channel-belts

Fluvial deposits, which is the focus of this thesis, encompass sediments generated by the actions of streams and rivers (Boggs, 2014). Sediments are generally deposited in channels as lateral accreting bars and as vertical accreting beds in levees, abandoned channels and crevasse-splays on the floodplain (Bridge, 2003). In meandering systems, helicoidal-spiralling flow are produced by water flowing around channel bends leading to a downward motion of water at the outer bend and upward motion of water paired with decreasing flow velocity towards the inner bend (e.g. Thomson, 1876; Einstein, 1954; Bridge, 2003; Boggs, 2014). This flow dynamic results in hydraulic action and erosion in the outer bend, and transport and

deposition by lateral accretion of upwards-fining sediments on the **point bars** in the inner bend (Figure 2.4) (Boggs 2014). This leads to a typical upwards fining of sediments within channel fill, often simplified to conceptual sedimentary logs of fluvial deposits; erosive gravel

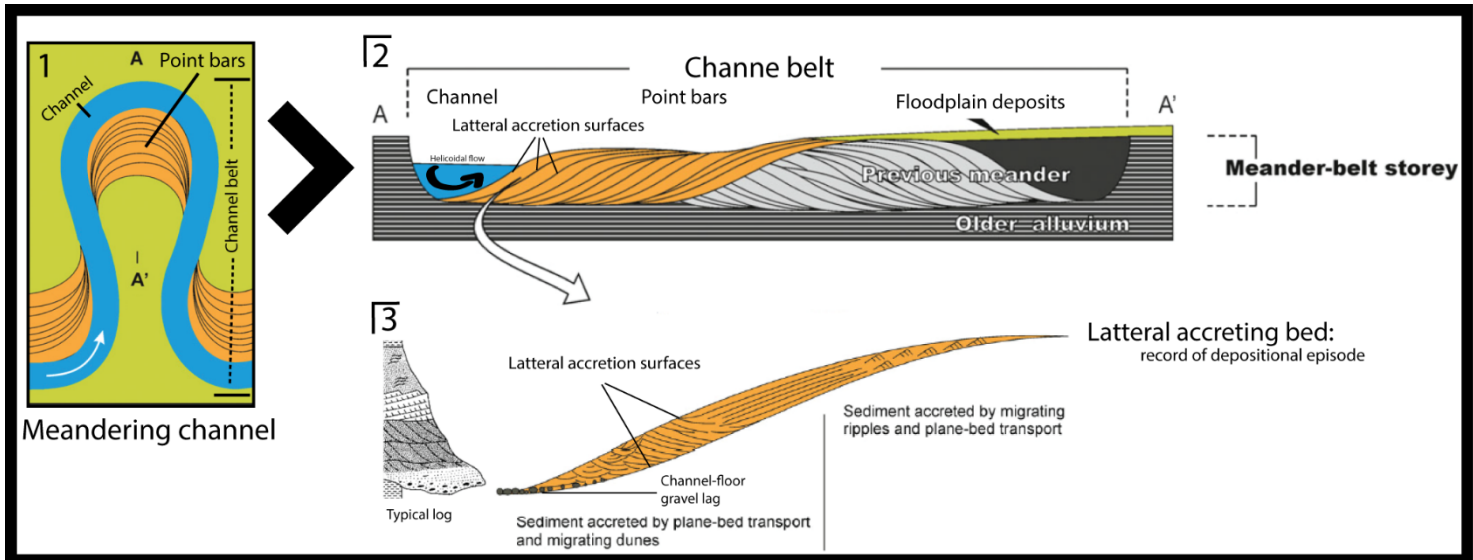


Figure 2.4: Illustration of terminology in relation to meandering channel-belt morphology. 1) Aerial view of a meandering channel with point visible in the inner bends. Channel belt represent the full width of the channel-point bars and channel-fill deposits, the channel is the active area of the channel belt where the stream is flowing. 2) Cross-section of channel belt, with the lateral accreting inclined packages building out as the stream erodes the outer bank. The lateral accreting beds have a typical sigmoidal shape building out from the river bank down-lapping onto the channel base. 3) A single lateral accreting point bar. Point-bar accretion involves plane-bed transport formation of 3D and 2D dunes (cross-stratification), and deposition of sand as ripples and small dunes in the uppermost part. where mud-drapes can occur. Typical sedimentary log of a meandering channel and its point bar. Modified from Ghinassi et al., (2014)

base fining upwards into mud (Figure. 2.4). In the field, point bars are often recognized in outcrops sections as **lateral accretion surfaces**; inclined sigmoidal bounding surfaces that record the progressive migration of point bars (Figure. 1.2 & 2.4) (Ghinassi, 2014). Lateral migration of point bars on the inner bank as the channel migrates towards the outer bank lead to the formation of a sand-body known as a **channel belt** (Figure 2.4). In the Brushy Basin Member lateral accretion surfaces in the channel belts are generally mud-draped and therefore easy to identify (Galli, 2014).

Crevasse-splays

On the floodplain, the strip of land surrounding a river channel, deposition mainly happens when the river breaches its banks and natural levees during overbank floods (Bridge, 2003; Boggs 2014). Floodplain deposits that settle out of floodwater occurs as fine-grained and laminated muds, prone to soil-forming processes (Retallack, 2001, Turner & Peterson 2004). Sediment may also be deposited as **crevasse-splays**; fan- or lobe-shaped mounds of sand

and mud that can display a wide range of geometry, commonly hundreds of meters to kilometres long and wide in large rivers (Bridge, 2003).

Distributary fluvial systems (DFS)

A **distributary fluvial system** (DFS) (Figure 2.5) is a fluvial system which in planform display a radial fan distributive channel pattern (e.g. Friend, 1978; Hartley et al., 2010). This radial pattern spreads out from an apex where the originally confined stream enters a sedimentary basin and becomes unconfined (Weissmann et al., 2010). The active part of the distributary fluvial system, where the river channel is flowing at any given time, is called a river tract. A river tract displays all the characteristics of a distributary fluvial system: 1) a change from amalgamated channel deposits in proximal areas to smaller fixed channels in distal areas; 2) a decrease in grain size downstream; 3) an increase in preservation of floodplain deposits relative to channel deposits downstream; and 4) a decrease in channel size and abundance downstream (Friend 1978; Nichols 1987; Hirst 1991; Stanistreet and McCarthy 1993; Nichols and Fisher 2007; Cain and Mountney 2009; Hartley et al. 2010; Weissmann et al. 2010; 2013; Owen et al., 2015). The radial fan-shape of the fluvial system builds up by repeated avulsion of river tracts due to compensational stacking (Nichols and Fisher, 2007). The areas that does not contain an active river tract are termed abandoned river tracts (Figure 2.5). Depending on the criteria above the distributary fan is divided into a proximal, medial and distal zone as shown in Figure. 2.5. Interestingly, distributary systems can have more than one entry point which can be active at different stages in the evolution of the system, or have several coeval entry points (Williams, 2000; Arenas et al., 2001).

Fluvial channels and overbank deposits in aggradational settings are dominated by distributary fluvial systems. Degradational tributary fluvial systems have a very limited preservation potential, hence distributary fluvial systems are expected to constitute a substantial part of the continental geologic record (Bristow et al., 1999; Weissman et al., 2010; Owen et al., 2015). The length of individual distributary fluvial systems varies between <1 km and >700 km, depending on size of the basin and the river flowing into the basin (Weissman et al., 2010).

A conceptual model of a fluvial distributary system is shown in Figure 2.5.

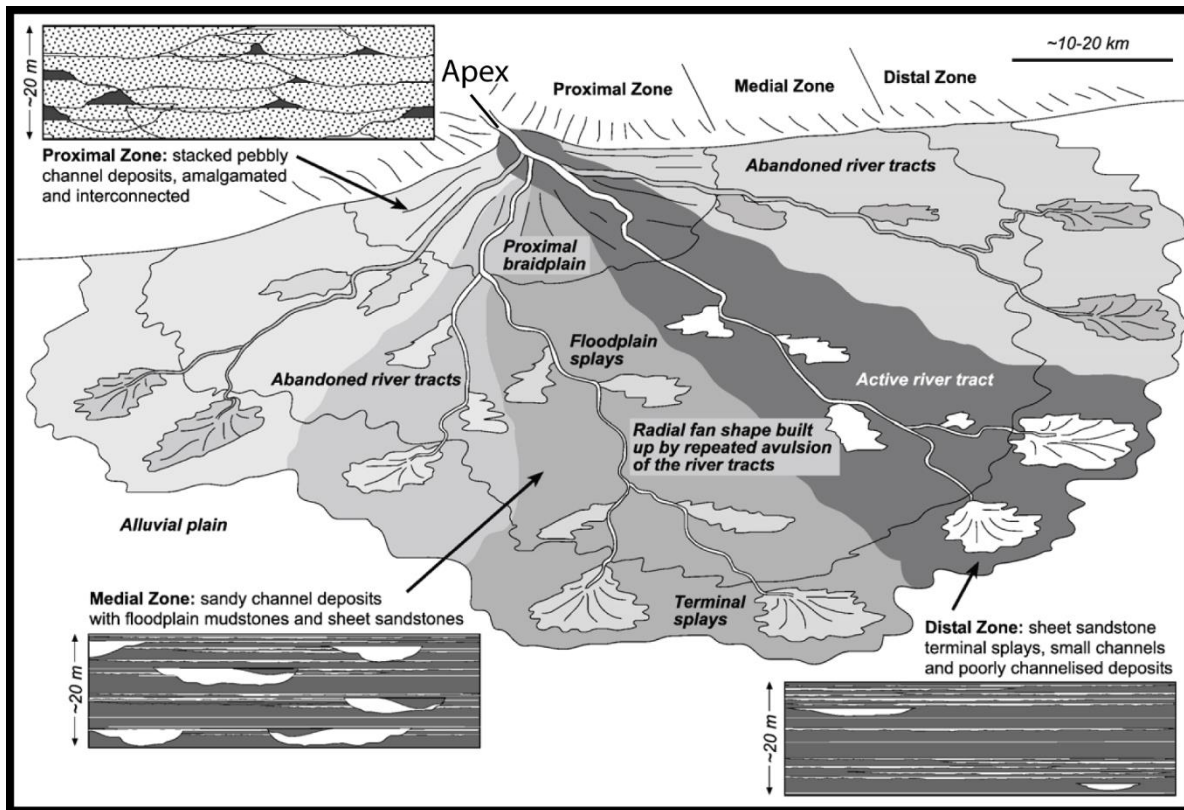


Figure 2.5: Conceptual model of a fluvial distributary system. The fan-shaped body radiating from and apex is constructed by repeated avulsions of the river channel (river tract). Note the architectural characteristics of the proximal, medial and distal zones of the fluvial distributary system. From Nichols and Fisher (2007)

While distributary fluvial systems radiate out from an apex, axial tributary fluvial systems have the opposite characteristic with an increase in discharge and channel size downstream which are fed by tributaries (Weissmann et al., 2010). The axial tributary systems are degradational and not aggregational as the distributary fluvial systems (Weissmann et al., 2010). Figure 2.6 show a typical axial system fed by tributary rivers.

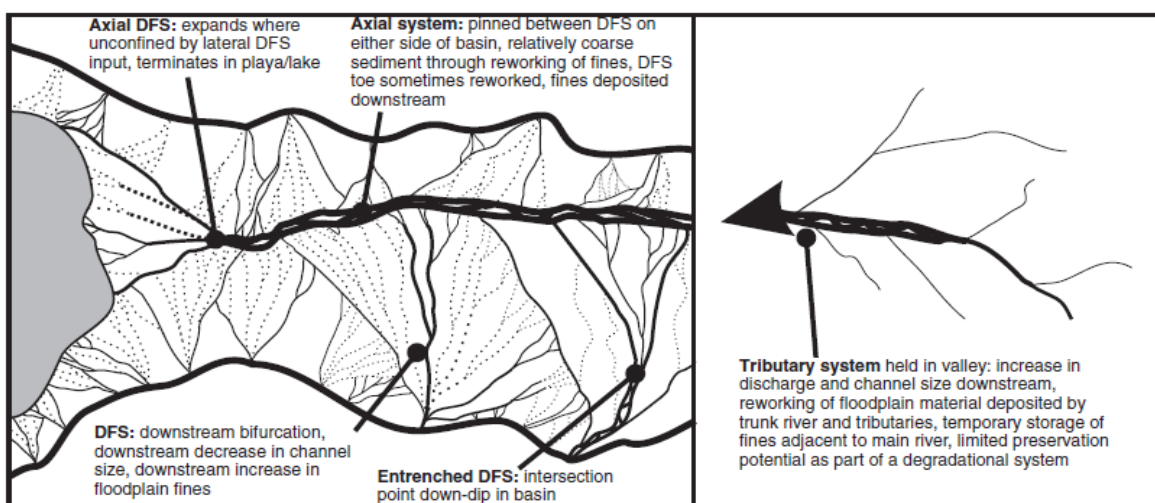


Figure 2.6: Schematic summary of key characteristics and differences between distributive fluvial systems and tributary fluvial systems (Weissmann et al., 2010)

3.0 Methodology

3.1 Data acquisition

The findings of this thesis are based on data collected during two field seasons in Utah, USA, in May 2017 and May 2018. Data was collected through the means of traditional sedimentological field work and by an Unmanned Aerial Vehicle (UAV) photographing a large part of the outcrop. Correlating the UAV photos and the logs, both during the fieldwork and after, was a crucial part of getting an understanding of the succession that was studied.

3.1.1 Fieldwork

The sedimentological fieldwork includes logging and photographing channel bodies and sedimentary structures. Particular emphasis was placed on lithologies, boundaries, architectural elements and recognizing channel geometries. Most of the outcrop was partly or fully covered by scree and substantial amounts of digging was required in order to achieve this. Standard field equipment such as compass, measuring tape, binoculars, geological hammer, camera and grain size chart were used. The logs were recorded on millimetre paper at 1:50 scale and later merged into continuous logs covering the units as seen in Chapter 4. Paleocurrent measurement were collected at all logged channels and crevasse-splays that had good sedimentary structures preserved. The outcrop was accessible by a short walk from the car. Digitalizing the logs was done in Adobe Illustrator.

3.1.2 UAV and the virtual outcrop

UAV photographing of the outcrop was performed by drone (model Phantom Dji 4) during the first field season. A GoPro camera was mounted underneath the drone and photographing was done through remote controlling the drone and camera with an iPad. A total of 800 photos was taken. The photos were georeferenced and stitched together into a 3D-model with *Agisoft Photoscan 1.3.2*. The workflow that was used to make the virtual outcrop is shown in Figure 3.1.

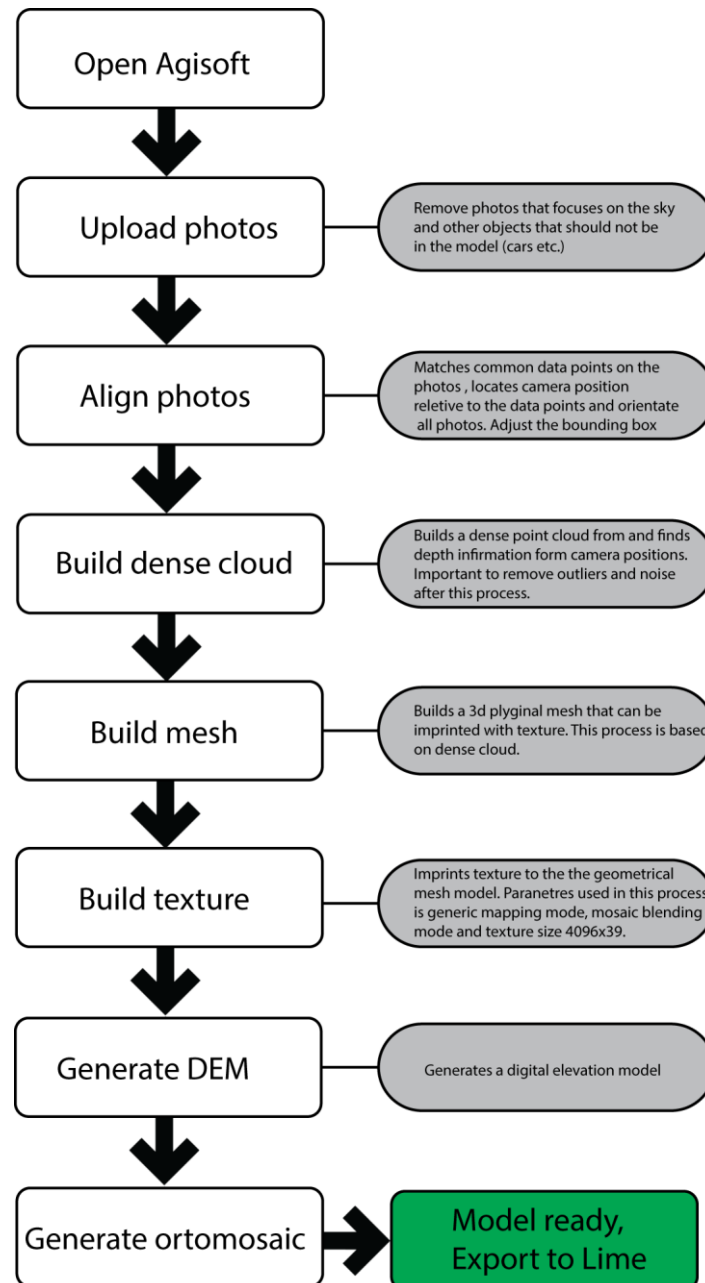


Figure 3.1: Simple workflow of how the virtual outcrop model was generated in AgiSoft.

after importing the model to LIME interpretation was done by outlining channels and sand-sheets and correlating with the logs. During the second field season, an understanding of the succession had been established by interpreting the model, logs and photos. An example of this is shown in Figure. 3.2. The model served as an excellent tool to locate channels in an otherwise difficult terrain, highly improving the efficiency of the fieldwork. After outlining sandstone channel bodies and sheet sandstones, a screenshot was taken of the

interpretation, uploaded to ImageJ which calculated the outlined areas relative to the rest of the photo giving a rough sand percentage in each unit.

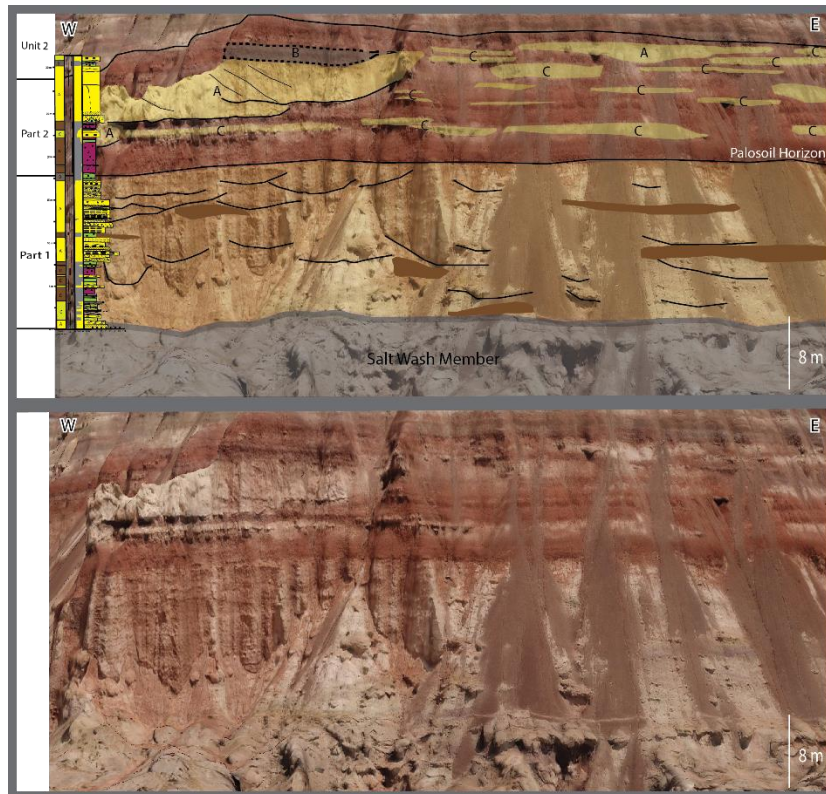


Figure 3.2: Example of interpretation of the virtual outcrop and correlation with logs. Letters (A,B,C) are different facies associations that are covered in chapter 4. This picture was uploaded to ImageJ and the percentage of sand was estimated based on the coloration of the areas. Vertical exaggeration x2.

3.1.3 Reservoir model and flow simulation

The following steps were performed to create a gridded geological reservoir model of the scanned Brushy Basin Member outcrop:

- Exported Unit boundaries interpreted in LIME and imported these lines as point to Petrel.
- Create surfaces of these points using a convergent interpolation algorithm.
- Copied the surfaces and added point in order to have several datum surfaces in order to extend interpretations into areas without data and make a bigger reservoir model.
- Added point, make/edit polygon, add point in right toolbar) to add 3d variability to the surfaces away from the interpreted lines. This was done by recreating the observed variability from the field and with the help of Google Earth. The whole outcrop is folding.
- Created surfaces of all the edited point with 2x2m grid increment.
- Created confining surfaces above and below the model-
- Created a grid using the *Make Simple grid* process. *Insert surfaces* in input data.
- Selected the 3d model and used *Corner point gridding/Layering process*. Follow base for all zone, with cell thickness 0.2m.

- Facies modelling was then performed by zone, adding channels, crevasse splays, and mudstone as facies. Used *property modelling*, *facies modelling*. Porosity and permeability values were assigned to the grid model. For the setting used in each zone, see table 4.3.1 and 4.4.1.
- Cell based flow simulation of the model was performed in RMS, this was done due to license issues. The model was exported from Petrel in Rescue format, and imported into RMS.
- The parameters used in the simulation is visible in Table 4.4.2. Two experiment were simulated, S1 and S2. In scenario S2 the crevasse splay facies were then removed.
- The results from the simulations was plotted using the Excel software.

4.0 Results

The purpose of the chapter is to give the reader an understanding of the fluvial system at the outcrop location, from small scale to large scale.

Chapter 4.1 starts by giving the reader a thorough presentation of the facies associations and depositional environments. Detailed observation about the different facies associations are accompanied by pictures and some of the logs from the fieldwork.

In Chapter 4.2 the outcrop as a whole is presented together with the large-scale architecture of the channels and the lateral and vertical variation of facies associations in the outcrop

that eventually led to the figure below (Figure. 4.0.1).

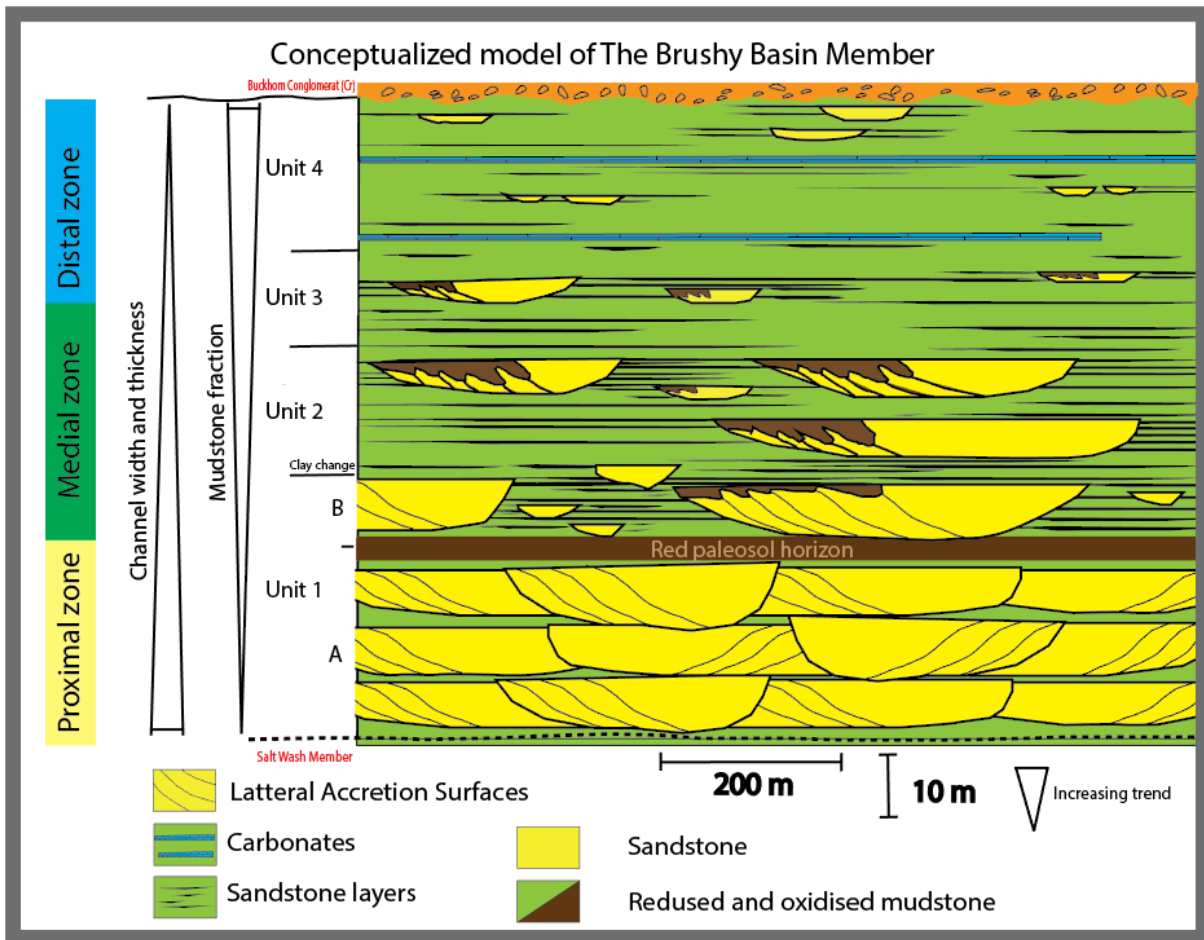


Figure. 4.2.12: Conceptualized model that summarize the upwards change in channel architecture presented in chapter 4.2. Channels become smaller, finer grained and, mudstone fraction increases upwards.

In chapter 4.3. the observation illustrated in the conceptual model is made into a reservoir model using the Petrel software package. This chapter presents the results as well as the parameters that went into creating the model.

Chapter 4.4 presents flow simulation results from two different simulations (scenario S1 & S2) done of the reservoir model made in chapter 4.3.

4.1 Facies and Facies association

Twenty sedimentary facies and five facies association have been recognised in the studied succession based on the fieldwork logging. The facies are listed in table 4.1 and the facies associations are described and interpreted in detail in this chapter.

Table 4.1. Facies discovered in the field at the study location. The facies are divided into Mudstones and Sandstones and a brief description is assigned to each facies. The facies have been put into the different facies associations that are described in the section below.

Facies	Description
Mudstones	
M1	Green featureless mudstone. (Slikenside/slikenlines visible sporadically)
M2	Red featureless mudstone. (Slikenside/slikenlines visible sporadically)
M3	Green mudstone with varying degree of red and brown mottles, root traces and burrows. Oxidation also visible in some layers. Small millimeter sized black ships in some layers
M4	Red to dark purple mudstone with varying degree of green mottling, root traces and burrows
M5	White to porcelain like featureless mudstone, conchoidal fractures
M6	Black to gray mudstone with millimeter sized white spots
M7	Green to white cm thin discontinuous layers of silt, occasionally mottled red and brown.
M8	Green to white siltstones with horizontal to low-angle bedding. Often weakly cemented.
M9	Laminated green silt.
M10	Carbonate rock
Sandstones	
S1	Planar parallel medium coarse sandstone (PPS), extraformational clasts 1-5mm in diameter
S2	Very fine-to- medium-grained sandstone with current ripples.
S3	Very fine-to-fine and medium-grained sandstone with tangential ripples. Occurs as climbing ripples
S4	Very fine to coarse grained cross-bedded sandstones. Both angular and tangential, with extraformational clast and mudchips 0.5-2.0 cm in the foresets. (Planar and trough cross-beds).
S5	Bioturbated/rooted very fine-fine grained sandstone
S6	Pebbly sandstone
S7	Conglomerate, matrix supported
S8	Medium-to- coarse grained sandstones, intraformational clasts, mudclasts, and erosional features
S9	Homogenous fine-to-medium coarse sandstones with little to no visible sedimentary structures
S10	Centimeter-scale layers of sandstone ranging from very fine to fine grained surrounded by dark red mudstone, often bioturbated and rooted.

4.1.1 Facies Association A- Channel belt

This facies association consist predominantly of very fine- to medium grained sandstone. However, coarse to very coarse-grained sandstones and conglomerates with sharp erosive base Figure. 4.1.1.F exists in a few places. Examples of conglomeratic sandstones occurs mail the lowermost and uppermost part of the outcrop.

The sandstones in Facies Association A form discontinuous lens-shaped bodies, <100 meters to >500 meters wide and 1-12-meter-thick, with relatively flat bases that show little erosional relief into the strata below (Figure. 4.1.1.A, B&C). The sandstone bodies generally have a fining upwards trend and lateral accretion surfaces (laterally down-lapping beds) (Figure. 4.1.1.B&C) are visible in almost all well-preserved sand bodies regardless of size. They commonly contain increasing amounts of mud and mud-drapes towards the top of the sandstone bodies.

Internally the sandstone bodies are highly complex and range from layers of massive homogenous structureless beds of fine-to-medium grained sandstone to layers with clear sedimentary structures and a fining upwards trend. Sedimentary structures observed within the sandstone bodies range from planar parallel stratification (PPS) Figure. 4.1.1.E, trough cross-stratification (TCS) Figure.4.1.1.E tangential & tabular cross-bedding to low-angle cross-bedding, and current ripples. Paleocurrent measurements of the current ripples and cross-bedding show a large variety of directions, mostly towards the north and east. Mud chips and extraformational clasts are presents throughout, and often occur in larger quantity in the foresets of cross-beds, in the planar parallel stratified layers or at the base of the sandstone bodies (Figure 4.1.1.G).

The discontinuous lens-shaped sandstone bodies with a generally fining upwards trend and multiple indicators of unidirectional current observed in this facies association are interpreted as the deposits of fluvial channel belts and will be referred to as channel sandstones or channel belts for the rest of the thesis (Miall, 2013; Bridge 2003). The channels range from being stacked fluvial channels that are difficult to map out completely (Figure. 4.1.1.C), to more isolated channels as shown in Figure. 4.1.1.A. The fluvial architecture of the succession is addressed in Chapter 4.2.

The channel belts show clear indication of sinuosity. Lateral accretion surfaces are observed in almost all the larger channels, and some of the smaller ones. These lateral accretion surfaces are interpreted to be fining-upward point-bar sequences deposited in the meander bend as the channels were expanding, translating or rotating laterally (Ghinassi et al., 2014).

The alternation between upper flow regime to lower flow regime sedimentary structures within the channel sandstones implies a “flashy” fluvial system that probably reached maximum discharge several times during the wet season (Bridge 2003; Galli, 2014). The abundant rip-up clasts/mud-chips and mud-clasts implies that the channel was eroding the banks as it moved laterally (Galli, 2014). Which also indicate some seasonal variation in stream power and instability of the banks (Demko et al., 2004; Galli, 2014,). Mud-draped lateral accretion surfaces, passive infill of channels, ripples and cross-beds indicates a mixed load fluvial system where the rivers were transporting both sand and mud (Miall, 2014). In addition, the flat bases of the channels and lack of major erosional relief at channel bases suggests that the channels were low-gradient, sinuous and meandering. The complex sandstone layers within the sandstone belts are interpreted as fluvial channel bars that were deposited in the channel (Ghinassi et al., 2014). These bars probably migrated downstream and varies somewhat in grainsize and sedimentary structure depending on stream-power, sediment supply and the curvature of the river at the time of deposition (Bridge, 2003; Ghinassi et al., 2004).

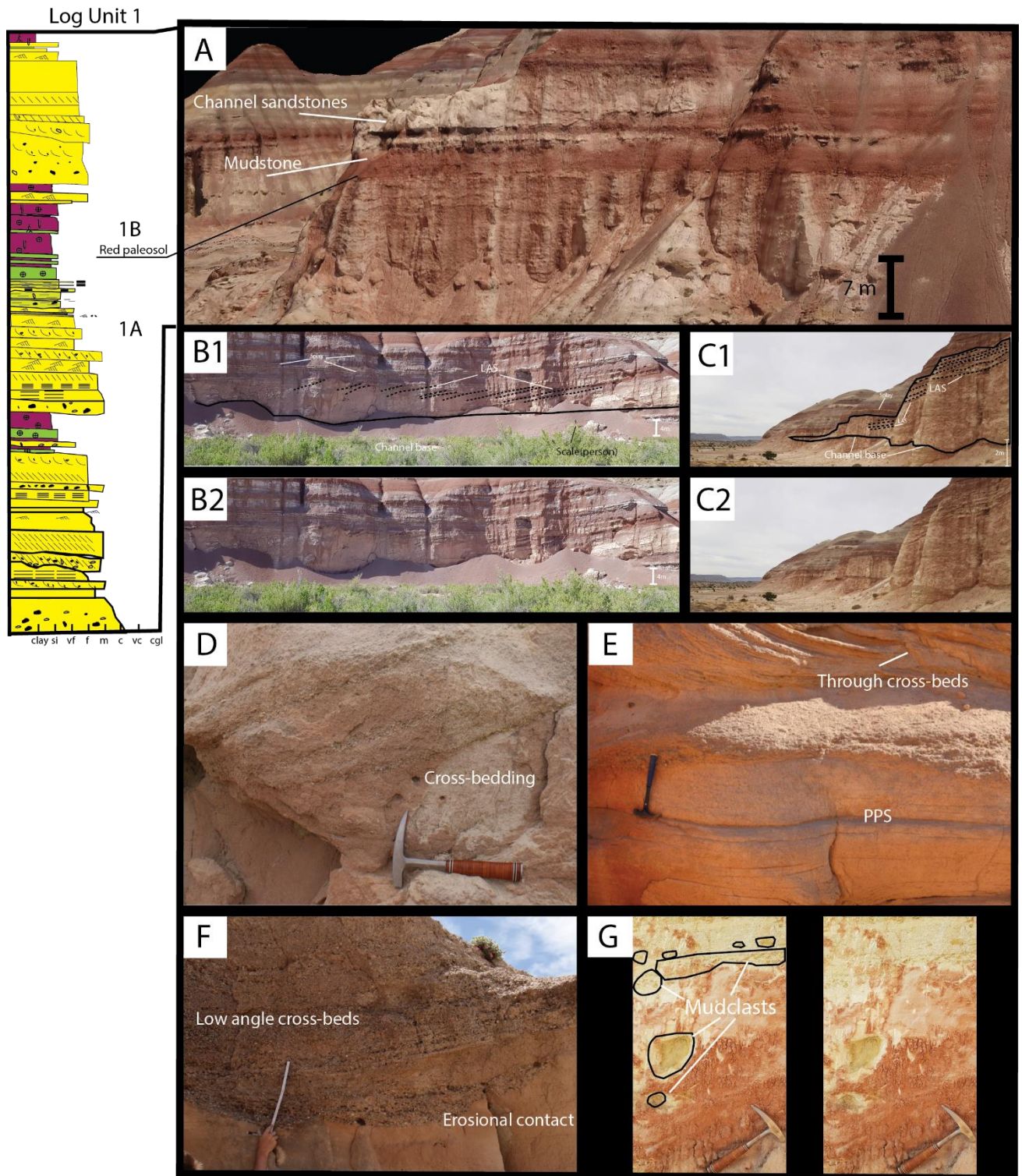


Figure 4.1. 1: A) White coloured channel sandstone surrounded by red and brown mudstone. B) Channel-belt from upper parts of Brushy Basin Member with muddy lateral accretion surfaces. C) Thick channel-belt from the lower parts of the Brushy Basin Member with lateral accretion surfaces. D) Cross-bedded sandstone with coarser grains in the foresets found in the channel-belts. E) Planar parallel stratification overlain by trough cross-beds within the channel-belts. F) Low angled cross-beds interpreted as dunes within the fluvial channel eroded down into finer grained sandstone below. G) Small and large mud-clasts within the channel-belts.

4.1.2 Facies Association B - Abandoned Channel

This facies association consists mostly of red to green mudstone. Interbedded within the mudstone are thin lateral continuous layers of very fine-grained sandstone Figure. 4.1.2.E. The large-scale geometry of the mudstone is lenticular with a flat top and curved base Figure. 4.1.2.A. In addition, the facie is surrounded by sandstones on all sides but the top. The mudstone shows little or no internal lamination and the sandstone layers are typically structureless Figure 4.1.2.B. The thicker sandstone layers show sharp base and a top grading into red mudstone Figure 4.1.2.B. Varying degree of mottling, root traces and bioturbation are common throughout Figure 4.1.2.C-D.

This facies association is interpreted as deposits accumulated in an abandoned, or cut of, channel, forming a mud-plug. The thin sand layers within the mudstone is interpreted to be spill-over deposits from the avulsed channel during floods (Bridge, 2003). The sand layers possibly originally had sedimentary structures. However, bioturbation, burrowing and pedogenesis has reworked the deposits and rendered them structureless (Retallack 2001, Boggs, 2014).

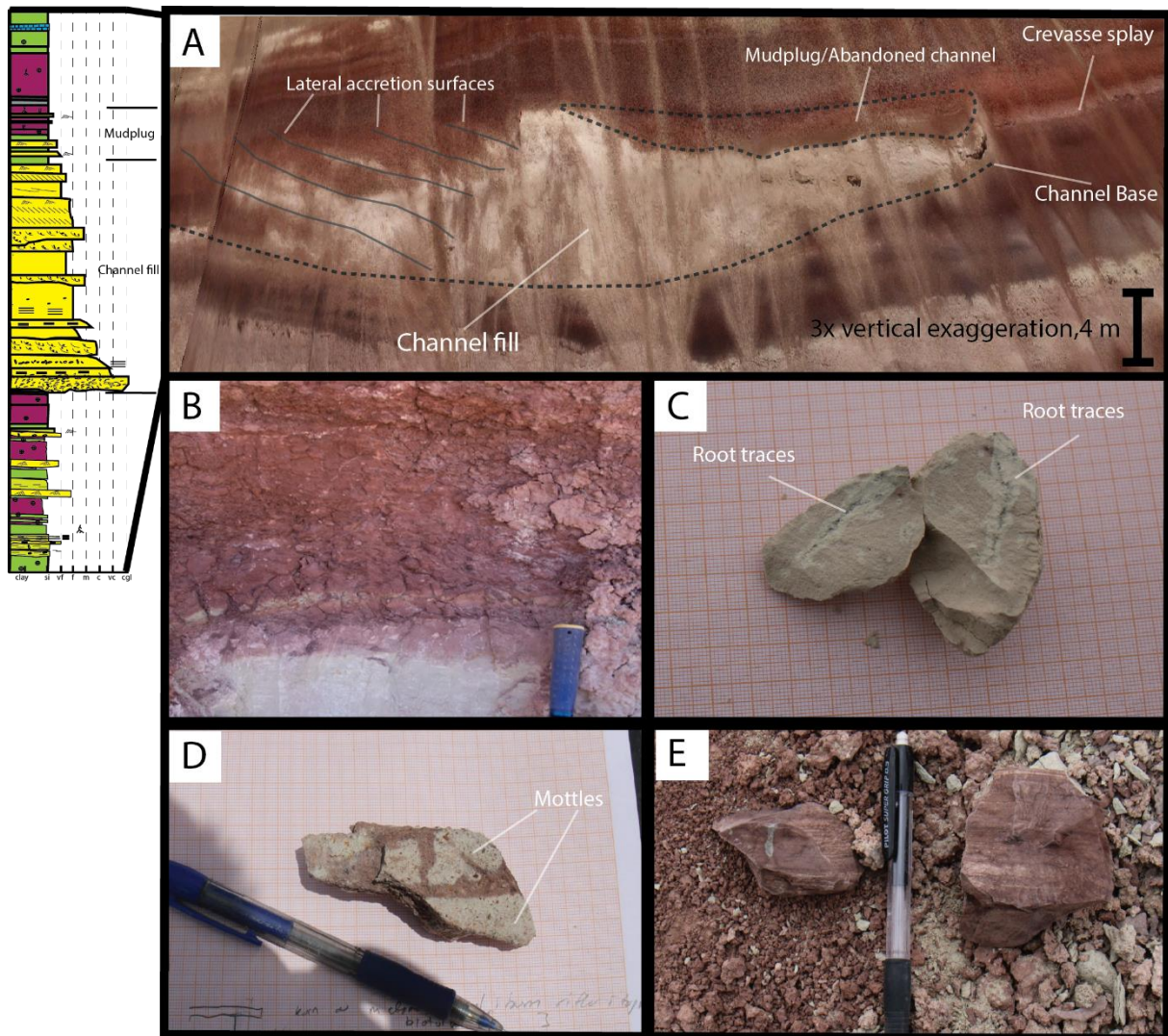


Figure 4.1. 2: A) White channel sandstone from upper Brush Basin Member with channel base (dashed black line), lateral accretion surfaces (indicated by black lines), and a mud-plug (dashed black lines) from passive infill when the channel was abandoned. B) Structureless red-brown mudstone. C) Root-traces in silty mudstone. D) Heavily mottled mudstone. E) Red-brown mudstone with thin white green silt laminae.

4.1.3 Facies Association C- Crevasse splay deposits

This facies association consist of resistant 2-50 cm thick sandstone beds within mudstone that forms layers of sandstone adjacent and below facies Association A and B, channel-belts and mud-plugs (Figure 4.1.3.A). The sandstones vary from very fine- to medium grain size and display mud-chips and quartz-clasts. The sandstone beds often thicken towards the channels-belts and gradually thins away from the channel-belts. They also have uniform consistent paleo-flow direction and commonly a fining-upwards trend. Tangential cross-bedding (Figure 4.1.3.C) and climbing ripples (Figure 4.1.3.B) often occurs at the top of the layers. Some places the sandstone layers are amalgamated forming thick sand layers within the mudstone. Thickness of the sandstone layers vary from a couple of centimetres to tens

of cm where the benches are isolated to, meter thick packages where the layers are stacking. Bioturbation and root traces are visible at the top of some of the layers.

The prominent ledge sandstone layers of limited extent, unidirectional current ripples and uniform paleo-flow direction are interpreted to be crevasse splays deposited from when the stream broke through its levees and deposited sediments on the floodplain (Bridge, 2003; Boggs, 2014). Rocks of this type will be referred to as crevasse splays for the rest of the thesis.



Figure 4.1. 3: Typical examples of facies association C – Crevasse splay deposits. A) 3 sandstone benches above a channel belt. B) Climbing ripples in the top of one of the benches. C) Small tangential cross-bedding at the top of a sandstone bench.

4.1.4 Facies Association D- Overbank deposits

This facies association consists mostly of light green and dark red mudstone and is the most frequent facies association in the study area. The colour-heterogeneity of the mudstones form the distinct colour banding of the Brushy Basin Member, which is shown in Figure.

4.2.2. Two types of coloured mudstone dominate the succession; Green-gray mudstone with black, white or red-brown mottles and red-brown mudstone with white or grey mottles.

Root traces, bioturbation, horizon with white cm sized white carbonate nodules (Figure.

4.1.4.A) and slickensides (Figure. 4.1.4.B) are visible occasionally. Thickness of the mudstone

layers varies from 10-centimetre thin layers in between sandstone bodies to more than 6-meter-thick packages. Both the green-gray and red-brown mudstones are almost completely void of sedimentary structures, faint lamination can occur close to large sandstone bodies, has conchoidal fractures and weather to a characteristic popcorn texture (Demko et al., 2004). The mudstone shows different degree of mottling ranging from a few small millimetre sized (Figure 4.1.4.D) to centimetre sized mottles (Figure. 4.1.2.D & FIG 4.1.4.C). The mudstone layers are associated with undulating boundaries, often sharp erosive features as shown in Figure 4.1.4.A where a sandstone body has eroded down into the mudstone.

The mudstones observed in Facies Association D are interpreted as weakly to well-developed paleosols formed on the floodplain associated with the meandering streams of the Brushy Basin fluvial system (e.g., Demko et al., 2004; Turner & Peterson, 2004; Galli, 2014).

Postpositional modification of the mudstone formed these paleosols and the degree of pedogenesis within the horizons dependent on a myriad of different controls like; magnitude and frequency of depositional events, distance from sediment source, parent material, inherent local topography, position and fluctuation of groundwater profile, composition of biotic communities, and the climatic setting with regard to temperature and precipitation resulting in a high degree of spatial heterogeneity (Bown and Kraus, 1987; Kraus, 1987; Hasiotis and Bown, 1996; Hasiotis, 2004). This makes studying the overbank deposits complex.

In general, the most mature paleosols are found in the lower Brushy Basin member where the soils typically have a deep red colour with carbonate nodule horizon, mottles, reddened clay accumulations, root traces and termite-nests traces (Demko et al., 2004; Galli, 2014). The mudstones in the Upper Brushy Basin are characterized by a distinct colour change into grayish, popcorn-weathered, ash-rich mudstones with volcanic ash layers and weakly to moderately developed paleosols (Galli, 2014). Slickensides and subparallel fractures exist in both the red and grey layers and was formed by expansion and contraction of ash-rich smectitic mudstone do to wetting and drying, indicating alternating wet and dry conditions (Hasiotis, 2004).

Based on the pedogenic features, colour, trace fossils caliche horizons and indication of dry and wet conditions the paleosols of the Brushy Basin member are typically classified as vertisols, and the more carbonate nodule rich horizons are also referred to as calcisols,

which form in subhumid to semiarid climates with a pronounced dry season (Retallack 2001; Hasiotis, 2004; Turner & Peterson 2004; Demko et al., 2004; Galli, 2014).

The mudstone described and shown here will be referred to as paleosol horizons, overbank mudstones or mudstones for the rest of the thesis.

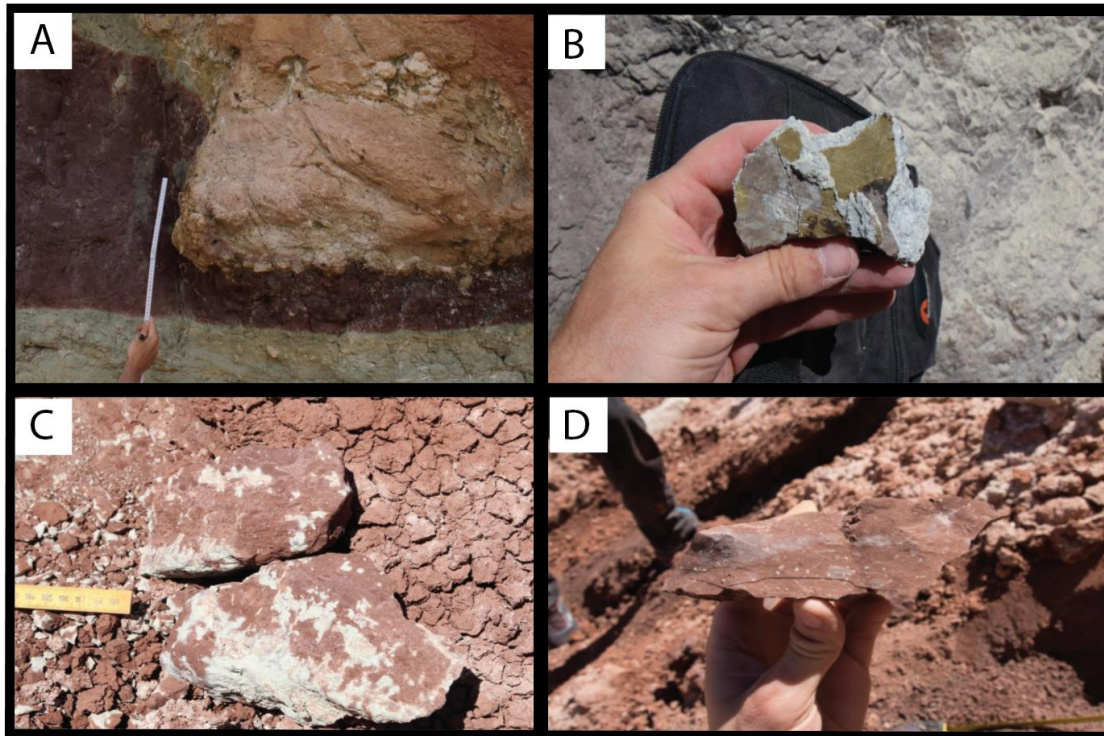


Figure 4.1. 4: A) White channel sandstone eroding down into red-brown mudstone. White caliche nodules visible in the green-grey mudstone below B) Slickensides in mudstone. C) Heavily mottled mudstone. D) Lightly mottled mudstone

4.1.5 Facies Association E- Volcanic ash-layers

This facies association consists of dark grey or white porcelain-like rock layers with no internal structuring and thicknesses between 10-50 centimetres that make up extensive continuous layers that can be followed laterally in the upper part of the outcrop throughout the study area. The rocks have conchoidal fractures and occasional black or green millimetres-sized patches. The frequency of these layers increases in the upper part of the Brushy Basin member.

Dark layers and white mudstone have been identified by others (e.g. Turner & Peterson, 2004; Demko et al., 2004; Galli, 2014) as silica-replaced volcanic ash layers rich in bentonite from volcanic ash. A proof of the volcanic activity in the calderas to the west and south-west of the Morrison basin. The frequency of these layers increases in the upper Brushy Basin

member indication voluminous outpourings of volcanic ash and a possible increase in eruptions in the last stages of the Brushy Basin member time interval (Turner & Peterson, 2004). The ash layers are missing where the channels belts are located. This could be explained by the rivers having eroded the layers away or hindered the settling and preservation of the ash.

4.2 Virtual outcrop

Chapter 4.2 starts by presenting an overview figure of the virtual outcrop in Figure 4.2.1 & Figure. 4.2.2 the outcrop is visible on these figures prior to interpretation. Blue lines that show how the thesis divides the outcrop into units has been added.

Every unit is presented with observation and interpretations from the virtual outcrop and total outcrop. The aim of the chapter is to build an understanding of fluvial architecture of the succession, and how the units relate to the large-scale distributary fluvial system in terms of proximal, medial and distal zones. This is done through outlining channel features in the virtual outcrop and correlate with the lithological data acquired in the field. Every unit will therefore consist of several photos taken in the field accompanied by field logs and screenshots from the virtual outcrop.

The outcrop is divided into 4 units, 1 through 4 from the bottom and up. The division is based on the vertical colour change, the change in mud-to-sand ratio and the abundance of channels. Sandstone percentages in the units have been estimated using ImageJ on the virtual outcrop interpretations (see Chapter 3 Methods). In other literature the norm is a twofold division between the upper and lower Brushy Basin member (e.g. Demko et al., 2004; Galli, 2014; Turner & Peterson, 2004), but in this thesis a fourfold division that best represent the data is used to systematically assess the succession of rocks that exist in the outcrop. In the context of Upper and Lower Brushy Basin Member; Unit 1 correspond to the Lower Brushy Basin, and Unit 2-4 corresponds to the Upper Brushy Basin Member. The division between lower-and upper Brushy Basin member is shown in Figure. 4.2.2.

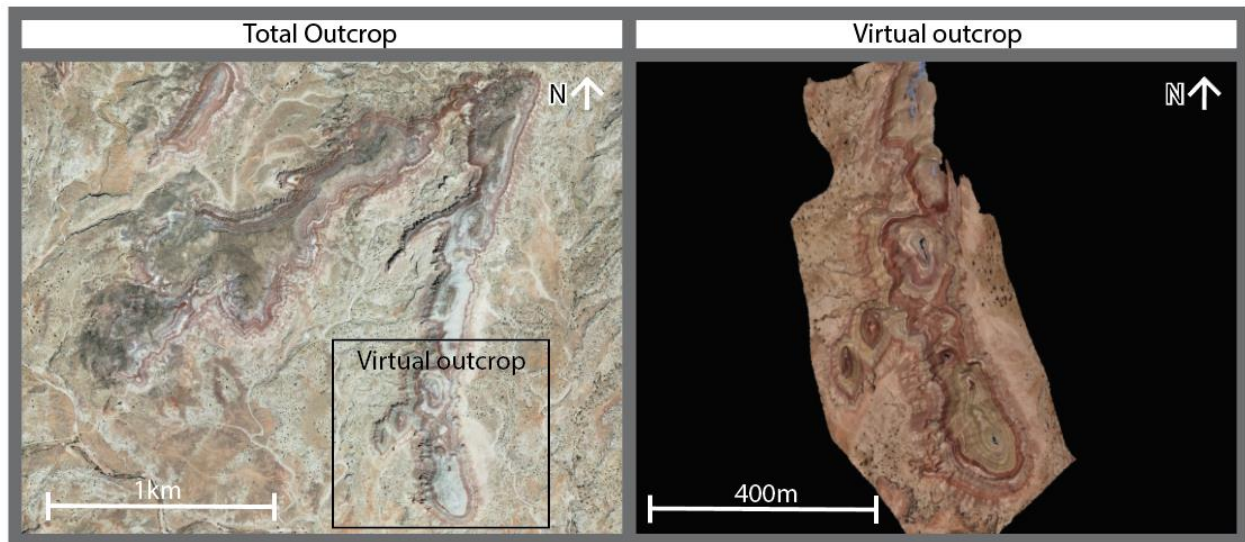


Figure 4.2. 1: V-shaped outcrop of The Brushy Basin Member where fieldwork was conducted, Western and Eastern limb converging towards the north. The Virtual outcrop was constructed from data gathered at the lower most part of the eastern limb. Fieldwork was conducted on the whole outcrop, but time restrictions and equipment-limitations did not allow for the construction of a virtual outcrop covering the whole outcrop.

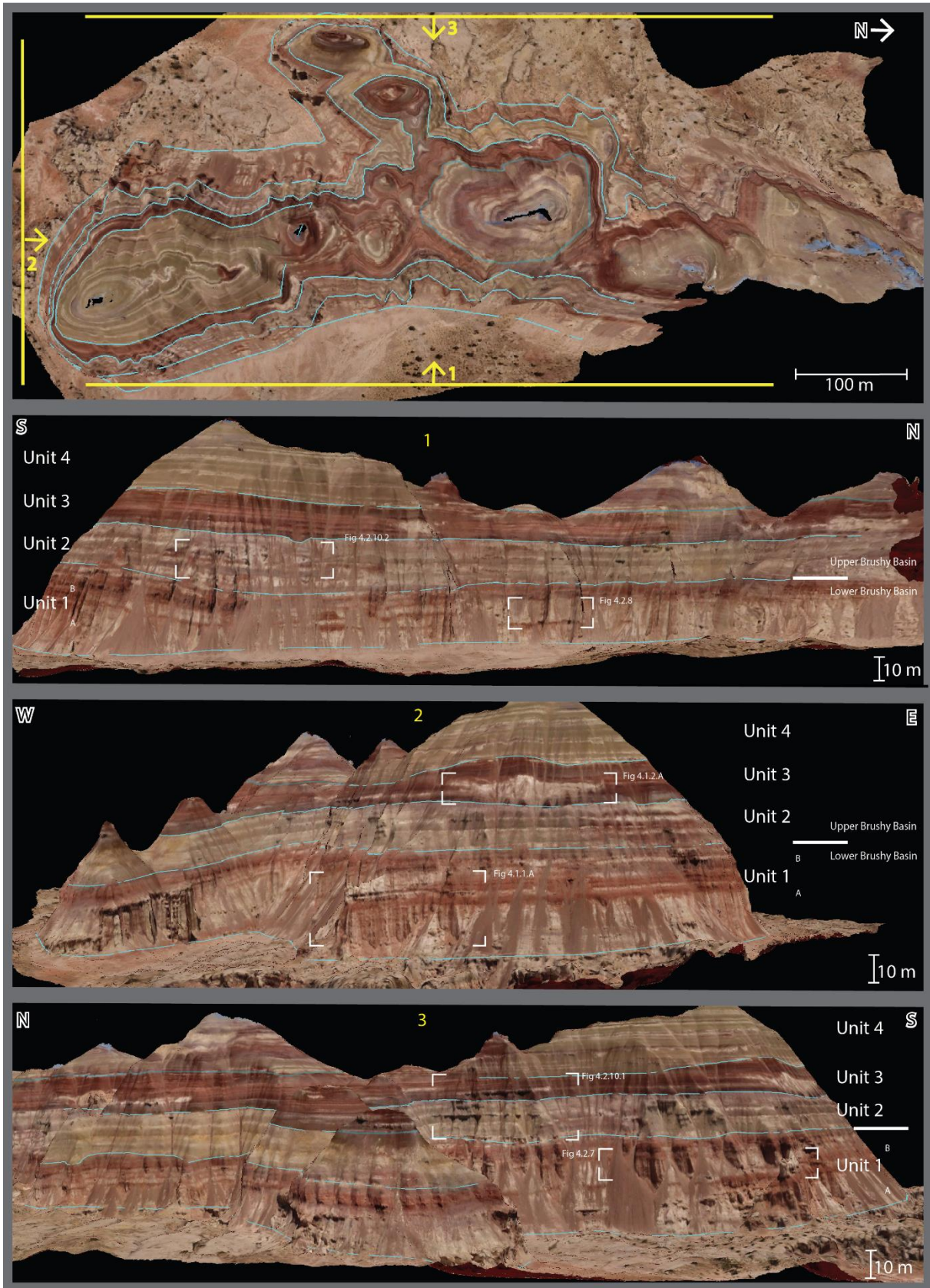


Figure 4.2. 2: Virtual outcrop presented from birds view (top) and from east (1), south(2) & west(3). Blue lines represent the different Unit boundaries and Units that will be presented from Unit 1-4 in this chapter. Figures that are presented later in the chapter have been indicated for reference purposes.

Unit 1A

Unit 1A is the lowermost 30 meters of rock poorly exposed in large parts of the virtual outcrop, but visible in certain areas outside the virtual outcrop where it forms steep cliffs near gullies or creeks. It consists of several laterally extensive 8-12-meter-thick channel-belts stacked on top of each other, separated by laterally discontinuous weakly developed paleosol layers (Figure. 4.2.3). The cliffs can be seen in Figure. 4.2.2 picture 1 & 2 beneath the first thick red paleosol layers, and close-up in Figure. 4.2.3. The sandstone percentage relative to mudstone in Unit 1A is estimated to be between 60-80 %.

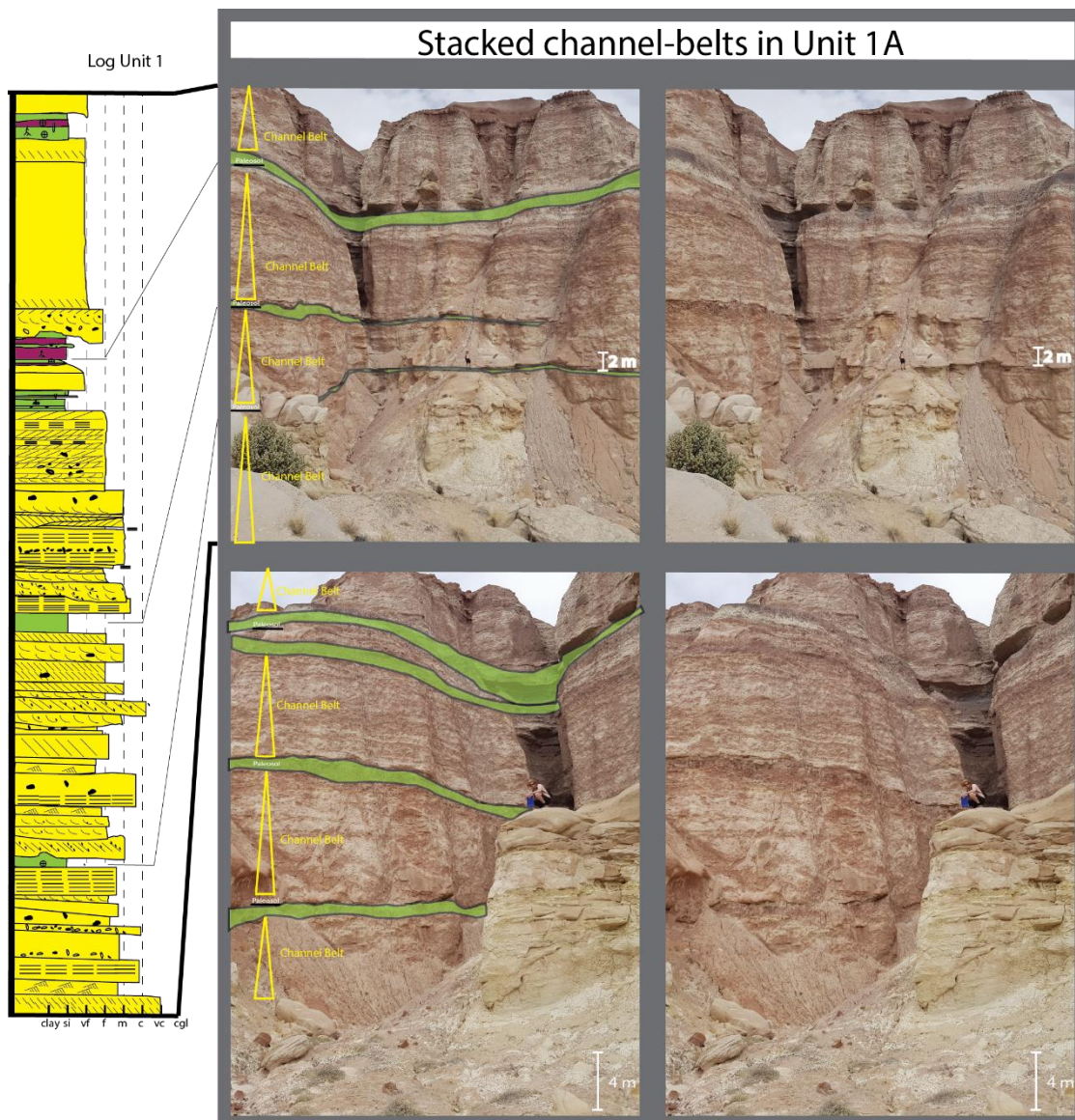


Figure 4.2. 3: Stacked channel-belts in Unit 1A. Pictures on the right side are without interpretations. Left-hand pictures have mud-layers in green. White-yellow channel sandstones are visible between the mud-layers. The channels fine upwards internally, this is represented by yellow triangles.

The bank/pinchouts of the belts are not preserved or exposed which makes them difficult to map out completely. The channel-belts are however visible in the same stratigraphic height on both the southern and eastern side of the virtual outcrop as well as on the western limb of the total outcrop (Figure 4.2.1). It is not possible to locate an end to the channel belts which therefore covers the whole study area where Unit1A is exposed. This means that the belts are at least 300 meters to over 1000 meters wide. A possible explanation for this extensive width could be that the channel belts, showing that they consist of multiple channel belts vertically (Figure 4.2.3), also stem from several channels migrating laterally forming a network of multilateral channels as illustrated in Figure 4.2.4 (Miall, 2014). The size and extent of the channel-belts resulting from this lateral migration does not imply that the size of the original channels was equally large (Bridge,2004), but is rather a testimony to the low rate of accommodation that forced the channels to deposit laterally at meander-bends and point bars (Bridge, 2004; Miall, 2014).

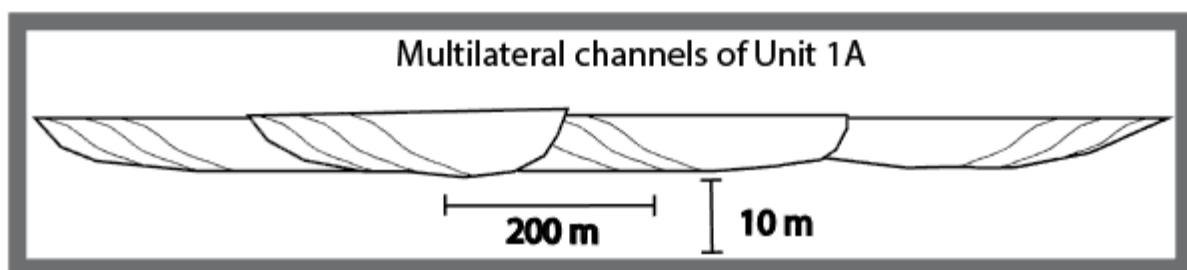


Figure 4.2. 4: Multilateral channels interpreted to have deposited the sandstone succession in Unit 1A. The down-lapping black lines within the channels represent lateral accretion surfaces. After Miall, 2014.

These multilateral channels reworked and cannibalised already deposited point-bars and channel-deposits, leading to a succession of sandstone belts that stack on top of each other and makes the lower most part of Unit 1 especially complex. The system both horizontally and vertically is conceptualized in Figure 4.2.4, where the yellow bodies represent the channels, the green bodies mudstone that are discontinuous and has varying thickness, and connection in certain places between the sandstone belts. A large quantity of mud-clasts ranging in size between 1cm to 40 cm are found throughout large parts of the belts which support the interpretation of laterally erosive channels. The mud-clasts are shown in the

Facies Association A Figure 4.1.1.

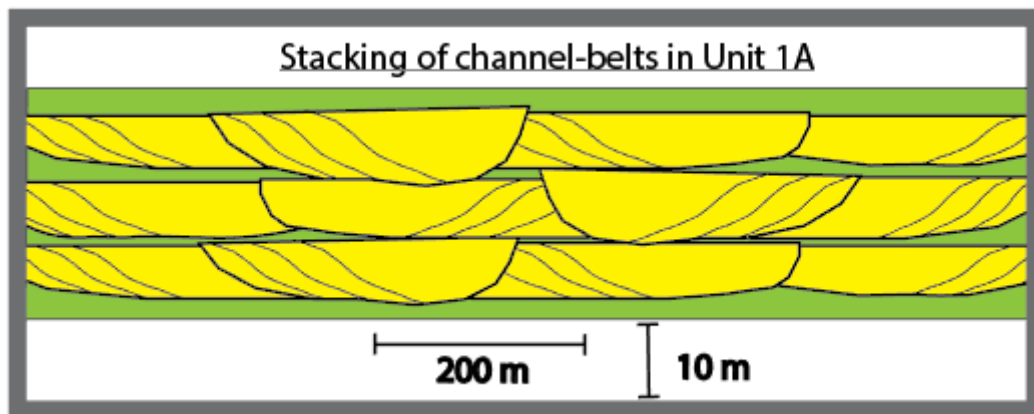


Figure 4.2. 5: Schematic illustration of stacked multilateral channels in Unit 1A. Note discontinuous mud-layers and vertical connection between channel-belts in a few places. The opposite of this would be singlestory and unilateral, one channel with no amalgamation vertically or horizontally (Miall, 20014).

Due to the complex nature of the channel-belts in the lower part, clear lateral accretion surfaces were not identified, although several dunes, erosive features and faint fining upwards sequences typical for channels deposits were found within the belts and could potentially have been deposited as part of the point bars. The lack of apparent lateral accretion surfaces could be that they are not easily visible due to the relative homogeneous grainsize composition at the top of the belts (mostly fine-medium, with pebbly sandstones at base)(log 1, Figure. 4.2.3) within the lower most channel belts (apart from large mud-clasts). Mud-drapes or muddy dipping layers near the top of the channels is often needed to spot the lateral accretion surfaces in the Brushy Basin Member.

Unit 1B

The upper part of Unit 1 is better exposed then the lower part. The unit is about 15 meters thick and form step cliffs near the bottom of the virtual outcrop. Unit 1B start at the first thick red paleosol horizon, 2-5-meter-thick with several interbedded crevasse splay sandstones, that can be traced all along the study area. Unit 1B in the virtual outcrop consists of one channel belt that can be traced both at the west side and east side of the exposure as shown in the yellow areas in Figure. 4.2.6. The sandstone percentage in Unit 1B is estimated to be between 40-60 %.

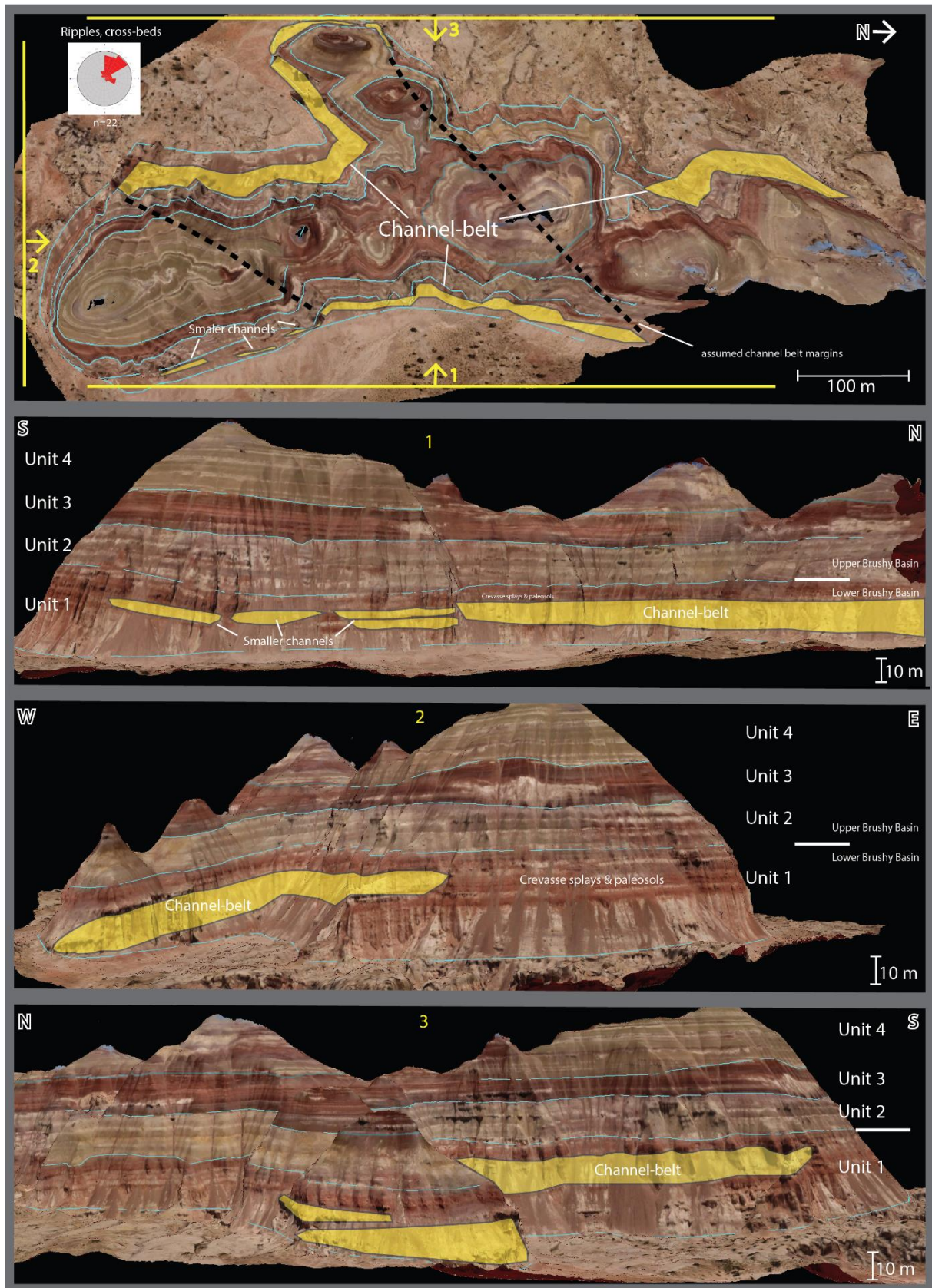


Figure 4.2. 6: Virtual outcrop with channel belts in Unit 1B marked yellow. The channel belts have been correlated in field on all sides of the outcrop and an approximate channel-belt width and mudstone/sandstone

ratio is inferred from that. Crevasse splays and overbank mudstones can be seen on the flanks of the channel belt.

The belt in Figure 4.2 is between 8-12 meters thick, and more than 400-500 meters wide. Lateral accretion surfaces are faintly visible at the very top along parts of the channel belts (Figure 4.2.7). The lack of clearly defined lateral accretion surfaces in much of Unit 1B can be explained in the same way as in Unit 1A; relative homogenous composition of grain size at the top of the channel belts. However, mud-draped and muddy lateral accretion surfaces in Unit 1B occurs and are especially visible when viewed from some distance (Figure 4.2.7). Several smaller channel belts are present in the same interval next to the large channel belt, together with abundant overbank fines. These channels could be chute channels or splay channels, an important part of the overbank drainage during floods (Miall, 2014).

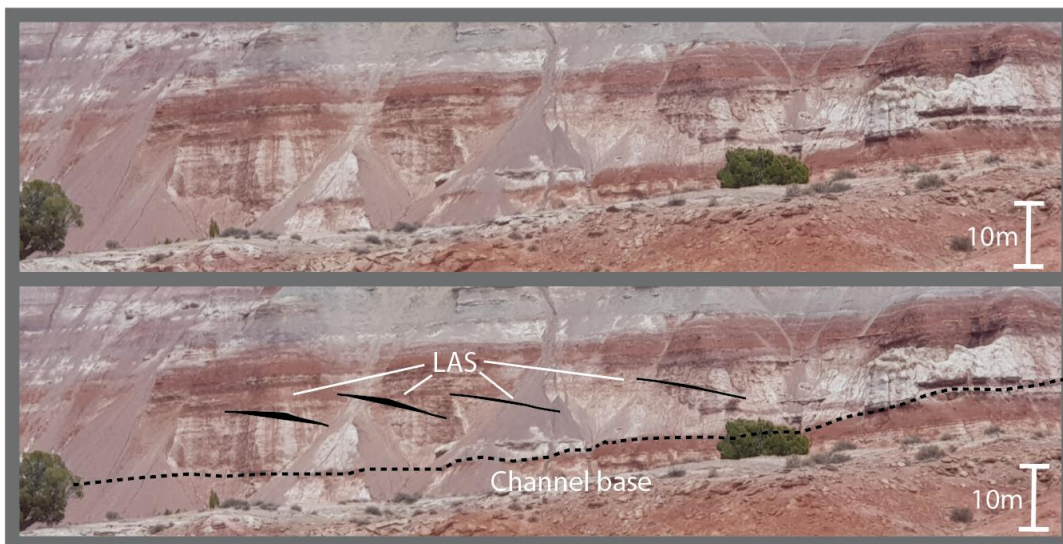


Figure. 4.2. 7: Lateral accretion surfaces (LAS) visible at the top of the channel-belt in Unit 1B at the virtual outcrop.

The channel belt depicted in Figure 4.2.6 and Figure 4.2.7 are in places thicker than the channel belts in Unit 1A below. Figure 4.2.8 show a close-up picture of the belt taken at the location where the sandstone erodes the most down into the dividing paleosol horizon between Unit 1A and Unit 1B. The red-brown coloured mudstone, although being at its thinnest here, is clearly visible at the base of the channel. Grain size decreases towards the top of the channel and the sandstone-belt have less pebbly content and are generally finer grained, but the difference is minor. The largest change in channel grain-size composition is an increased fraction of fines within the channel belts, especially towards the top.

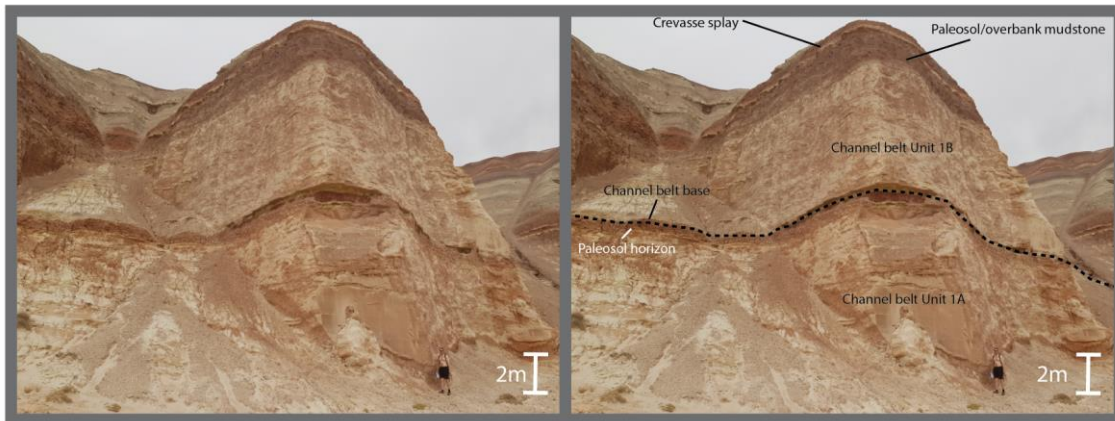


Figure 4.2. 8: Channel-belts from Unit 1A and B divided by red-coloured paleosol. The base of the uppermost channel erodes slightly down into the paleosol which is at its thinnest at this location. Crevasse splays and paleosol/overbank mudstone can be seen above the sandstones.

There are thicker more extensive mudstone layers in Unit 1B than in Unit 1A. Several meter-thick red mudstones and 50-100 cm thick hundreds of meter extensive crevasse splays form a complex stacking of alternating mudstone, paleosols and crevasse-splays that close-up resembles a layer-cake that does not occur, or is not preserved, in Unit 1A. This red-brown layer-cake is visible above the channel in Figure 4.2.8 and above and at the sides of the yellow coloured channel belt in Figure 4.2.6.

The stacking of channels and vertical and lateral change from Unit 1A to Unit 1B is illustrated in Figure 4.2.9.

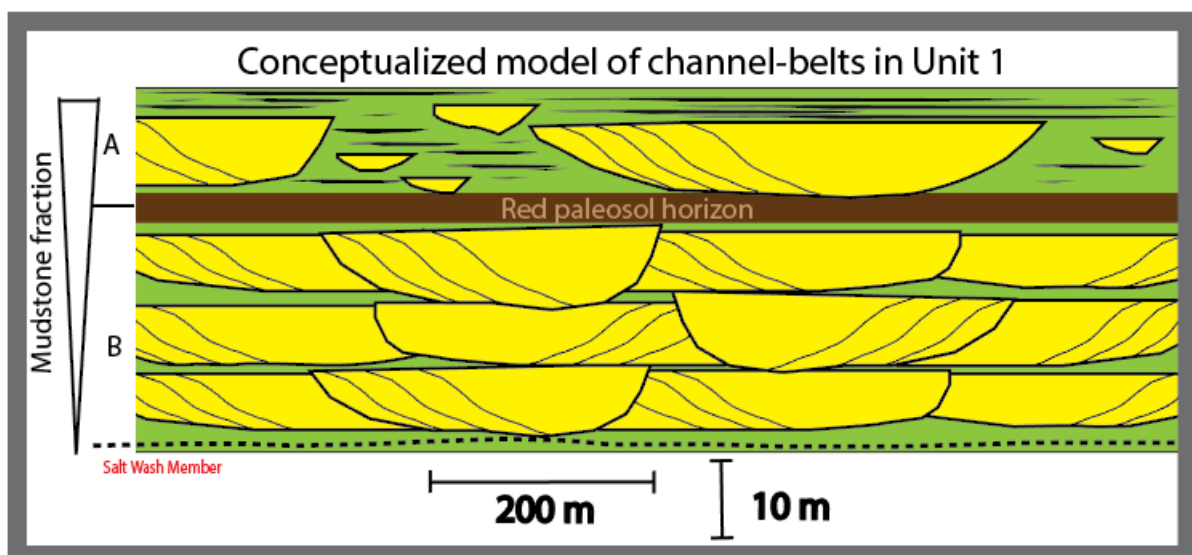


Figure 4.2. 9: Complete conceptualized model of Unit A & B. The channels retain much of the same thickness but the lateral extent decreases. Mud-fraction within the channel-belts as well as the amount of overbank mudstone increases upwards.

In terms of proximal, medial and distal zones (Figure. 2.5) in a distributary fluvial system, Unit 1A is interpreted to resemble the proximal zone; stacked channel deposits, amalgamated and interconnected. Whereas Unit 1B resemble the medial zone; channel deposits with floodplain mudstones and sheet sandstones.

Reservoir aspect Unit 1

The channel sandstones in Unit 1 could make up substantial reservoir volumes, and in the outcrop itself the channels belts amount to a total of around 30-40-meter thickness. Especially the amalgamated, multistore channels in Unit1A makes up a large connected sand volume (Donselaar and Overeem, 2008). A potential problem for fluid flow in Unit 1 is however the mudstone layers between the channel belts, aswell as mud-chip lag within the channel bodies themselves which may impede connectivity (Chapin and Mayer, 1991). The continuous red-brown paleosoil will probably be a barrier for vertical fluid flow. The paleosol horizon is therefore added to the conceptual model (Figure. 4.2.9).

Unit 2

Unit 2 shows a distinct change in colour from Unit 1 and can be traced as a 10-15-meter-thick grey-green band above the red-brown Unit 1 (Figure 4.2.2). The Unit form less ledges and cliffs than Unit 1, which is possibly an indication of lower competence rocks and increasing mud-content. The colour change has been attributed to the increased smectitic content of the mudstones that originate from abundance of silicic ash blown eastward from the volcanic arc to the west (Cordilleran Arc, Nevada orogeny) (Galli et al., 2014). Extensive porcelain-white ash layers can be found at several intervals in this Unit.

The white-green Unit 2 consist primarily of mudstones that, apart from the colour change, display similar paedogenic features as the mudstones in Unit 1. The sandstone percentage in Unit 2 is estimated to be between 15-30 %. Continuous sheet like sandstone layers form ledges within the mudstone (Figure 4.2.10). These layers are interpreted as crevasse splays and display varying thickness and extent. Most are between 5-110 cm thick, but some are thicker than 1 meter and can be traced all over the virtual outcrop. Only two clear channel sandstones are visible in the virtual outcrop. These channel sandstones are embedded in the mudstone package and are small compared to the previous channels, between 3-6 meters

thick and 50-100 m wide, as shown in Figure. 4.2.10. They are associated with crevasse splays, marked C, and overbank mudstones on all sides.

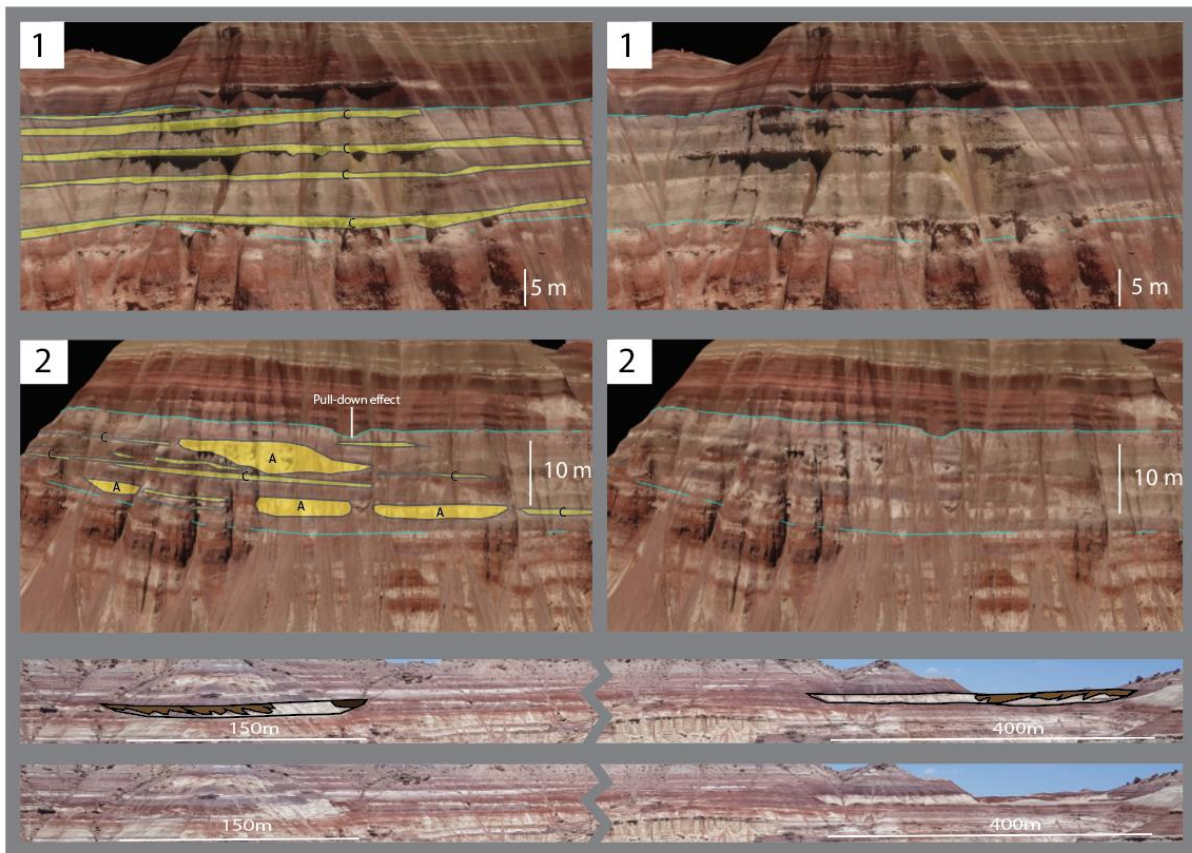


Figure 4.2. 10: 1) Lateral extensive sandstone benches in the red coloured overbank mudstones and paleosols of Unit 2. The sandstones are interpreted as crevasse splays and marked as Facies association C. 2) Sandstone bodies of different thickness and lateral extent. Some have been interpreted as smaller fluvial channels (marked with A), possibly seasonally active, and the thinner more extensive have been interpreted as crevasse splays (marked C). 3) Wide channel belts with muddy lateral accretion surface and mud plugs from the western limb outside the virtual outcrop.

Several large channel belts outside the virtual outcrop also exist in this unit and can explain the origin of the thick splay deposits. The channel belts are singlestorey and they appear isolated, a clear change from the multilateral multistorey channels of Unit 1. In addition, the channels are smaller and finer grained than the channel belts in Unit 1. They range between 6-9 meters thick and between 100-400 meters wide. Muddy lateral accretion surfaces are visible in all channels (Figure 4.2.10). The content of fines within the medium to fine sandstone in the channels are even more apparent here than in Unit 1B. Unidirectional paleocurrent indicators from ripples in the channel belts give an eastward trend.

Brown lateral accretion surfaces consisting of mud and silt suggest a fluctuating water level (Bridge, 2003). Some channel also shows mud draped lateral accretion surfaces extending

far into the sandstones belts. Example of this is shown in two separate channels in the figure below (Figure 4.2.11). Mud draped surfaces that extends far into the sandstone belts could point towards a fluvial environment with highly fluctuating water level where the energy within the channels at times are weak enough to deposit mud in the channel itself. A possible explanation for this is seasonal drought which fit well with the interpretation of a semi-arid environment made by Demko et al., (2004) and Turner & Peterson (2004) who both have interpreted the channels in the upper brushy basin to be channel that at times were completely dried out.

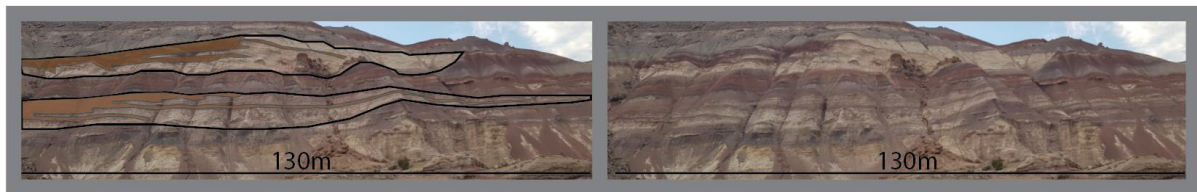


Figure 4.2. 11: Close-up of two 6-10m thick channel-sandstones in Unit 2. The channel has muddy lateral accretion surfaces, in the lowermost channel one of the mud-surfaces stretches all the way across the belt. This is interpreted to stem from extremely variable water level in the channel. The mud is coloured brown.

The fluvial system in Unit 2 has been conceptualized in the same style as Unit 1 (Figure 4.2.12). The channel belts observed in Part 2 are interpreted to be the deposits of sinuous meandering rivers. The channels display typical meandering features like point-bar accretion, crevasse-splays and mud-plugs from when the channels were abandoned due to avulsion and transported sediments both as bedload and in suspension. The paleosol horizon is well developed, preserved and thicker which indicate a change in sediment influx, water discharge and bank stability from Unit 1 (Bridge 2004; Miall, 2014)

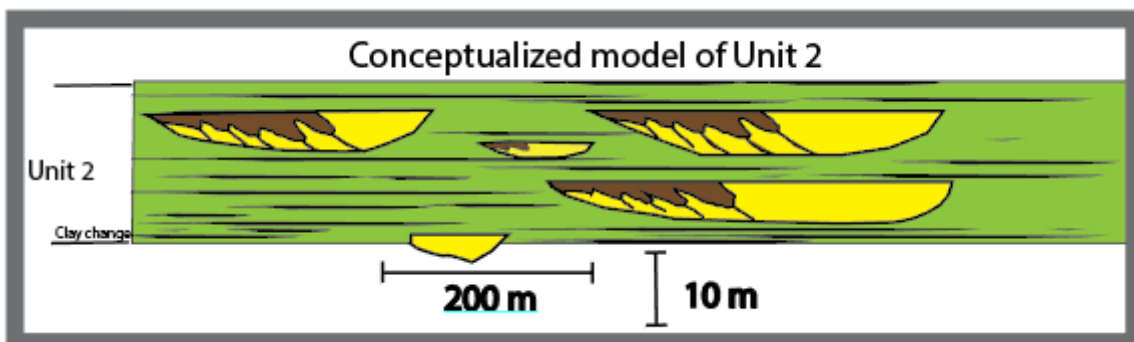


Figure 4.2. 12: Yellow channel belts embedded in overbank mudstone and splays. The channels still have a lateral reach of several 100 meters. Muddy lateral accretion surfaces represent the varying water level and abundance of fines in the fluvial system.

In terms of proximal, medial and distal zones (Figure 2.5) in a distributary fluvial system, Unit 2 is interpreted to resemble the medial zone; channel deposits with floodplain mudstones and sheet sandstones.

Reservoir aspect Unit 2

The channels in this unit make up around 6-9-meter-thick reservoir bodies. They are however spaced out and not connected as the multilaterally connected channels of Unit 1. Fines within the channel sandstones could impact fluid flow negatively. The relative thick crevasse splays add to the total volume of sand in the unit. Mudstone layers within the channel belts and between the channel belts, will work as non-reservoirs and fluid barriers.

Unit 3

Unit 3 is the dark red -brown 10-15-meter-thick band above the white-green Unit 2 visible in Figure 4.2.2. The unit consists for the most part of scree covered slopes of mudstones. The sandstone percentage in Unit 3 is estimated to be between 10-20%. A few channel belts exist embedded within the paleosol mudstones, all identified channels in this unit are single-story and unilateral. The width of these channels varies from around 100 meters to over 200 meters. In the virtual outcrop three 4-7-meter-thick channel-sandstones have been identified as shown in Figure 4.2.13 bellow.

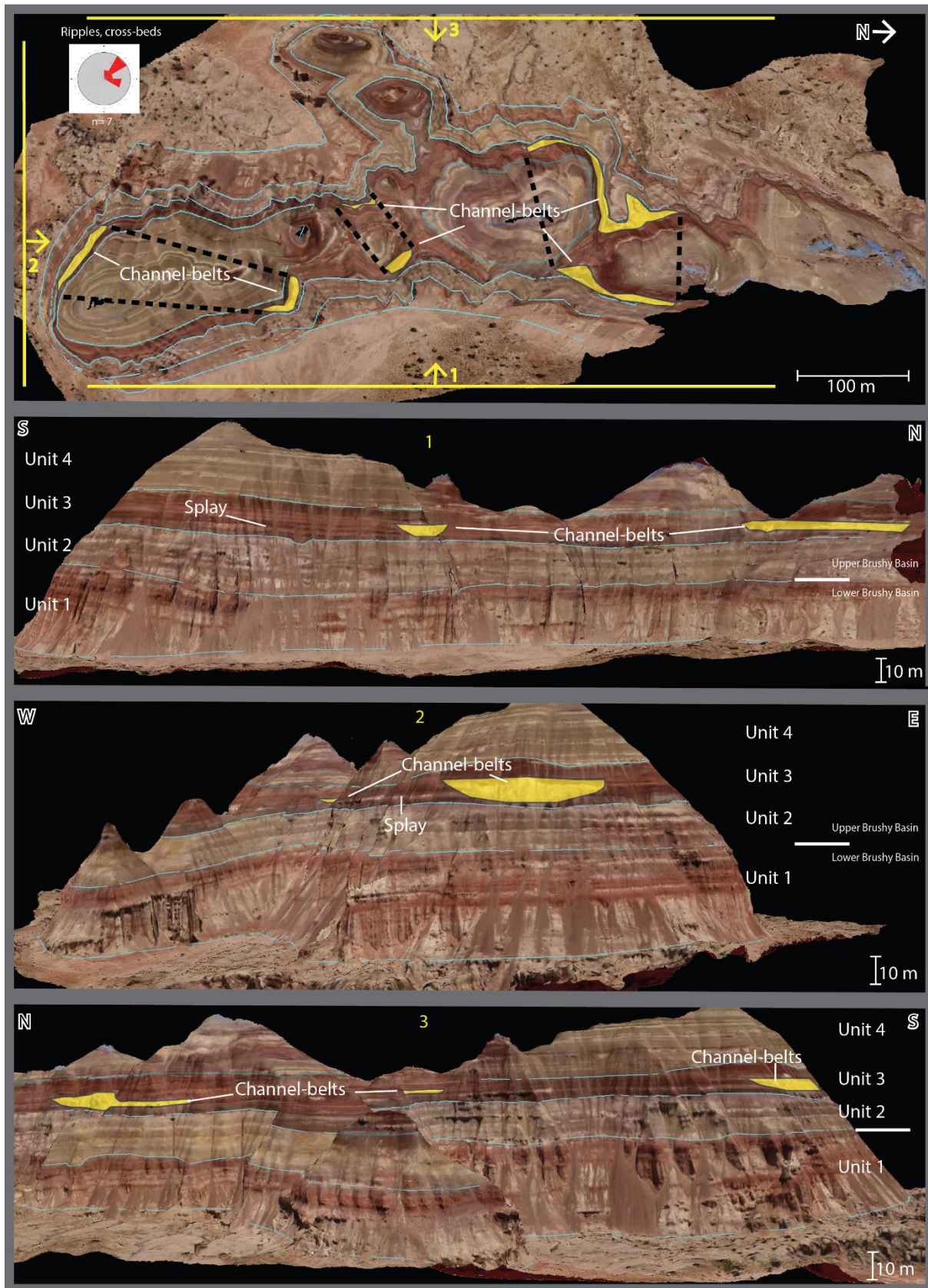


Figure. 4.2.12: Virtual outcrop with channel belts (yellow) in the red-brown mud dominated Unit 3. Crevasse splays and overbank mudstones can be seen on the flanks of the channel belt. Note that the channels are

connected and runs through the outcrop, in on the western side and out on the eastern side. Unidirectional paleocurrent indicators from ripples in the channel sandstones give a north-eastward trend.

The channel sandstones display fining upwards trends with grain sizes ranging from a 40-50 cm thick conglomerate bed at the base, to very-fine sandstone at the top of the channel (Figure 4.1.2.A). Mud-clasts like in the units below are not common, but several extraformational quartz clasts occurs in the foresets of cross-beds. The most common grain size in the channels are very fine and fine sand. Mud draped low angled fining upwards lateral accretion surfaces and passively infilled channels occurs in all observed channels in the unit.

The decrease in channel size, lateral accretion surfaces and mud-plugs (Figure 4.1.2 & 4.2.13) from channel abandonment, paired with the variable grain size composition and increase of overbank mudstone, has been interpreted to mean that the channel-belts were deposited by a sinuous meandering river system in a low gradient setting typical for the medial-to-distal zone of the distributary fluvial system (Nichols and Fisher 2007). The decrease in mud-clasts within the channels and the limited lateral reach of the channel-sandstones could point towards an increase in bank stability and a wetter more vegetated system that confined the channels for the most part (Bridge 2004; Galli, 2014). Laterally extensive sand-layers that thins out into mudstone interpreted as crevasse splays are common, but they are thinner than in the units below. Root traces in the mudstone and in the tops of crevasse splays are common in this unit.

A picture of a typical fine-grained channel-sandstone associated overbank fines and passive infilled mud-plug as described above is shown in Figure 4.2.13.

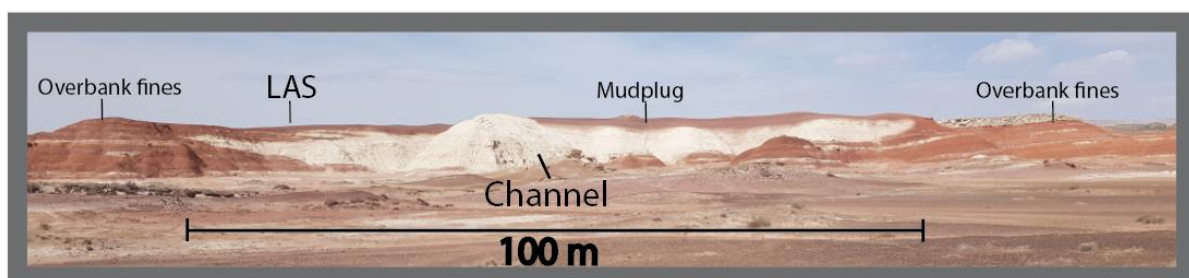


FIG. 4.2.13: White clear channel sandstones embedded in dark-red paleosol and crevasse splays. Note the muddy low angled lateral accretion surfaces that stretches far into the sand body. This channel has a conglomeratic base, but most of the channel fill is fine-to-very fine-grained sandstone. Vertical exaggeration x2

The fluvial system in Unit 3 has been conceptualized in the same style as before (Figure 4.2.14).

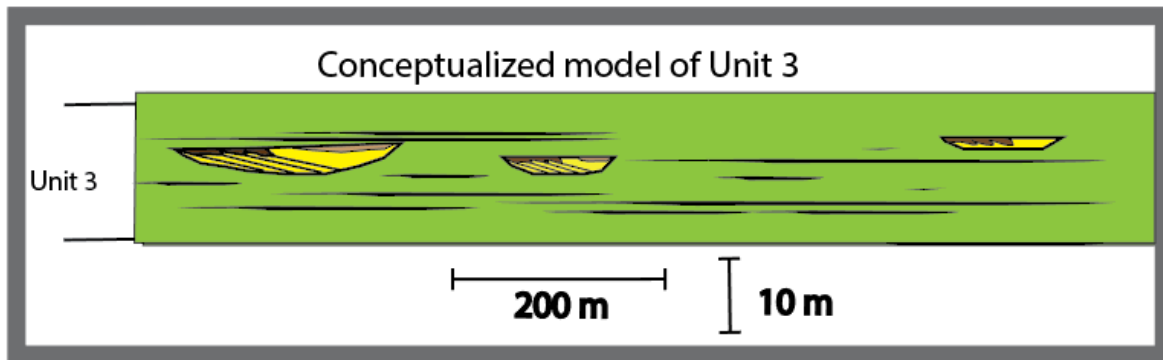


Figure. 4.2.14: Small yellow channels embedded in a package dominated by mudstone. Thin crevasse splays within the mudstone are at the side of the channels are visible as black lines. Muddy low angled lateral accretion surfaces and brown mud-plugs are visible in the channels.

Reservoir aspect Unit 3

Direct sandstone-body connectivity is clearly very poor and a major risk in Unit 3. The sand bodies appear isolated and surrounded by non-reservoir mudstone. No stacked channel-belts was observed in the study location in this unit. The crevasse-splays are extensive and adds to the total volume of sandstone in the system, but they are thin and often thinning out into mudstone.

Unit 4:

Unit 4 is the uppermost 10-25-meter grey succession of weathered and eroded rocks on the top the Virtual outcrop visible on Figure 4.2.2. It is the least studied unit at the study location due to the lack of cliffs and requiring digging to get sections of rock suited for logging. Unit 4 consists predominantly of mudstone and extensive thin layers of very-fine sand interpreted as paleosols, overbank fines and splays. Most of the channels in this unit is between 1-4 meters thick and less than 50 meters wide and appears as smaller ribbon shaped channels. However, two largest channels exist in this unit. They are about 100 meters wide and 4 meters thick and have a conglomeratic base as the channels in Unit 3.

Relative to the other units the amount of channel sand-bodies is very low. The sandstone percentage in this unit is estimated to be between 5-15%. The smaller channels are very fine grained with high mud content but no mud- or extraformational clasts from erosion and bank collapse occurs as in the other units. Few bedforms are visible in the channel-sandstone deposits, but measurements of 3 current ripples indicate an eastward

paleocurrent direction. No lateral accretion surfaces were identified in the channels hence the degree of sinuosity of the channels are unknown.

At two levels in the unit 20-40-centimetre-thick carbonate layers form benches that are easily mistaken for crevasse splays in the virtual outcrop. These beds have been identified as lacustrine micrite limestones deposited in conjunction with several major zones of altered silicic ash falls (Galli, 2014; Parrish et al., 2004). The fluvial system at the time is thought to have been low gradient, decreasing accommodation setting with a relatively high-water table (Demko et al., 2004; Turner & Peterson 2004; Galli, 2014).

In terms of proximal, medial and distal zones in a distributary fluvial system Unit 4 is interpreted to resemble the distal zone with thin isolated small channels and a high mudstone percentage.

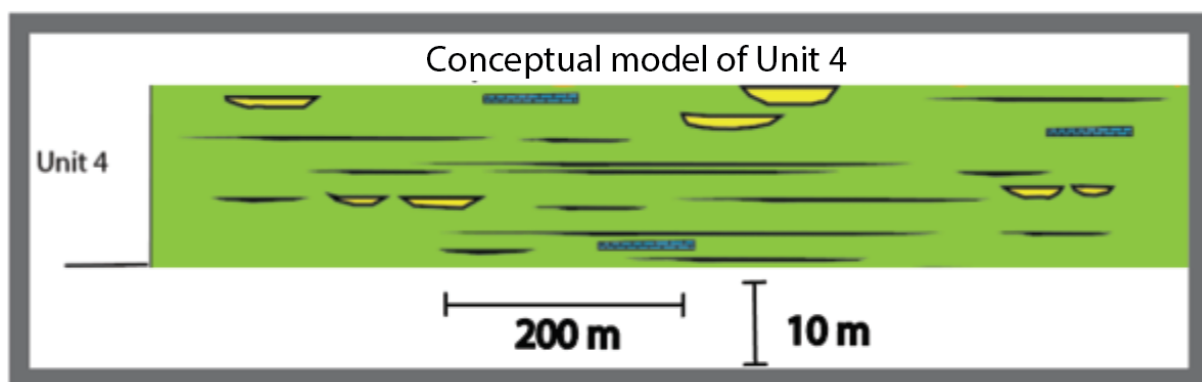


Figure 4.2.15: Conceptual model of Unit 4. Small isolated ribbon channels. Thin crevasse-splays and abundant mudstone. Occasional lacustrine limestones.

4.2.5 The conceptual model put together, summary of results.

The lithologies, facies associations and the vertical changes described in Chapter 4.1 & 4.2 have been put into one complete conceptual model of the Brushy Basin member (Figure 4.2.16). This model summarizes the major vertical changes that is of interest when building the reservoir model of the Brushy Basin Member mud-rich fluvial system.

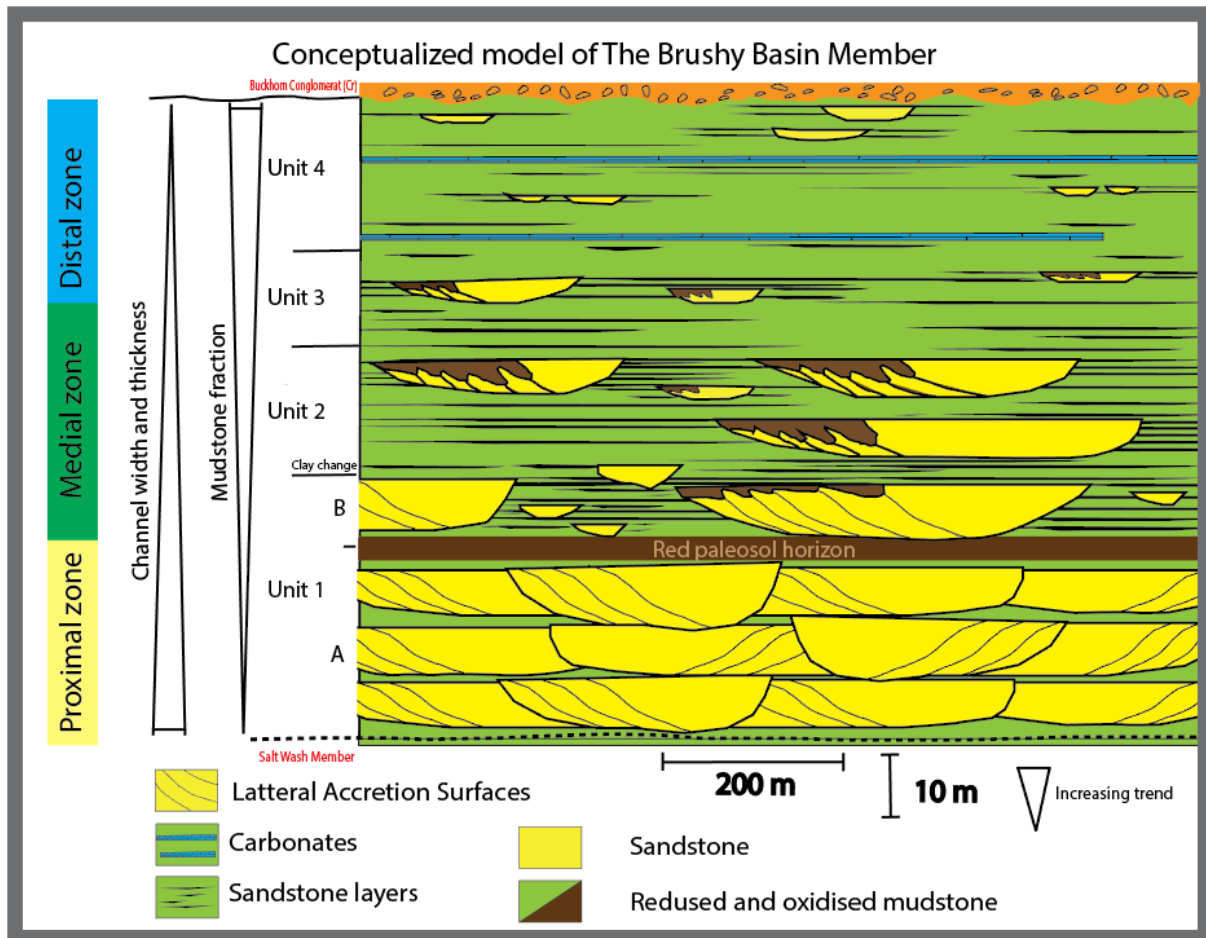


Figure 4.2.16: Conceptual model of the Brushy Basin Member. The figure summarizes the lateral and vertical changes presented in Chapter 4.2. Note the DFS zones, channel width and thickness trend and mudstone fraction trend. The reservoir model in Chapter 4.3 is based on the conceptual model. The important changes illustrated in the figure are listed below.

Vertical changes upward in the conceptual model:

- Less sand-more mud, less channels more floodplain (Table 4.3.1)
- Channel-belts get thinner and smaller (Table 4.3.2)
- Internal channel-fill heterogeneity increases (mud-draped LAS and conglomeratic sandstones)
- Small channels generally finer grained than the larger, exception conglomeratic small channel in Unit 4.
- Less vertical and horizontal direct communication between channel belts
- Lacustrine deposits towards the top. (probably also in unit 3 and possibly unit 2 but this was not identified in the field (Galli,2014).
- Thickness and frequency of crevasse-splays decrease from Unit 1B-Unit 4. Mapping of crevasse-splays in Unit 1A was not possible.

- Palosols generally less developed. (Generally, well developed in Unit 1, poor to moderately developed in Unit 2-4 (Demko et al., 2004; Galli, 2014).

4.3 Reservoir model, Brushy Basin Member

Chapter 4.3 will present the gridded geological reservoir model of the scanned and studied outcrop.

The model has been constructed in Petrel by importing interpreted lines from the virtual outcrop in Lime and incorporate the observation and vertical changes presented in the conceptual mode in Chapter 4.2.5. This results in a model which represent an actual mudstone-rich fluvial system found in the geological record. For a detailed explanation of the steps performed to create the model see Chapter 3.0 Methods where this is covered.

The facies associations described in Chapter 4.1 have been simplified into three facies association in the reservoir model: 1. Channel-sandstone 2. Crevasse-splays. 3. Shale mudstone(overbank/non-reservoir). Numerical data used in order to construct the model and a short description of the units will be presented in Table 4.3.1 below. The amount of sandstone in each unit have been calculated using ImageJ on the virtual outcrop photos. Above Unit 4 and below Unit 1A confining zones of shale have been added to represent homogeneous layers that will not influence the flow simulation. The boundaries between units are conformable, but channels are allowed to erode downwards. The length (Y-axis) of the model is 1500 meters while the width (X-axis) is 1000 meter. Hight (Z-axis) is 142 meters. Total number of grid cells in the model is 1 841 250. No faults exist in the model, but a slight N-S trending folding is added from the virtual-outcrop.

Table 4.3.1 Reservoir modelling properties

Unit	Channel thickness	Channel belt width	Orientation	Sandstone (%)	Description
1A	8-12	>500	0-30	60-80	Stochastic object modelling. Shale background with amalgamating fluvial channel bodies, isolated areas of mud exists in the Unit. They represent channel abandonment fills and overbank muds. Crevasse-splays extend from channel-bodies with a thickness similar to that observed in the field: between 0.1 cm and 1 m.
1B	8-12	400-500	0-30	40-60	As Unit 1A
2	6-9	100-400	70-90	15-30	Stochastic object modelling. Shale background with large fluvial channel bodies encased in mudstone and crevasse-splays inserted. Some amalgamation occurs.
3	4-7	100-200	80-90	10-20	Stochastic object modelling. Isolated smaller channels with few instances of channel to channel connectivity. Crevasse-splays primary connection between sand-bodies.
4	1-4	<100	90	5-10	Stochastic object modelling. Completely isolated channels, no amalgamation, little connectivity between channel-bodes through crevasse-splays.

Screenshots of the model in X, Y and Z direction is shown in Figure 4.3.1 below. Two wells have been added in the model for flow simulation purposes.

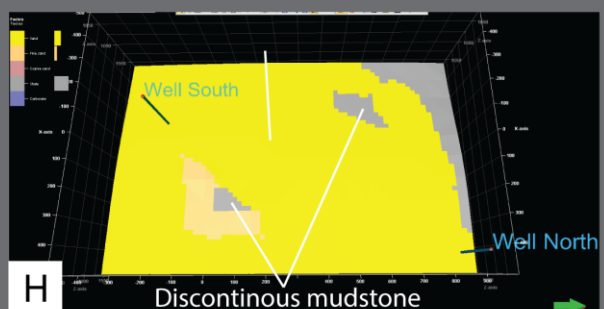
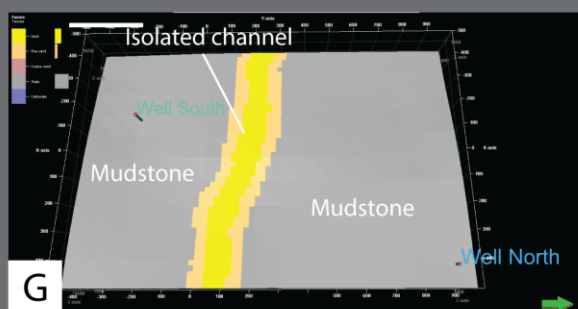
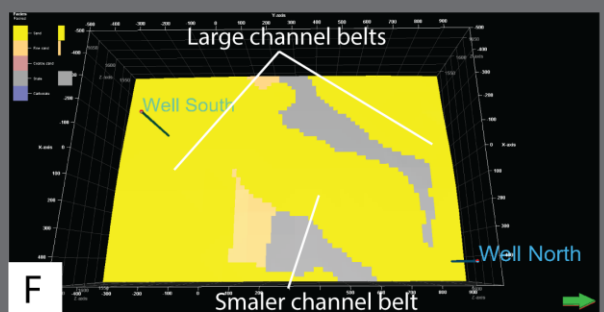
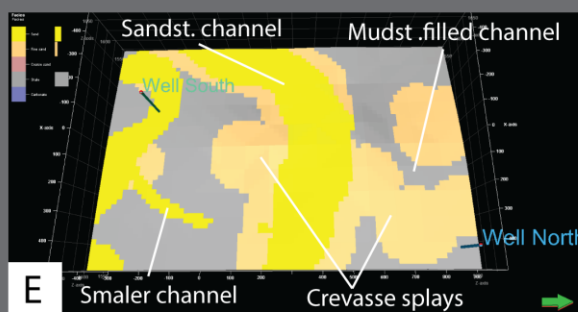
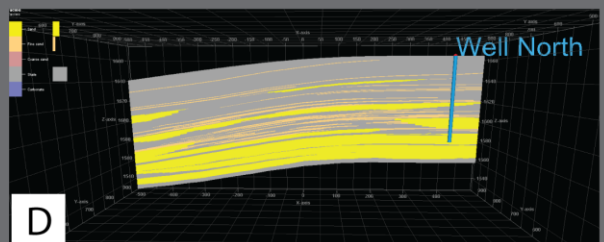
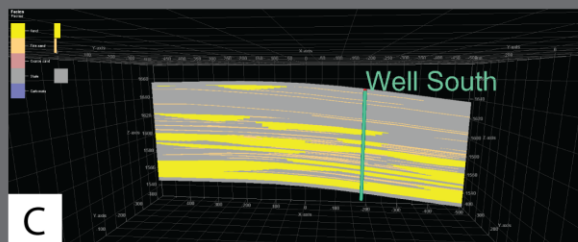
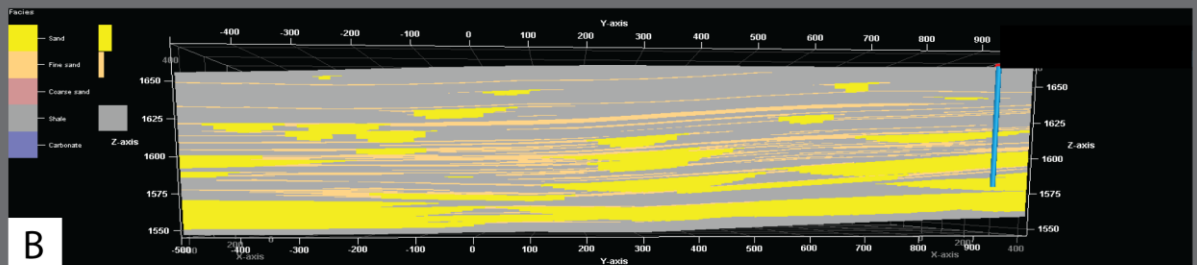
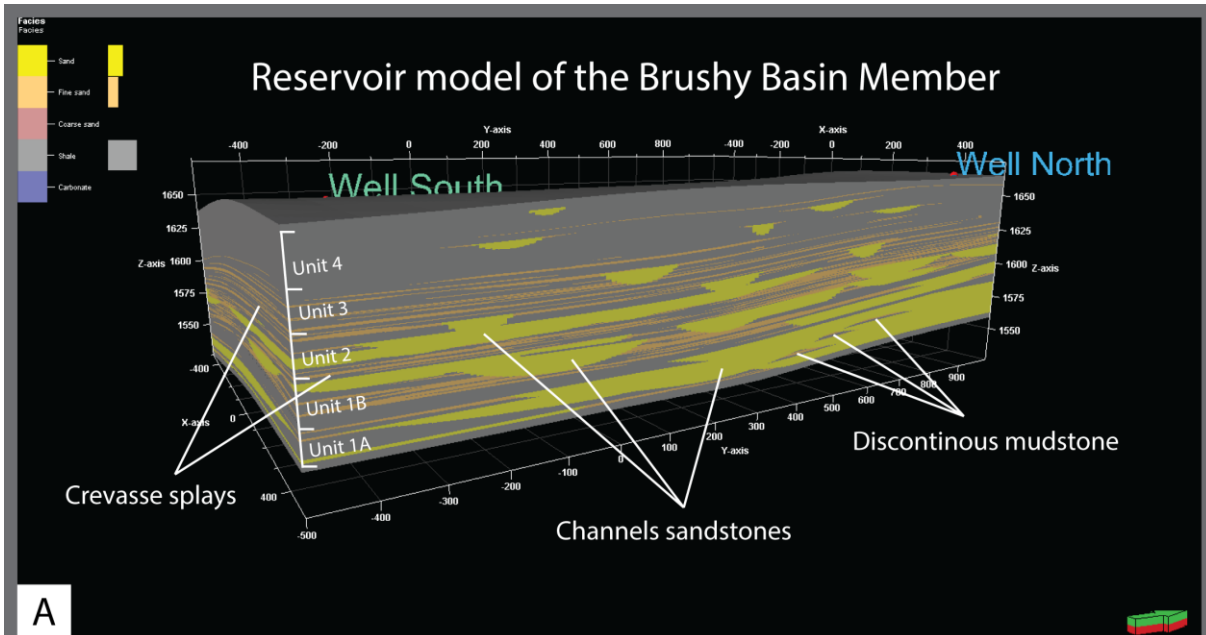


Figure 4.3.1: Reservoir model of the Brushy Basin Member built in Petrel. A) Three-dimensional view of the model with annotations showing the Units presented in chapter 4.2. Channel sandstone in yellow, crevasse-splay sandstone in orange and mudstone in grey. The decrease in the amount of sandstone upwards are clearly visible. In Unit 1 and 2 discontinuous mudstone layers are common, while in Unit 3 and 4 the thickness and continuity of the mudstone layers increases, while the thickness and width of the channels decrease upwards B) Westward cross-section of the model. C) Southward cross-section of the model. D) Northward cross-section of the model. E) Horizontal cross-section of Unit 2 showing eastbound channels with associated crevasse splays, smaller channels and mud-filled channels. F,H) Horizontal cross-section of Unit 1B and 1A with northeast trending amalgamating channels with discontinues bodies of mudstone. G) Horizontal cross-section of Unit 4 showing an east-trending isolated channel.

4.4 Flow simulation

The reservoir model presented in Chapter 4.3 was exported from Petrel, imported to the RMS software and run through a cell-based flow simulation. Chapter 4.4 contains the results from this simulation.

Cell-based flow simulation gives detailed information about production results like hydrocarbon production rate, water production rate, water cut, total fluids produces and how this change over time (RMS manual). Conducting a flow simulation on the Brushy Basin Member reservoir model created in this thesis will give interesting results as the model is constructed with empirical basis in an actual observable reservoir package where the channel-reservoir are typically separated from each other. The reservoir model, as previously shown, contains several units with varying sandstone mudstone percentages, channel-to-channel interconnectivity and a channel-belt architecture that changes dramatically from base to top. This mean that flow simulating the model will gives us an idea of how fluid flow changes depending on channel-belt connectivity in a mudstone-rich system like the Brushy Basin Member.

Petrophysical properties like porosity and permeability used in the model is real data from Barents Sea core plugs. Which were taken from Line et al., (2018) study of reservoir quality of fluvial channels in the Snadd formation. The data is sampled from wells located on the Loppa High, Bjarmeland Platform, Fingerdjupet Sub-Basin and the Nordkapp Basin giving a good representation of the petrophysical properties that can be expected in a mudstone-rich fluvial system.

The petrophysical properties that are used in the reservoir modelling is shown in Table 4.4.1.

Table 4.4.1 Facies and petrophysical properties

Facies	Porosity	Horizontal perm. (mD)	Vertical perm. (mD)
Channels (vf-c sand)	32	1100	900
Crevasse-splays (vf-m sand)	15	250	10
Overbank (Paleosol/mud)	0.1	0.1	0.01

A selection of the channel data taken from Lina et al., 2018 gives a Kv/kh: 0.8, close to Deveugle et al., (2011) who found a Kv/kh: 0.9 in distributary fluvial channels. For the purpose of this study a kv/kh: 0.8 is within the margin of reasonable relationship between horizontal and vertical permeability.

Table 4.4.2 Reservoir modelling parameters for fluid flow simulation

Modelling parameters	Value
Rock compressibility	$10 \cdot 10^{-7}$ /bar
Fluid compressibility	$10 \cdot 10^4$ /bar
Temperature	121 °C
Oil saturation ratio	0.8
OWC	-1545 m
Min. depth	-1660 m
Max depth	-1545 m
Simulation time	50 years
Injection rate	1000 m ³ /d
Model size	1.5 km ²
Reference pressure	150 bar
Injector pressure	175 bar
Producer pressure	130 bar
Viscosity	5 cP

The parameters used for the cell-based flow simulation are presented in Table 4.4.2. Two scenarios were simulated, S1 and S2. In scenario S1 the three facies shown in Table 4.4.1 were all present, while in scenario S2 the crevasse-splays was removed and replaced by non-reservoir rock. In terms of total reservoir pore volume, removing the crevasse splays

decrease the total pore volume in the reservoir model by 17%, meaning that 83% of the pore volume can be found in the channel sandstones. Both scenario S1 and S2 had the same production strategy. Two wells are drilled in the model, well South and well North. Both wells penetrate major channel bodies in the reservoir model and have been placed in the south western and north-eastern corners respectively. Well South reached the OWC at 1536m downdip from well North. Well South is the designated injector, while well North is the producer. Both wells are perforated in the 142-meter reservoir interval, meaning that production and injection happens in all Units in the reservoir model. A cross-section from well-to-well which display the facies distribution in the model that are simulated is visible in Figure 4.4.1.

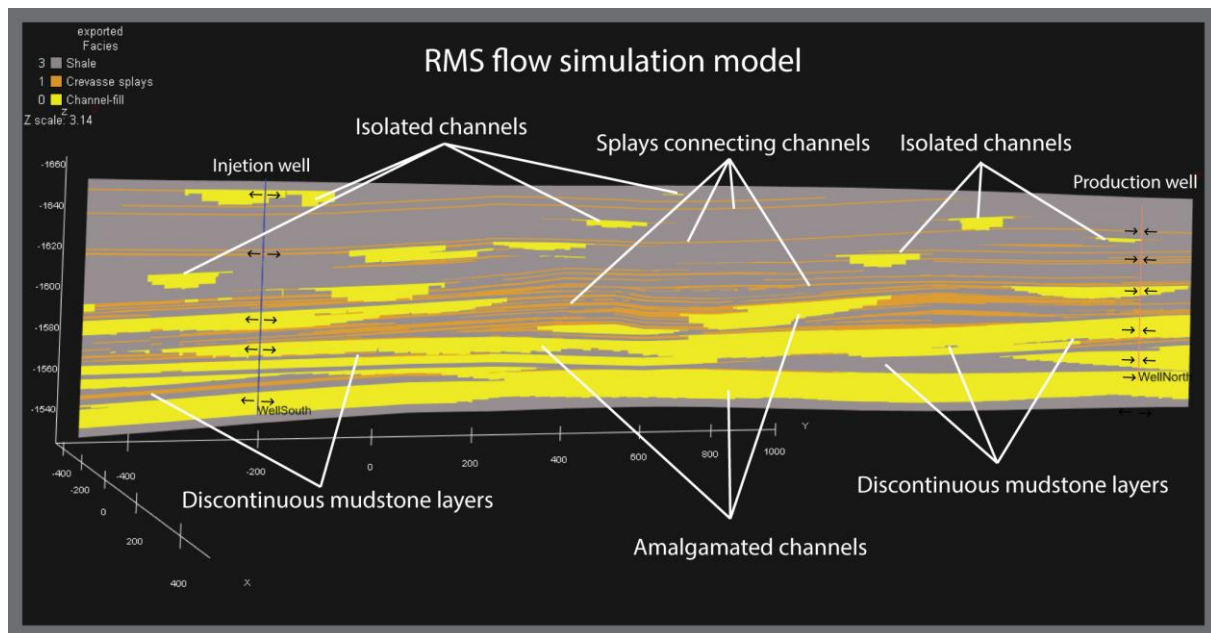


Figure 4.4.1: Well-to-well cross-section of the flow simulation model in RMS. The same features as the

The cell-based flow simulation in S1 and S2 simulates 50 years of production. Both simulation-runs took over 90 hours to complete. Screenshots from the runs are presented in Figure 4.4.2, where oil is represented by black colour, and increasing water percentages in each cell is represented by a progressively white colour. The pore volumes in the model is filled with oil down to the OWC prior to production start (Figure 4.4.2.A & F). Screenshots from S1 production after 10 years (Figure 4.4.2.B), water breakthrough (Figure 4.4.2.C),

water cut 50% (Figure 4.4.2.D), and water cut > 90 (Figure 4.4.2.E) are shown in the figure below. The production in S2 declines faster and water breakthrough is reached at an earlier stage (Figure 4.4.2.G). Consequently, production with a water cut of 50% (Figure 4.4.2.H) and water cut > 90 % (Figure 4.4.2.I) also happens at an earlier stage than in S1.

The flow simulation results from scenario S1 show that the lower units with amalgamated channels are swept relatively evenly and earlier than the upper units. The discontinuous overbank mudstone-layers (Figure 4.4.1) that exists in this part of the model, act as vertical barriers for the most part. But, where the mudstone is particularly thin communication between the channels occur (Figure 4.2.2.B). As time passes, breakthrough of injection-water happens within the lower parts of the model long before water is produced in the upper part of the model. In the upper part of the model, oil in the channels have to migrate through the low permeability crevasse splays in order to reach the production well. The simulation show that this is often the case and that the injected water follows the crevasse-splays and sweeps the non-amalgamated otherwise isolated channels. Where the crevasse-splays are not in connection and the channels are completely isolated and surrounded by overbank mudstone, the oil is bypassed (Figure. 4.4.2.E).

The results from scenario S2 show that breakthrough of water in the lower part of the model happens 4 years earlier (Figure 4.4.2.G). Production in the lower units are seemingly otherwise not affected by the lack of splays. This is not the case in the upper part of the model. The channel sandstones that was accessible through crevasse-splays in scenario S1 are not swept in scenario S2 (Figure 4.2.2 H-I), subsequently less oil is produced (Figure 4.2.3).

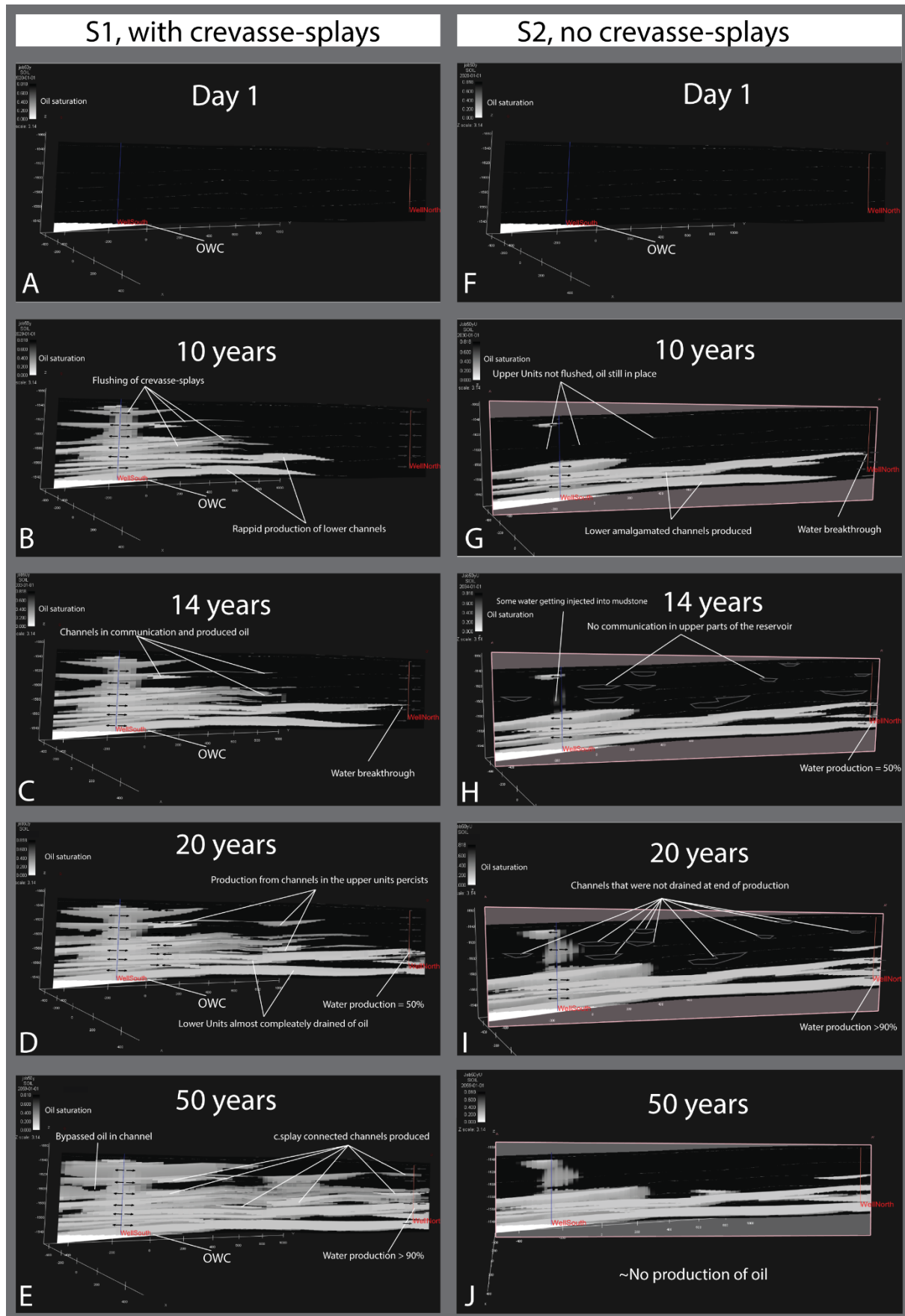


Figure 4.4.2: Results of flow simulations. A, F) The reservoir filled with oil prior to production. The Oil-water contact is visible at the lower left side. B) Oil saturation distribution after 10 years of production. Note the

efficient sweep of the amalgamated channels in the lower part of the model (Unit 1). Injected water is also sweeping crevasse splays in the upper part of the model (Unit 2-4). C) Oil saturation distribution after 14 years. At this time water from the injection well are produced at the production well resulting in decreasing oil production rate. D) Oil saturation distribution after 20 years. Most of the oil in the lower unit are already produced. The production water-cut is now 50%. Crevasse-splays and isolated channels in the upper part of the reservoir are still being produced. E) Oil saturation distribution after 40 years. Most of the channels and crevasse-splays have been swept, however the cells still have substantial amounts of oil in them (40-50%). Note bypassed oil in certain channels. G) Oil saturation distribution of scenario S2 after 10 years. Water breakthrough happens 4 years earlier then scenario S1. Seemingly no production from upper parts of the reservoir. H) Oil saturation distribution of scenario S2 after 14 years. Still no flow in the upper part of the reservoir. Production mainly from amalgamated now waterfilled channels. Water production hits 50%. I) Oil saturation distribution of scenario S2 after 30 years. Some water is injected into the mudstone near the injector. Most of the channels in the upper part of the model is not swept.

Production results (rate and total) from both simulations are plotted in Figure 4.2.3 and summarised below.

The total volume of oil in scenario S1 is 13 250 200 m³. After 50 years 7 871 575,5 m³ is produced, meaning that 59% of the oil originally in place is recovered. In scenario S2 11 016 200 m³ was originally in place in the reservoir. After 50 years of production 5 980 065 m³ of oil is produced, resulting in 54% of the originally in place oil being recovered.

The total volume of oil originally in place in the crevasse-splays in scenario S1 is 2 234 000 m³. Splays therefore make up 17% of the oil originally in place while 83% of the oil is situated in channels. In scenario S1 a total of 31.6% more oil is produced, clearly indicating sweep of channels that depend on crevasse-splays to get produced. When adjusted for the decrease in total oil volume originally in place when removing the crevasse splays in scenario S2, scenario S1 result in a 5% increase in recovered resources.

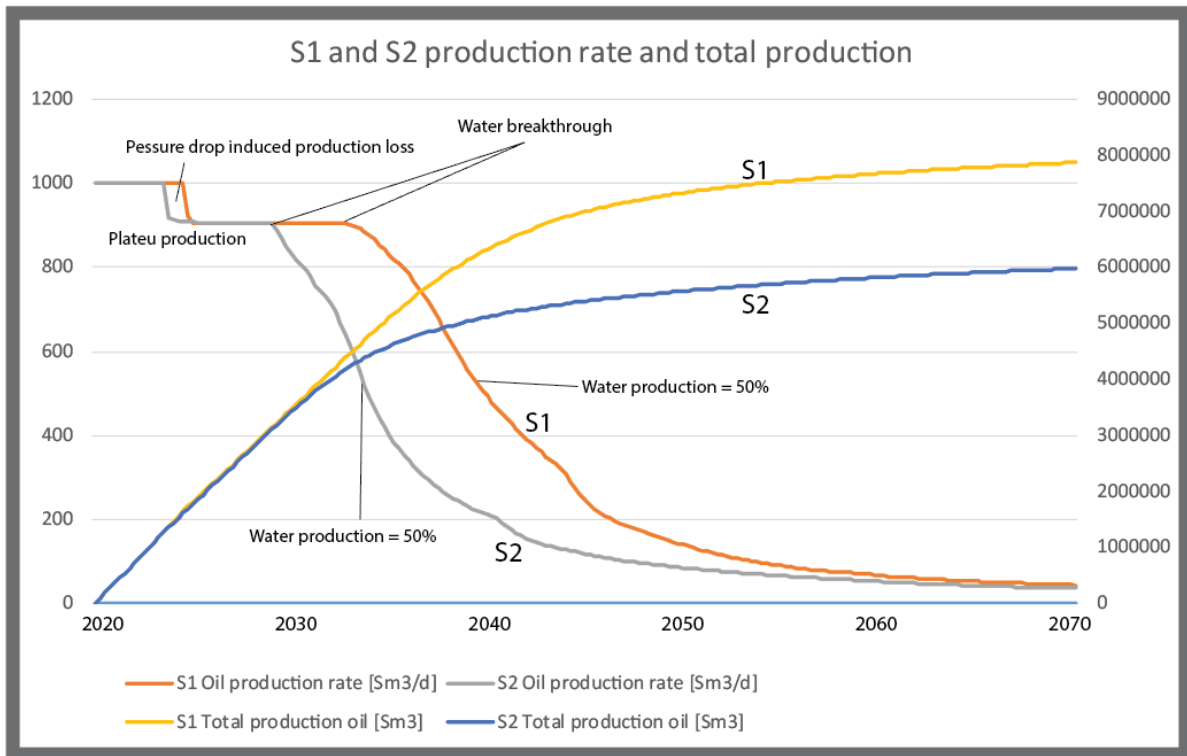


Figure 4.2.3: Production rate and total volume of oil produced plotted against time (years).

Given the production number visible and the graph above it is reasonable to suggest that the crevasse splays contributes to keeping oil production levels high in scenario S1 compared to scenario S2 (Figure 4.2.3).

5.0 Discussion

The purpose of this chapter is to discuss the results presented in Chapter 4. This is mainly done by: 1) Addressing how the upwards variability of facies at the study area relates to the regional fluvial system, 2) Consider the importance of crevasse-splays in the reservoir model revealed during the simulation runs, and 3) how sub-seismic smaller channels could represent a possible upside for exploration in similar mudstone-rich systems (low net-gross systems) such as those in the Triassic of the Barents Sea.

5.1 The Brushy Basin Member distributary fluvial system

A review of more than 700 continental sedimentary basin conclude that fluvial depositional landscapes are dominated by distributary systems, with tributary axial and incised river deposits composing a relatively minor proportion of the continental rock record (Weissmann et al., 2010). The Salt Wash Member, stratigraphically below the Brushy Basin Member, consist if a distributary fluvial system representing deposition from a single fluvial system (Owen et al., 2015,2015). The Salt Wash Member and the Brushy Basin Member was deposited in the same paleogeographic setting, with relatively similar basin-conditions and tectonic framework. It is therefore reasonable to suggest that the Brushy Basin fluvial system also is a distributary fluvial system.

Evident from the conceptual model and summary of vertical changes in Chapter 4, the overall sandstone ratio, channel width and channel thickness decrease upwards in the succession (Figure 4.4). The change is pretty dramatic from Unit 1 to Unit 4, going from sandstone ratios above 50% with amalgamating-multistorey channel-sandstones, to sandstone percentage less than 15% with isolated channel fill deposits encased in stacked paleosols and floodplain deposits. Channel-belt-thickness decreases from 14 m to around 1 m.

This trend is completely opposite of what have been found in the upwards increase in sandstone percentage (from 70% in the proximal facies to 8% in the distal facies) and channel-belt-width in the Salt Wash Member distributary fluvial system (Owen et al., 2015). This system has been interpreted as a prograding system with stacked distal-to-medial-to-

proximal facies (Figure 5.1.1) (e.g. Peterson, 1980,1984; Currie 1998; Kjemperud et al., 2008; Weissmann et al., 2014; Owen et al., 2015,2017).

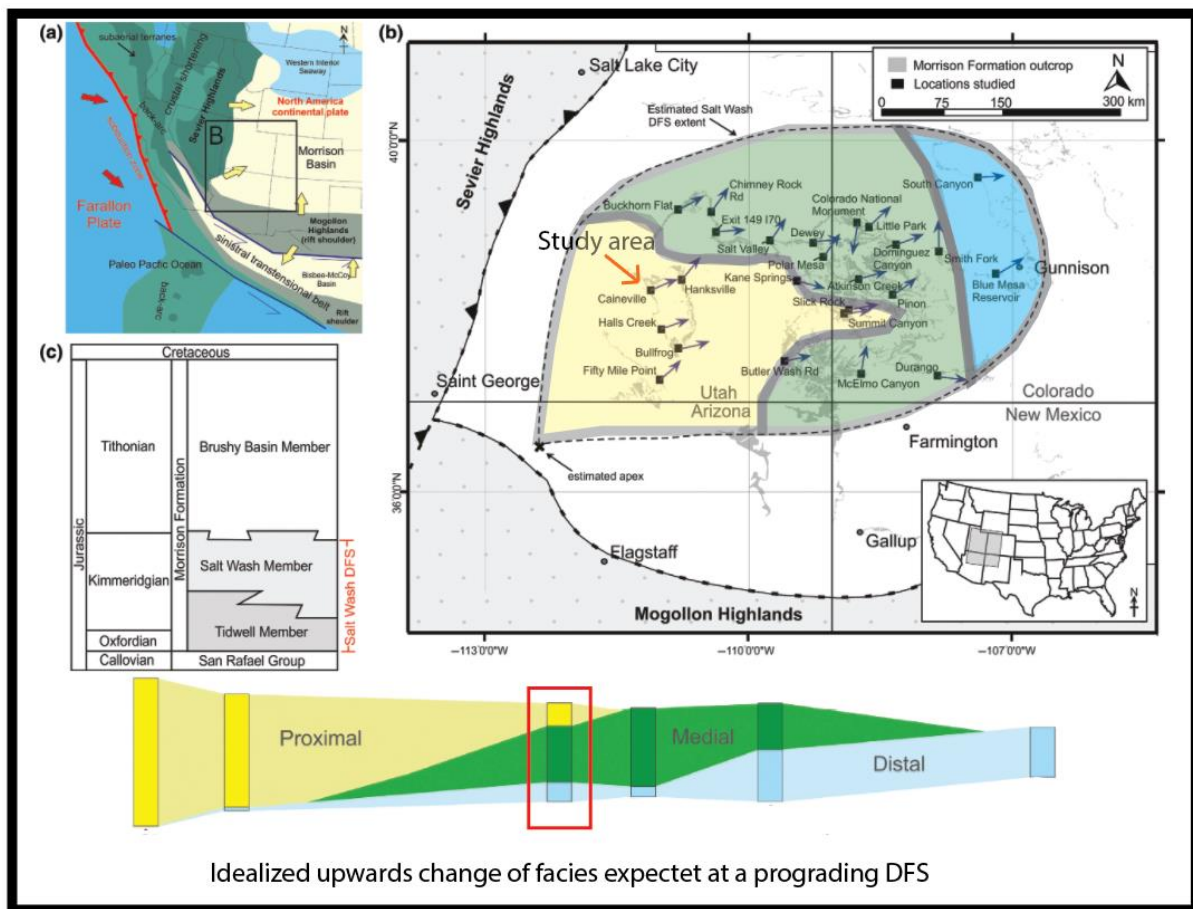


Figure 5.1.1: Location maps of the Salt Wash Member DFS uncovered by Owen et al., (2015). (a) Tectonic framework of the Late Jurassic during the deposition of the Morrison. Modified from Turner & Peterson (2004) and Blakey (2014). (b) Location map of the study area. Blue arrows indicate mean palaeocurrent direction at localities studied by Owen et al., 2017. Yellow, green and blue colour correspond to proximal, medial and distal facies in the idealized upward changes of facies from a prograding DFS visible below the map (c) Stratigraphic framework of the Salt Wash DFS relative to the Brushy Basin DFS. (modified from Owen et al., 2015)

The Brushy Basin Member itself have been described as both aggregational and progradational, with relatively long periods of little or no deposition at all (Currie, 1998, Demko et al., 2004). The observations at the study area does not fully comply with a progradational description.

If put into a distributary fluvial system facies model (proximal, medial, distal facies) Unit 1 and perhaps Unit 2 both resembles proximal to medial facies with interconnected amalgamating channels and relatively high sand-percentage, while Unit 3 and 4 can be characterized as typical distal facies with low sand-percentage and isolated (ribbon) channels (Nichols and Fisher, 2007). The vertical change from high to low sand-ratio and high to low

channel connection found at the study location therefore does not imply a typical prograding distributary fluvial system (Nichols and Fisher, 2007). Based on the observations revealed in the results chapter the succession at the study location could however indicate a retrograding distributary fluvial system.

An interesting question that follows from this is whether the observed trends in the study area is a local feature, or expresses the actual regional fluvial system. The combination of allocyclic and autocyclic controlling factors in a basin system can be responsible for any observed sedimentary succession variations, which makes this a very complex question (Ethridge et al., 1998, Miall, 2000; Owen et al., 2015). The intricate relationship between the controlling mechanisms that affect a fluvial system dictates sedimentary succession both locally and basin wide (Owen et al., 2015). Allocyclic controls work on the system as well as outside the system, controls like eustasy, tectonics and climate are termed allocyclic. Whereas controls which work within the system on a smaller scale like avulsion of streams, migration of bars and local changes in topography are termed autocyclic (Allen, 1971; Ethridge et al., 1998; Miall, 2000; Cecil, 2003).

The deposition of the Brushy Basin Member, like in the Salt Wash distributary fluvial system, probably was driven by upstream controls in the catchment (Owen et al., 2015). Eustasy, due to the distance from sea, is in this particular case disregarded as a major control, leaving climate, source area and basin subsidence as the dominant external controls (Shanley & McCabe, 1994). Overall accommodation in the basin is believed to have been increasing upwards in the Brushy Basin Member until the very end of the Member where the rate of accommodation declined until sedimentation stopped (Demko et al., 2004). It is reasonable so suggest that accumulation of large shallow lakes and wetlands in the Upper and eastern part of the Brushy Basin Member had a significant impact on the distributary fluvial system prograding, retrograding or aggrading (Demko et al., 2004, Turner & Peterson 2004). Expansion of a lacustrine wetland and accumulation of sediment and water in the basin could have forced the Brushy Basin distributary fluvial system to retrograde, either by movement of apex away from the lakes or simply by a shortening of the rivers leading out to the lakes.

The upwards trend observed at the study area could also just be a local feature and does not need to indicate whether the system as a whole is retrograding or aggrading. Instead, 1) The

succession could represent channel-deposits from two or more distributary fluvial fans partly or completely overlapping. The upper and lower parts of the model show differences in paleocurrent measurements orientation from ripples and cross-beds, and difference in channel-belt orientation visible from interpreting the virtual outcrop. The lower unit have measurements trending towards the north, while the measurements of the upper units are trending towards the east. A change in fluvial regime by paleocurrent measurements upwards in the Brushy Basin Member have also been identified by Galli et al., (2014) in different location of the basin, and could indicate that the basin was populated by multiple distributary fluvial systems (Figure 5.1.2).

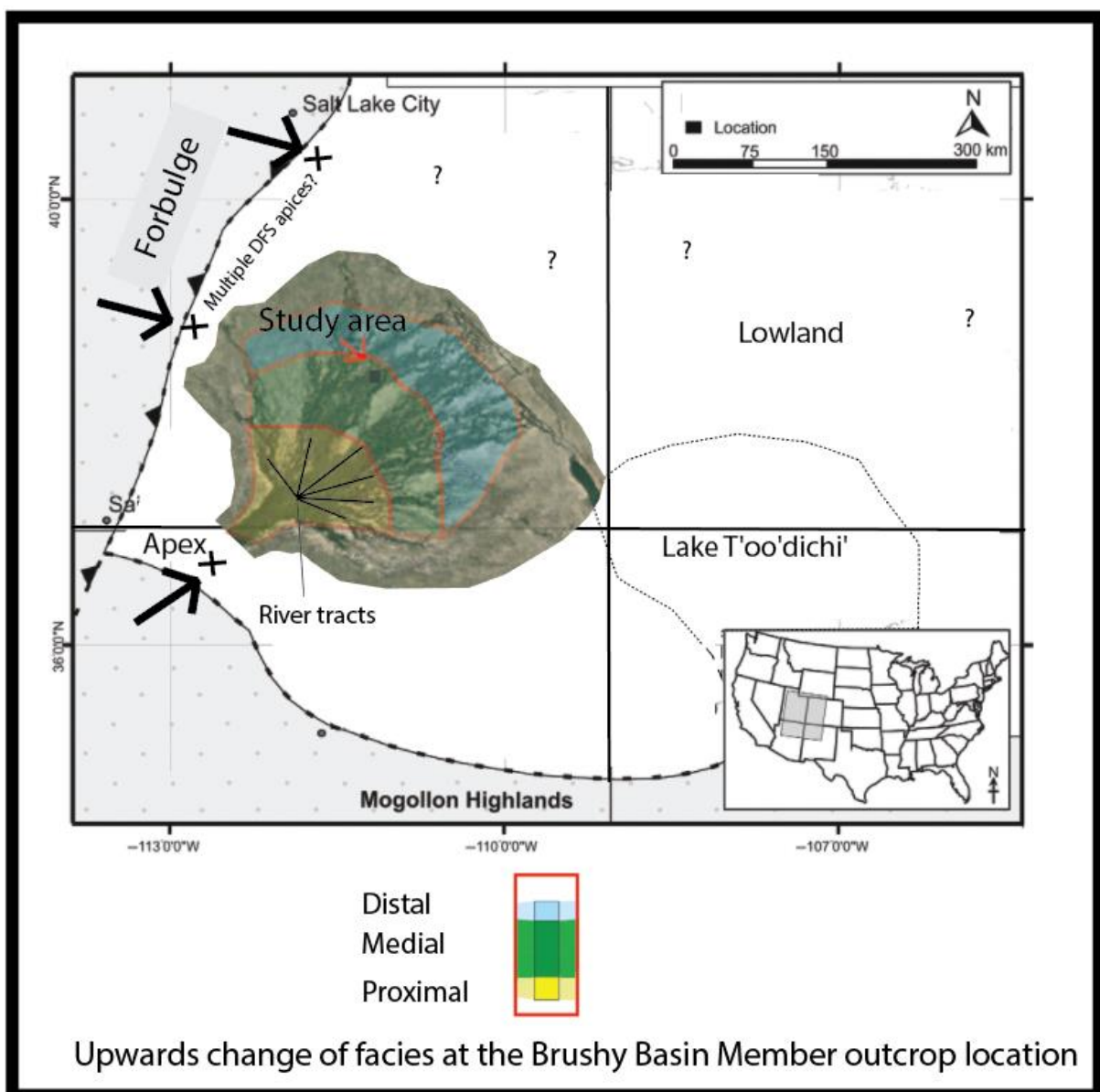


Figure 5.1.2: Map illustrating the distributary fluvial system that could have deposited the successions visible at the study area. The Okavango delta, Botswana, distributary system has been added to illustrate the

depositional setting of the Brushy Basin Member. The location of the DFS are purely illustrative, additional research is needed to establish the apex and reach of the system. The upward changes of facies are opposite of what is visible in the Salt Wash Member distributary fluvial system. River tracts are drawn on the Okavango delta. Apices for multiple eastward going distributary fluvial systems in the late Brushy Basin Member are indicated by crosses. (modified from Owen et al., 2015)

2) Alternatively, the upwards changes are not due to two different distributary fluvial systems but rather a consequent of the system avulsing, changing river tracts and moving away from the study area (Figure 5.1.2) (Nichols and Fisher, 2007). Distributary fluvial systems are constructed through avulsions of channel-belts across the sedimentary basin (compensational-stacking) (Nichols & Fisher, 2007; Weissmann et al., 2010; Buehler et al., 2011), leading avulsion as a key autocyclic process during the formation of distributary fluvial systems (Owen et al., 2015). Avulsion upstream may have been facilitated by massive increase of volcanoclastic sediment following the volcanic activity in the south-east resulting in a change in the amount of sediment entering the basin, changing the channel-pattern and geometry (Galli et al., 2014). Numerous studies have suggested that raise in rates of sediment supply can increase rates of avulsion frequency in a fluvial basin (e.g., Wright and Marriott, 1993; Mackey and Bridge, 1995; Heller and Paola, 1996; Kraus, 2002; Mack and Madoff, 2005; Lepre, 2017). More specific, sediment supply caused by explosive vulcanism have been linked to increase topographic relief of channels above the floodplain and increased avulsion frequency, aggradation and mud (Allen & Fielding, 2007, Lepre 2017).

Interestingly even though the net to gross ratio and channel-belt size decrease upwards, thicker conglomeratic sandstones are present mainly in the upper part of the member, proving that despite the increase in volcanic mud, the stream had high competence and where able to transport not only fine material but also bigger clasts right before the end of Jurassic deposition in the basin (Bridge, 2004; Demko et al., 2004; Boggs, 2014). This also complicates whether the upper Units really represent distal or proximal facies within the Brushy Basin Member distributary fluvial system. The upwards changes could be a reaction to the sediment input from the source area becoming increasingly mud-dominated.

If the succession studied in this thesis is from a retrograding distributary system, it will be one of the first reported cases of this and a possible interesting analogue to subsurface exploration. The changes observed in the study area could be the signature of an aggrading and retrograding system or be explained by different autogenic and allogenic controls as discussed. To infer locally observed trends and project the findings on a basin wide system

could lead to a false representation of reality (Kukulski et al., 2013). A spatial coverage of studies is needed to avoid false reconstruction of depositional architecture from local to basin scale (Owen et al., 2015, 2015). Therefore, without additional research spatially analysing a much larger area, confidently establishing whether the Brushy Basin Member is prograding, retrograding or aggrading, or if the observed trend is a local feature, is not possible in this thesis.

5.2 The Brushy Basin Reservoir model

5.2.1 Connectivity within the reservoir model

As stated in the introduction a key part of this thesis was to make a reservoir model of the fluvial system in Brushy Basin Member. The fluvial system investigated in this study has an average sandstone content less than 30%. Had it not been for the lowermost unit high sandstone content, the percentage would be even lower as other studied have found sand percentages between 5-20% (Demko et al., 2004; Galli, 2014). Evidently a system like this have a high degree of heterogeneity and a low net/gross ratio which puts the Brushy Basin fluvial system firmly into what could be called a mudstone-rich fluvial system. Compared to sandstone-rich fluvial systems where sandstone ratio could be above 80% (Galloway and Hobday, 1996). The most striking results from the modelling this heterogeneous mudstone rich fluvial system is the importance of crevasse-splays for flow especially in the upper mudstone-rich part of the model. Crevasse-splays are well documented part of a meandering low gradient fluvial system that are genetically related to the channel that sourced them (Stouthamer and Berendsen, 2001; Bridge, 2003; Boggs 2014). Their presence is therefore to be expected in most similar fluvial systems. The simulations in this thesis show that the most efficient flow happens where point bars are connected and work as conduit between channel belt sandstone bodies, this is mainly the case in Unit 1. However, the simulation also shows that connectivity between channels with little or no direct contact with other channels (Unit 2-4) can be established through crevasse splays. In the simulation crevasse splays account for a 5% increase in production from establishing connectivity with otherwise isolated channels. Due to time constraints, modelling of mud draped lateral accretion surfaces, and mudclast- lags that existed in almost all channels in the succession was not considered in this thesis. It could have reduced connectivity and

increased compartmentalisation within the reservoir, lowering the production results (Doyle and Sweet, 1995; Chapin and Mayer, 1991; Larue and Joseph, 2006; Willis and Tang, 2010).

Previous research that evaluate the impact of crevasse splays on reservoir connectivity have given results that align with the results from our simulation (Pranter., et al 2013; Stuart et., al 2014; Toorenenburg., et al 2016). Reservoir modelling from Williams Fork formation, USA, have found an 4% increase in connectivity when crevasse splays are included as reservoir-quality sandstone (Pranter., et al 2013). Crevasse splays in low net-to-gross fluvial deposits in the Ebro Basin, Spain, and Altiplano Basin, Bolivia, have been proven to significantly increase the connected reservoir volume in fluvial channels previously thought to have been isolated by floodplain fines, much in the same way as thin-bedded lobate deposits of deep-marine systems also contribute to connect reservoir volumes (de Ruig and Hubbard, 2006; Donselaar and Overeem, 2008; Toorenenburg et al., 2016). Ambrose et al., (1991) have pointed out the possible increase of resources in undepleted and partially depleted crevasse splays in the active La Gloria gas field in Texas, USA, with the overall production potential though to be significant. Similarly, exploitation of unconventional hydrocarbon resources in thin-bedded crevasse splays in low-net-to gross fluvial intervals have been suggested to prolong gas production in the North Sea (Sandén et al., 2016).

5.2.2 Upside in exploration of new areas

Crevasse splays have already been discussed (5.2.1) as a potential increase in both reservoir connectivity and reservoir volume. Many of the channels constructed in the reservoir model could themselves also represent a upside in similar low net-to-gross fluvial systems outside the main channel-belts (Klausen et al., 2014).

In the Triassic of the Barents Sea mud-rich fluvial systems are currently being explored as hydrocarbon reservoirs. Both the Snadd formation and the Kobbe formation consists of prograding, retrograding systems with proven highly mudstone-rich continental fluvial deposits (e.g., Klausen et al., 2014; Klausen and Mørk, 2014). Many of the mapped channel sandstones in the Snadd Formation are large and can reach up to 60 meters thick and 20km wide and make up exceptional exploration targets as show in Figure 5.2.2 (Klausen et al., 2014; Klausen and Mørk, 2014). Relative to these channels the channels in the reservoir model are very small. In Figure 5.2.2 the 1.5km² reservoir model have been added for comparison between the channels in the model and the channels that make up typical

exploration targets that in the Barents Sea (Figure 5.2.2). The simulation performed in this thesis offers a possible increase in total reservoir volume. Despite being small compared to the large channels, the associated overbank deposits between the channel-sandstone bodies contain heterolithic areas outside the easily mapped main-channels that probably contain numerous sub-seismic channels. Field observations of correlative units at the Hopen island outside Svalbard have found that a significant proportion of sub-seismic sandstones, which includes sandstone sheets and channels, must be assumed to exist within the Snadd formation (Klausen et al., 2014). Most of the channels (1-14-meter-thick) in the reservoir model are all probably of sub-seismic thickness, and correspond in size to the channels Klausen et al., (2014) refers to, not visible in the subsurface unless cored (Klausen et al., 2014). The whole systems of channels and crevasse splays, as shown in the simulations, could contain valuable hydrocarbon resources that add to the total volume of recoverables, and therefore should be considered as a potential upside when exploring areas with few or no cores.

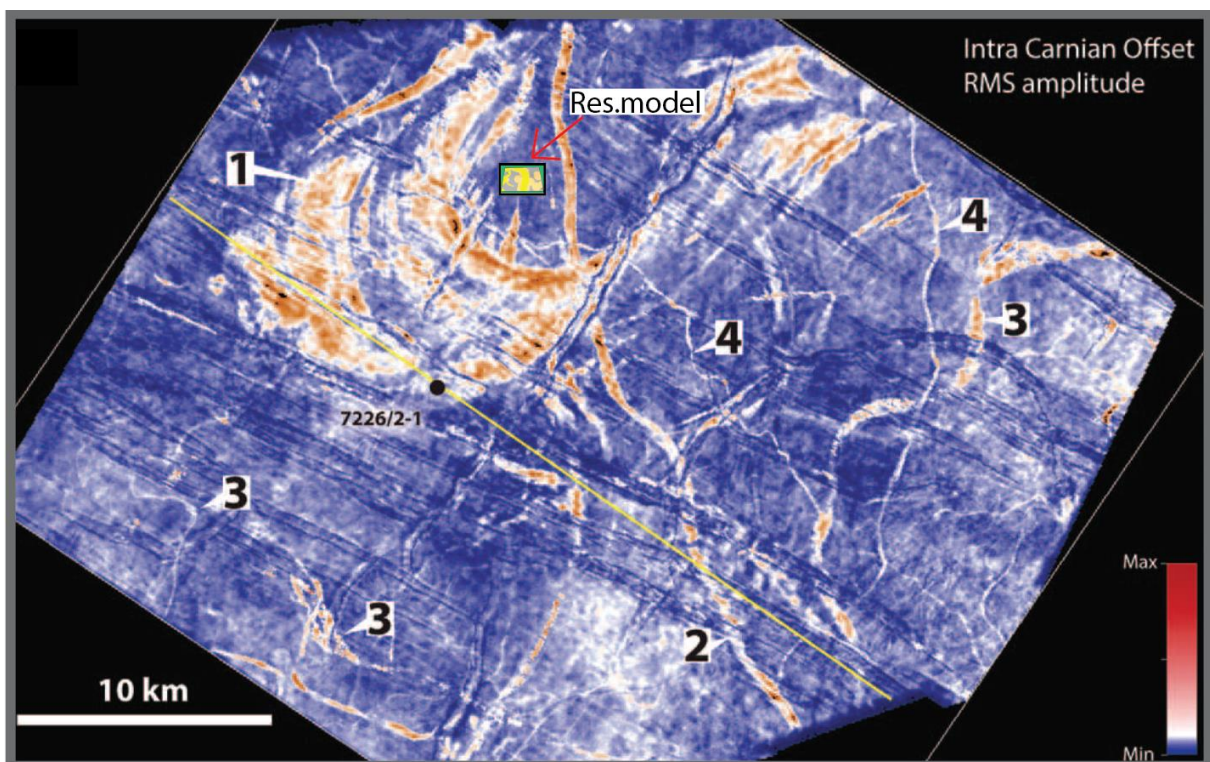


Figure 5.2.3.: RMS attribute map from immediately below the Snadd (intra Carnian flooding surface) highlighting different channel-sandstone geometries: 1) large, high-sinuosity, meandering-river sandstone body; 2) large ribbon-shaped channel sandstone body; 3) smaller, low-sinuosity, meandering channel bodies; and 4) thin, ribbon-shaped channel sandstone body. The size of the reservoir model constructed in this thesis have been

added for comparison. All but the biggest channels within the reservoir model would probably not be visible on this attribute map. (Modified from Klausen et al., 2014)

5.2.3 The reservoir model compared to the Goliat field

Every constructed model should be tested against the reality. Comparing the results from the flow simulation with production data from the Goliat field can shed some light on the credibility of the production results from the reservoir model presented in Chapter 4. Goliat is the only active producing field of fluvial sand-bodies in the Barents Sea that share some similarities with the heterogenous reservoir modelled from the Brushy Basin Member (NPD, 2018).

Production on the Goliat encompasses a substantial larger area (Figure 5.2.2) and has an estimated much higher oil originally in place (93.07 mill Sm³) (NPD, 2018) than the reservoir model (13.25 mill Sm³). The field is over 10 times larger than the model and subsequently have within the first three years of production produced over 9 times more oil than the flow simulations in scenario S1 did the first three years. This comparison points out that the production results from the model are realistic.

The Recovery factor on the Goliat is estimated to be around 35% substantially lower than the 59% in the model. This can however be linked to economic restrains on Goliat limiting the longevity of production which is estimated to end in 13 years, while the reservoir in scenario S1 was simulated for 50 years. Additionally, much of the reservoir in the Goliat field differ somewhat from the continental sedimentary environment in the reservoir model, consisting of tidally influenced deltaic system, but there are also fluvial dominated channels in Snadd producing from this field (NPD,2018). It would have been particularly interesting to address the impact of flow between these channels on the Goliat field, but this is beyond the scope of this work.

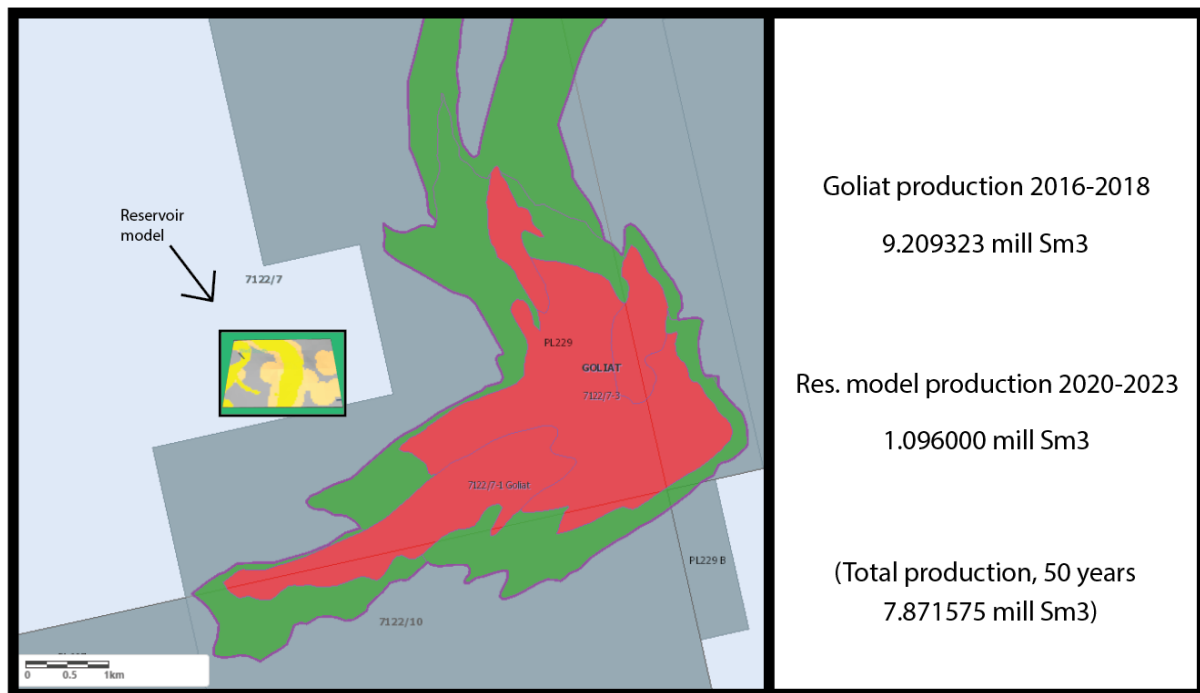


Figure 5.2.4: Size and production comparison between the Goliat field and the reservoir model from the Brushy Basin Member.

6.0 Summary and conclusions

By investigating the mudstone-rich Brushy Basin Member of the Morrison Formation, this thesis has characterised the facies and architectural elements of the fluvial system and built a reservoir model based on the observations. This is the first detailed petroleum geological study on the Brush Basin Member. It has presented a reservoir model based on field-work observations and UAV data gathering and done flow simulation to evaluate the importance of the different facies in the model. From the results and discussions presented in the thesis, the following conclusions are made:

- The Brushy Basin Member consists of overbank mudstone and fluvial channels that show a high degree of internal variability as well as architectural variability upwards in the succession: The fraction of mudstone increases while channel width, thickness and amalgamation of the channels decreases.
- In terms of a distributary fluvial system, the Brushy Basin Member display a change from proximal-to-medial-to-distal zones. This infers a retrograding distributary fluvial system, the complete opposite of the prograding distributary fluvial system that exist

in the lower parts of the Morrison Formation. Few retrograding distributary fluvial systems have been described to date, hence the Brushy Basin Member might be an interesting analogue for similar subsurface mudstone-rich systems.

- The observed proximal-to-distal trend could be a local feature and not represent the whole fluvial system in the basin. In addition, autogenic and allogenic control could explain the apparent proximal-to-distal trend observed at the study area.
- The simulations in this thesis show that the most efficient flow happens in the amalgamated, multistorey and multilateral part of the reservoir (Unit 1) where point bars from different channels belts are interconnected.
- Connectivity between singlestorey channels with little or no direct contact with other channels (Unit 2-4) can be established through crevasse splays. In the simulation crevasse splays account for a 5% increase in production from establishing connectivity with otherwise isolated channels.
- Channel-belts being explored and visible in the subsurface are generally much larger than the sand-bodies investigated in this thesis. The channel sandstones and associated crevasse splays in similar fluvial systems should be considered a potential upside in terms of communication and reservoir volumes when exploring new areas.
- Comparing the results from the flow simulation with data from the Goliat field show that the production results from the model are realistic.

Future work

After having conducted this study several questions concerning the Brushy Basin Member itself, and the impact of the observed facies on hydrocarbon production remains. Some ideas for further work that would improve the understanding of mudstone-rich systems like this could be:

- Building a geological model that incorporate the observed internal variability (mud-chips, mud-lag, mud-drapes, conglomerate etc.) within the channels in the reservoir model. Hence, giving much more realistic simulation of production results.

- Investigate the Brushy Basin Member distributary fluvial system in other locations to establish whether it is actually is a distributary fluvial system and whether it retrogrades or not.
- Investigate the importance of crevasse-splays in the fluvial parts of the Goliat field and compare them with the conclusions drawn in this thesis.
- Do a study that gathers petrophysical values for crevasse splays in similar mudstone-rich fluvial systems.

7.0 List of references

- Allen, J.P. and Fielding, C.R., 2007, Sedimentology and stratigraphic architecture of the Late Permian Betts Creek Beds, Queensland, Australia. *Sed. Geol.*, 202, 5–34.
- Allen, J.R.L., 1971, A theoretical and experimental study of climbing-ripple cross-lamination, with a field application to the Uppsala Esker. *Geogr. Ann. Ser. A Phys. Geogr.*, 53, 157–187.
- Ambrose, W. A., N. Tyler, and M. J. Parsley., 1991, Facies heterogeneity, pay continuity, and infill potential in barrier-island, fluvial, and submarine-fan reservoirs: Examples from the Texas Gulf Coast and Midland Basin, in A. D. Miall and N. Tyler, eds., *The three-dimensional facies architecture of terrigenous clastic sediments and its implication for hydrocarbon discovery and recovery: SEPM Concepts in Sedimentology and Paleontology* 3, p. 13–21
- Arenas, C., Millán, H., Pardo, G., Pocoví, A., 2001, Ebro Basin continental sedimentation associated with late compressional Pyrenean tectonics (north-eastern Iberia): controls on basin margin fans and fluvial systems. *Basin Research* 13, 65–89.
- Bilodeau, W.L., 1986, The Mesozoic Mogollon Highlands, Arizona: an Early Cretaceous rift shoulder. *Journal of Geology* 94/5, 724– 735.
- Blakey R., 2011, Southwestern North America paleogeographic maps; Late Jurassic. Colorado Plateau Geosystems, <http://cpgeosystems.com/swnam.html>
- Blakey, R. and Ranney, W., 2018, *Ancient landscapes of western North America*. 1st ed. Springer Nature.
- Blakey, R. C. 2011, Palaeogeographic maps, URL: <http://jan.ucc.nau.edu/~rcb7/globaltext2.html>, [Accessed: 14.04.2018].
- Blakey, R. C., and Ranney, W, 2008, *Ancient landscapes of the Colorado Plateau*, Grand Canyon Assn.
- Boggs, S, 2006, *Principles of sedimentology and stratigraphy*. Upper Saddle River, N.J., Pearson Prentice Hall. Pp, 564
- Boggs, S, 2006, *Principles of sedimentology and stratigraphy*, Upper Saddle River, NJ, Pearson Prentice Hall. pp 585.
- Boggs, S., 2011, *Principles of sedimentology and stratigraphy*, Prentice Hall New Jersey.
- Bown, T.M., Kraus, M.J. 1983. Ichnofossils of the alluvial Willwood Formation (lower Eocene), Bighorn Basin, northwest Wyoming, USA. *Palaeogeography, Palaeoclimatology, Palaeoecology* 43, 95– 128.
- Bralower, T.J., Ludwig, K.R., Obradovich, J.D., Jones, D.L. 1990. Berriasian (Early Cretaceous) radiometric ages from the Grindstone Creek section, Sacramento Valley, California. *Earth and Planetary Science Letters* 98, 62– 73.
- BRISTOW, C.S., SKELLY, R.L., AND ETHRIDGE, F.G. 1999. Crevasse splays from the rapidly aggrading, sand-bed, braided Niobrara River, Nebraska: effect of base-level rise: *Sedimentology*, v. 46, p. 1029–1047.
- Buehler, H.A., Weissmann, G.S., Scuderi, L.A. & Hartley, A.J. 2011. Spatial and temporal evolution of an avulsion on the Taquari River Distributive Fluvial System from satellite image analysis. *J. Sediment. Res.*, 81, 630–640.
- CAIN, S.A., AND MOUNTNEY, N.P. 2009. Spatial and temporal evolution of a terminal fluvial fan system: the Permian Organ Rock Formation, South east Utah, USA: *Sedimentology*, v. 56, p. 1774–1800.

- CECIL, C.B. 2003. The concept of autocyclic and allocyclic controls on sedimentation and stratigraphy, emphasizing the climatic variable. In *Climate Controls on Stratigraphy* (Ed. by Cecil C.B. & Edgar N.T.) SEPM Special Publication, 77, 13–20.
- Chapin, M. A., and D. F. Mayer., 1991. Constructing a three-dimensional rock property model of fluvial sandstones in the Peoria field, Colorado, in A. D. Miall and N. Tyler, eds., *The three dimensional facies architecture of terrigenous clastic sediments and its implication for hydrocarbon discovery and recovery*: SEPM Concepts in Sedimentology and Paleontology 3, p. 160–171.
- Chapin, M. A., and D. F. Mayer., 1991. Constructing a three-dimensional rock property model of fluvial sandstones in the Peoria field, Colorado, in A. D. Miall and N. Tyler, eds., *The three dimensional facies architecture of terrigenous clastic sediments and its implication for hydrocarbon discovery and recovery*: SEPM Concepts in Sedimentology and Paleontology 3, p. 160–171.
- Christiansen, E.H., Kowallis, B.J., Dorais, M.J., Hart, G.L., Mills, C.N., Pickard, M., and Parks, E. 2015. The record of volcanism in the Brushy Basin Member of the Morrison Formation: Implications for the Late Jurassic of western North America, in Anderson, T.H., Didenko, A.N., Johnson, C.L., Khanchuk, A.I., and MacDonald, J.H., Jr., eds., *Late Jurassic Margin of Laurasia—A Record of Faulting Accommodating Plate Rotation*: Geological Society of America Special Paper 513, p. 399–439,
- Currie, B. 1998. Upper Jurassic-Lower Cretaceous Morrison and Cedar Mountain Formations, NE Utah-NW Colorado [Colorado]. *JOURNAL OF SEDIMENTARY RESEARCH*, pp.VOL. 68, NO. 4, JULY, 1998, P. 632–652.
- Currie, B.S. 1997. Sequence stratigraphy of nonmarine Jurassic– Cretaceous rocks, central Cordilleran foreland-basin system. *Geological Society of America Bulletin* 109, 1206– 1222.
- David K. L.,Hovadik, J. 2006. Connectivity of channelized reservoirs: a modelling approach. *Petroleum Geoscience* ; 12 (4): 291–308.
- De Ruig, M. and Hubbard, S.M. 2006. Seismic facies and reservoir characteristics of a deepmarine channel belt in the Molasse foreland basin, Puchkirchen Formation, Austria. *AAPG Bull.*,90, 735–752 (PDF) Interplay between an axial channel belt, slope gullies and overbank deposition in the Puchkirchen Formation in the Molasse Basin, Austria.
- DeCelles, P.G. 2004. LATE JURASSIC TO EOCENE EVOLUTION OF THE CORDILLERAN THRUST BELT AND FORELAND BASIN SYSTEM, WESTERN U.S.A, *American Journal of Science*, Vol. 304, February, 2004, P. 105–168]
- DeCelles, P.G., Currie, B.S., 1996. Long-term sediment accumulation in the Middle Jurassic– Early Eocene Cordilleran retroarc foreland-basin system. *Geology* 24, 591– 594.
- Demko T.M., Parrish J.T., 1998 — Paleoclimatic setting of the Upper Jurassic Morrison Formation. *Modern Geology*, 22: 283–296.
- Demko, T.M., and Parrish, J.T., 1998, Paleoclimatic setting of the Morrison Formation: *Modern Geology*, v. 22, p. 283–296.
- Demko, Timothy & Currie, Brian & Nicoll, Kathleen. 2004. Regional paleoclimatic and stratigraphic implications of paleosols and fluvial/overbank architecture in the Morrison Formation (Upper Jurassic), Western Interior, USA. *Sedimentary Geology*. 167. 10.1016/j.sedgeo.2004.01.003
- Deveugle, P., Jackson, M., Hampson, G., Farrell, M., Sprague, A., Stewart, J. and Calvert, C. 2011. Characterization of stratigraphic architecture and its impact on fluid flow in a fluvial-dominated deltaic reservoir analog: Upper Cretaceous Ferron Sandstone Member, Utah. *AAPG Bulletin*, 95(5), pp.693-727.
- Dickinson, W.R. 1981. Plate tectonic evolution of the southern Cordillera. In: Dickinson, W.R., Payne, W.D. (Eds.), *Relations of Tectonics to Ore Deposits in the Southern Cordillera*. *Arizona Geological Society Digest*, vol. 14, pp. 113–135.

- Donselaar, M. E., and I. Overeem, 2008, Connectivity of fluvial point bar deposits: An example from the Miocene Huesca fluvial fan, Ebro basin, Spain: AAPG Bulletin, v. 92, no. 9, p. 1109–1129.
- Doyle, J. D., and M. L. Sweet, 1995, Three-dimensional distribution of lithofacies, bounding surfaces, porosity, and permeability in a fluvial sandstone—Gypsy Sandstone of northern Oklahoma: AAPG Bulletin, v. 79, no. 1, p. 70–95.
- Dunagan, S. and Turner, C., 2004. Regional paleohydrologic and paleoclimatic settings of wetland/lacustrine depositional systems in the Morrison Formation (Upper Jurassic), Western Interior, USA. *Sedimentary Geology*, 167(3-4), pp.269-296.
- Eide, C., Klausen, T., Katkov, D., Suslova, A. and Helland-Hansen, W., 2017. Linking an Early Triassic delta to antecedent topography: Source-to-sink study of the southwestern Barents Sea margin. *GSA Bulletin*, 130(1-2), pp.263-283.
- Einstein, A., 1954, The cause of the formation of meanders in the courses of rivers and of the so-called Baer's Law, pp. 249-253 in *Ideas and Opinions*: New York, Bonanza Books, 337 p.
- Ethridge, F.G., Wood, L.J. & Schumm, S.A., 1998, Cyclic variables controlling fluvial sequence development: problems and perspectives. In: *Relative Role of Eustasy, Climate, and Tectonism in Continental Rocks* (Ed. by Shanley K.W. & McCabe P.J.), SEPM Spec Pub., 59, 17–29.
- Friend, P.F., 1978, Distinctive features of some ancient river systems, in Miall, A.D., ed., *Fluvial Sedimentology*: Canadian Society of Petroleum Geologists, Memoir 5, p. 531–541.
- Galloway, W. E. & Hobday, D. K. 1996. *Terrigenous Clastic Depositional Systems. Applications to Fossil Fuel and Groundwater Resources*, 2nd ed. xvi + 489 pp. Berlin, Heidelberg, London, Paris, New York, Tokyo, Hong Kong: Springer-Verlag
- Ghinassi, M., Ielpi, A., Aldinucci, M. and Fustic, M., 2016. Downstream-migrating fluvial point bars in the rock record. *Sedimentary Geology*, 334, pp.66-96.
- Ghinassi, M., Nemec, W., Aldinucci, M., Nehyba, S., Özaksoy, V. and Fidolini, F., 2014. Plan-form evolution of ancient meandering rivers reconstructed from longitudinal outcrop sections. *Sedimentology*, 61(4), pp.952-977.
- Good, S.C., 2004. Paleoenvironmental and paleoclimatic significance of freshwater bivalves in the Upper Jurassic Morrison Formation, Western Interior, U.S.A. *Sedimentary Geology* 167, 165—178
- Graham, G., Jackson, M. and Hampson, G., 2015. Three-dimensional modeling of clinoforms in shallow-marine reservoirs: Part 1. Concepts and application. *AAPG Bulletin*, 99(06), pp.1013-1047
- Graham, G., Jackson, M. and Hampson, G., 2015. Three-dimensional modeling of clinoforms in shallow-marine reservoirs: Part 2. Impact on fluid flow and hydrocarbon recovery in fluvial-dominated deltaic reservoirs. *AAPG Bulletin*, 99(06), pp.1049-1080.
- Gulliford, A., Flint, S. and Hodgson, D., 2017. Crevasse splay processes and deposits in an ancient distributive fluvial system: The lower Beaufort Group, South Africa. *Sedimentary Geology*, 358, pp.1-18.
- HARTLEY, A.J., WEISSMANN, G.S., NICHOLS, G.J., AND WARWICK, G.L., 2010, Large distributive fluvial systems: Characteristics, distribution, and controls on development: *Journal of Sedimentary Research*, v. 80, p. 167–183.
- Hasiotis, S., 2004. Reconnaissance of Upper Jurassic Morrison Formation ichnofossils, Rocky Mountain Region, USA: paleoenvironmental, stratigraphic, and paleoclimatic significance of terrestrial and freshwater ichnocoenoses. *Sedimentary Geology*, 167(3-4), pp.177-268.

- Hasiotis, S.T., Bown, T.M., Kay, P.T., Dubiel, R.F., Demko, T.M., 1996. The ichnofossil record of hymenopteran nesting behaviour from Mesozoic and Cenozoic pedogenic and xylic substrates: example of relative stasis. North American Paleontological Convention, NAPC-96, Washington, DC, 165.
- Heller, P.L. and Paola, C., 1996. Downstream changes in alluvial architecture: an exploration of controls on channelstacking patterns. *J. Sed. Res.*, 66, 297–306.
- Hintze, L. F. & Kowallis, B. J. 2009. Geologic history of Utah, Provo, Utah, Brigham Young University Studies. 225pp.
- Hirst, J.P.P., 1991, Variations in alluvial architecture across the Oligo-Miocene Huesca fluvial system, Ebro Basin, Spain, in Miall, A.D., and Tyler, N., eds., *The Three Dimensional Facies Architecture of Terrigenous Clastic Sediments and Its Implications for Hydrocarbon Discovery and Recovery: SEPM, Concepts in Sedimentology and Paleontology* 3, p. 111–121.
- Ingersoll, R. V., and Schweickert, R. A., 1986, A plate-tectonic model for Late Jurassic ophiolite genesis, Nevadan orogeny and foreland initiation, northern California. *Tectonics*, v. 5, pp. 901–912.
- J. Pranter, M & C. Hewlett, A & D. Cole, R & Wang, H & Gilman, J., 2013. Fluvial architecture and connectivity of the Williams Fork Formation: Use of outcrop analogues for stratigraphic characterization and reservoir modelling. Geological Society, London, Special Publications. 387. 57-83. 10.1144/SP387.1.
- Jackson, C., Grunhagen, H., Howell, J., Larsen, A., Andersson, A., Boen, F. and Groth, A., 2010. 3D seismic imaging of lower delta-plain beach ridges: lower Brent Group, northern North Sea. *Journal of the Geological Society*, 167(6), pp.1225-1236.
- James, W. C., Mack, G. H., and Monger, H. C., 1993, Classification of paleosols: Discussion and reply, *Geological Society of America*, v. 105, p. 1637.
- K. Galli, 2014, Fluvial architecture element analysis of the Brushy Basin Member, Morrison Formation, western Colorado, USA", "Volumina Jurassica", "Vol. 12, no. 2", pages = "69--106",
- Kjemperud, A., Schomacker, E. and Cross, T., 2008. Architecture and stratigraphy of alluvial deposits, Morrison Formation (Upper Jurassic), Utah. *AAPG Bulletin*, 92(8), pp.1055-1076.
- Klausen, T. and Mørk, A., 2014. The upper Triassic paralic deposits of the De Geerdalen Formation on Hopen: Outcrop analog to the subsurface Snadd Formation in the Barents Sea. *AAPG Bulletin*, 98(10), pp.1911-1941.
- Klausen, T., Ryseth, A., Helland-Hansen, W., Gawthorpe, R. and Laursen, I., 2014. Spatial and Temporal Changes In Geometries of Fluvial Channel Bodies From the Triassic Snadd Formation of Offshore Norway. *Journal of Sedimentary Research*, 84(7), pp.567-585.
- Kowallis B.J., Christiansen E.H., Deino A.L., Peterson F., Turner C.E., Kunk M.J., Obradovich J.D., 1998 The age of the Morrison Formation. *Modern Geology*, 22: 235–260.
- Kowallis, B., Christiansen, E. and Deino, A., 1991. Age of the Brushy Basin Member of the Morrison Formation, Colorado Plateau, western USA. *Cretaceous Research*, 12(5), pp.483-493.
- Kraus, M., 1999. Paleosols in clastic sedimentary rocks: their geologic applications. *Earth-Science Reviews*, 47(1-2), pp.41-70.
- Kraus, M., 1999. Paleosols in clastic sedimentary rocks: their geologic applications. *Earth-Science Reviews*, 47(1-2), pp.41-70.
- Kraus, M. J., 1999. Paleosols in clastic sedimentary rocks: Their geologic applications. *Earth-Science Reviews*, 47(1-2), 41-70. doi:10.1016/s0012-8252(99)00026-4
- Kraus, M.J., 2002. Basin-scale changes in floodplain paleosols: implications for interpreting alluvial architecture. *J. Sed. Res.*, 72, 500–509.

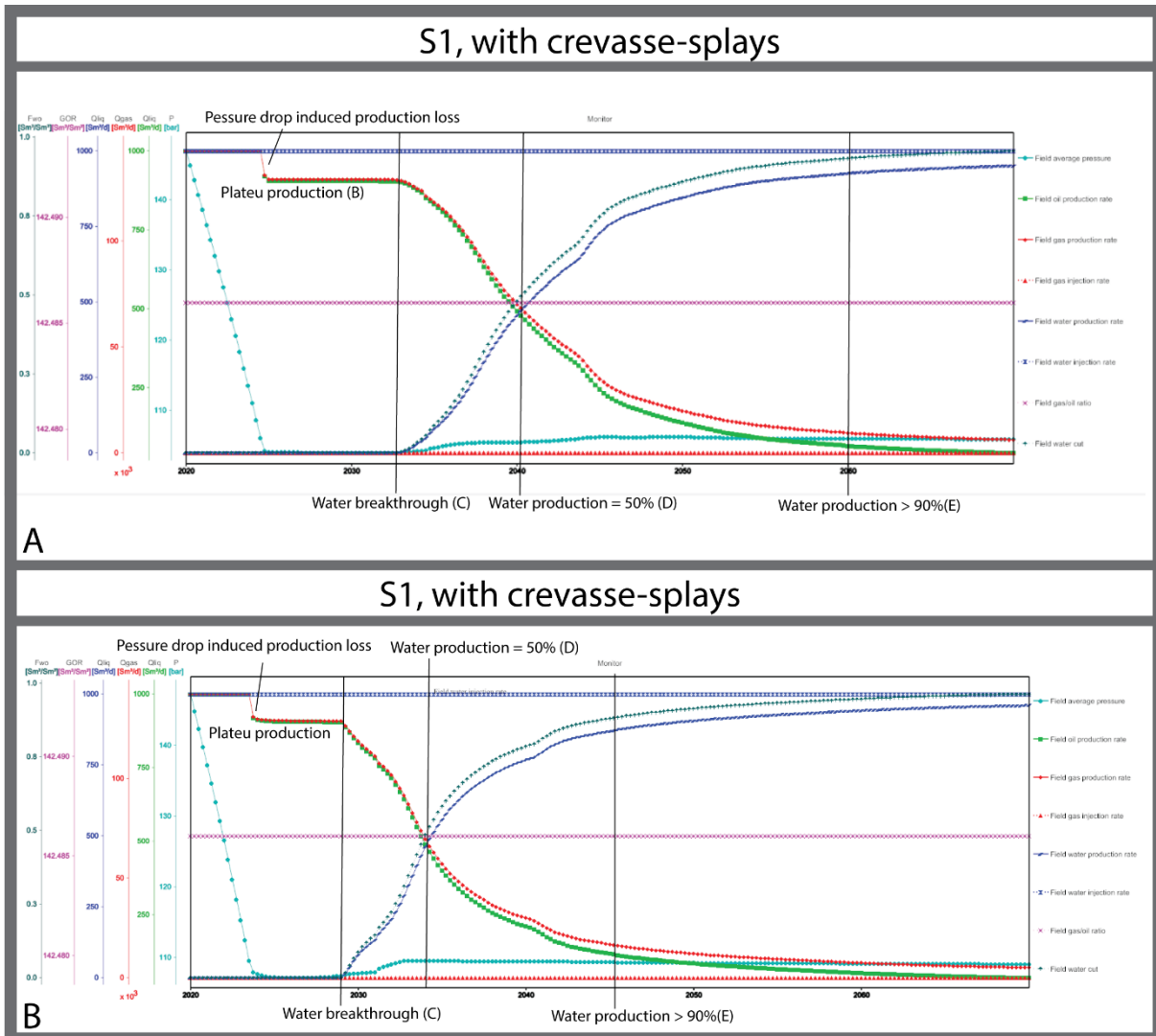
- Kraus, M.J., 1987. Integration of channel and floodplain suites: II. Vertical relations of alluvial paleosols. *Journal of Sedimentary Petrology* 57, 602–612.
- Kukulski, R.B., Hubbard, S.M., Moslow, T.F. & Keegan Raines, M., 2013. Basin-scale stratigraphic architecture of upstream fluvial deposits: Jurassic-Cretaceous Foredeep, Alberta Basin, Canada. *J. Sediment. Res.*, 83, 704–722.
- Lawton, T.F., 1994. Tectonic setting of Mesozoic sedimentary basins, Rocky Mountain region, United States. In: Caputo, M.V., Peterson, J.A., Franczyk, K.J. (Eds.), *Mesozoic Systems of the Rocky Mountain Region, USA*. Rocky Mountain Section of SEPM (Society for Sedimentary Geology), Tulsa, Oklahoma. U.S.A. pp. 1–25.
- Lepre, C., 2017. Crevasse-splay and associated depositional environments of the hominin-bearing lower Okote Member, Koobi Fora Formation (Plio-Pleistocene), Kenya. *The Depositional Record*, 3(2), pp.161-186.
- Line, L., Jahren, J. and Hellevang, H., 2018. Mechanical compaction in chlorite-coated sandstone reservoirs – Examples from Middle – Late Triassic channels in the southwestern Barents Sea. *Marine and Petroleum Geology*, 96, pp.348-370.
- Lucas, S.G., Zeigler, K.E., Lawton, T.F., Filkorn, H.F., 2001. Late Jurassic invertebrate fossils from the Little Hatched Mountains, southwestern New Mexico. *New Mexico Geology* 23/1, 16–20.
- Lundschieen, B.A., Høy, T. & Mørk, 2014.: Triassic hydrocarbon potential in the Northern Barents Sea; integrating Svalbard and stratigraphic core data. *Norwegian Petroleum Directorate Bulletin*, No. 11, pp. 3–20. Stavanger.
- Mack, G.H. and Madoff, R.D., 2005. A test of models of fluvial architecture and palaeosol development: Camp Rice Formation (Upper Pliocene-Lower Pleistocene), southern Rio Grande rift, New Mexico, USA. *Sedimentology*, 52, 191–211.
- Mackey, S.D. and Bridge, J.S., 1995. Three-dimensional model of alluvial stratigraphy: theory and application. *J. Sed. Res.*, 65, 7–31.
- Martinius, A.W., Ravnås, R., Howell, J.A., Steel, R.J. and Wonham, J., 2014, From Depositional Systems to Sedimentary Successions on the Norwegian Continental Margin. *International Association of Sedimentologists Special Publications* 46,
- Martinsen, O., Ryseth, A., Helland-Hansen, W., Flesche, H., Torkildsen, G. and Idil, S., 1999. Stratigraphic base level and fluvial architecture: Ericson Sandstone (Campanian), Rock Springs Uplift, SW Wyoming, USA. *Sedimentology*, 46(2), pp.235-263.
- MIALL, A., 2016. *FLUVIAL DEPOSITIONAL SYSTEMS*. Springer Cham Heidelberg New York Dordrecht London : SPRINGER INTERNATIONAL PU.
- Miall, A. D., 1985, Architectural-element analysis: A new method of facies analysis applied to fluvial deposits: *Earth-Science Reviews*, v. 22, p. 261-308.
- Miall, A. D., 1992, Alluvial deposits, in R. G. Walker and N. P. James, *Facies models: Response to sea level change*: Geological Society of Canada, p.119-142.
- Miall, A. D., 2006, Fluvial facies models: Recent developments, in H. W. Posamentier, and R. G. Walker, eds., *Facies Models Revisited*, SEPM Special Publication, no. 84, p. 85-170.
- Miall, A. D., ed. 2008: *The Sedimentary Basins of the United States and Canada: Sedimentary basins of the World*, v. 5, K. J. Hsü, Series Editor, Elsevier Science, Amsterdam, Chapter 7, s.246-292
- Miall, A. D., ed. 2008: *The Sedimentary Basins of the United States and Canada: Sedimentary basins of the World*, v. 5, K. J. Hsü, Series Editor, Elsevier Science, Amsterdam, Chapter 9, s.330-358

- Miall, A. D., ed. 2008: The Sedimentary Basins of the United States and Canada: Sedimentary basins of the World, v. 5, K. J. Hsü, Series Editor, Elsevier Science, Amsterdam, Chapter 11, s.395-428
- Miall, A.D, 2011. The geology of fluvial deposits. Berlin: Springer.
- Miall, A.D, 2014. Fluvial Depositional Systems. Berlin: Springer.
- Newell, D.L., 1997. Geology of the Brushy Basin Member of the Morrison Formation, Fruita Paleontological Resource Area, Colorado. MS Thesis. Colorado State University. 197 pp.
- Nichols, G. and Fisher, J. 2007. Processes, facies and architecture of fluvial distributary system deposits. *Sedimentary Geology*, 195(1-2), pp.75-90.
- Norwegian Petroleum Directorate, 2018, RESSURSRAPPORT LETING 2018., URL: [<http://www.npd.no/no/nyheter/nyheter/2018/velkommen-til-presentasjon-av-oljedirektoratets-nye-ressursrapport-/>], [Accessed: 14.04.2018]. s. 1-38
- Norwegian Petroleum Directorate, 2018, Goliat Info cite., URL: [<http://factpages.npd.no/FactPages/default.aspx?nav1=field&nav2=PageView%7CAll&nav3=5774394/>], [Accessed: 14.04.2018].
- Nourse, J.A., 1995. Jurassic –Cretaceous paleogeography of the Magdalena region, northern Sonora, and its influence on the positioning of Tertiary metamorphic core complexes. In: Jacques- Ayala, C., Gonzalez-Leon, C.M., Roldan-Quintana, J. (Eds.), *Studies on the Mesozoic of Sonora and Adjacent Areas*. Geological Society of America Special Paper 301, pp. 59– 78.
- Owen, A., Nichols, G., Hartley, A. and Weissmann, G. (2015). Vertical trends within the prograding Salt Wash distributive fluvial system, SW United States. *Basin Research*, 29(1), pp.64-80.
- Owen, A., Nichols, G., Hartley, A., Weissmann, G. and Scuderi, L. (2015). Quantification of a Distributive Fluvial System: The Salt Wash DFS of the Morrison Formation, SW U.S.A. *Journal of Sedimentary Research*, 85(5), pp.544-561.
- Parrish, J.T., Curtis, R.L., 1982. Atmospheric circulation, upwelling, and organic-rich rocks in the Mesozoic and Cenozoic Eras. *Palaeogeography, Palaeoclimatology, Palaeoecology* 40, 31–66.
- Parrish, J.T., Peterson, F., Turner, C., 2004. Jurassic “savannah” — plant taphonomy and climate of the Morrison Formation (Jurassic, Western U.S.A.). *Sedimentary Geology* 167, 139—164
- Peterson, F., 1994. Sand dunes, sabkhas, streams, and shallow seas: Jurassic paleogeography in the southern part of the Western Interior Basin. In: Caputo, M.V., Peterson, J.A., Franczyk, K.J. (Eds.), *Mesozoic Systems of the Rocky Mountain Region*,
- Pranter, M., Hewlett, A., Cole, R., Wang, H. and Gilman, J., 2013. Fluvial architecture and connectivity of the Williams Fork Formation: use of outcrop analogues for stratigraphic characterization and reservoir modelling. Geological Society, London, Special Publications, 387(1), pp.57-83.
- Retallack, G. J. 2001. *Soils of the Past. An Introduction to Paleopedology*, 2nd ed. xi+404 pp. Oxford: Blackwell Science.
- Retallack, G.J., 1997. Dinosaurs and dirt. In: Wolberg, D.L, Stump, E. (Eds.), *Dinofest International Proceedings. Dinofest (TM)*, pp. 345– 359.
- Roca, X. and Nadon, G., 2007. Tectonic Control on the Sequence Stratigraphy of Nonmarine Retroarc Foreland Basin Fills: Insights from the Upper Jurassic of Central Utah, U.S.A. *Journal of Sedimentary Research*, 77(3), pp.239-255.

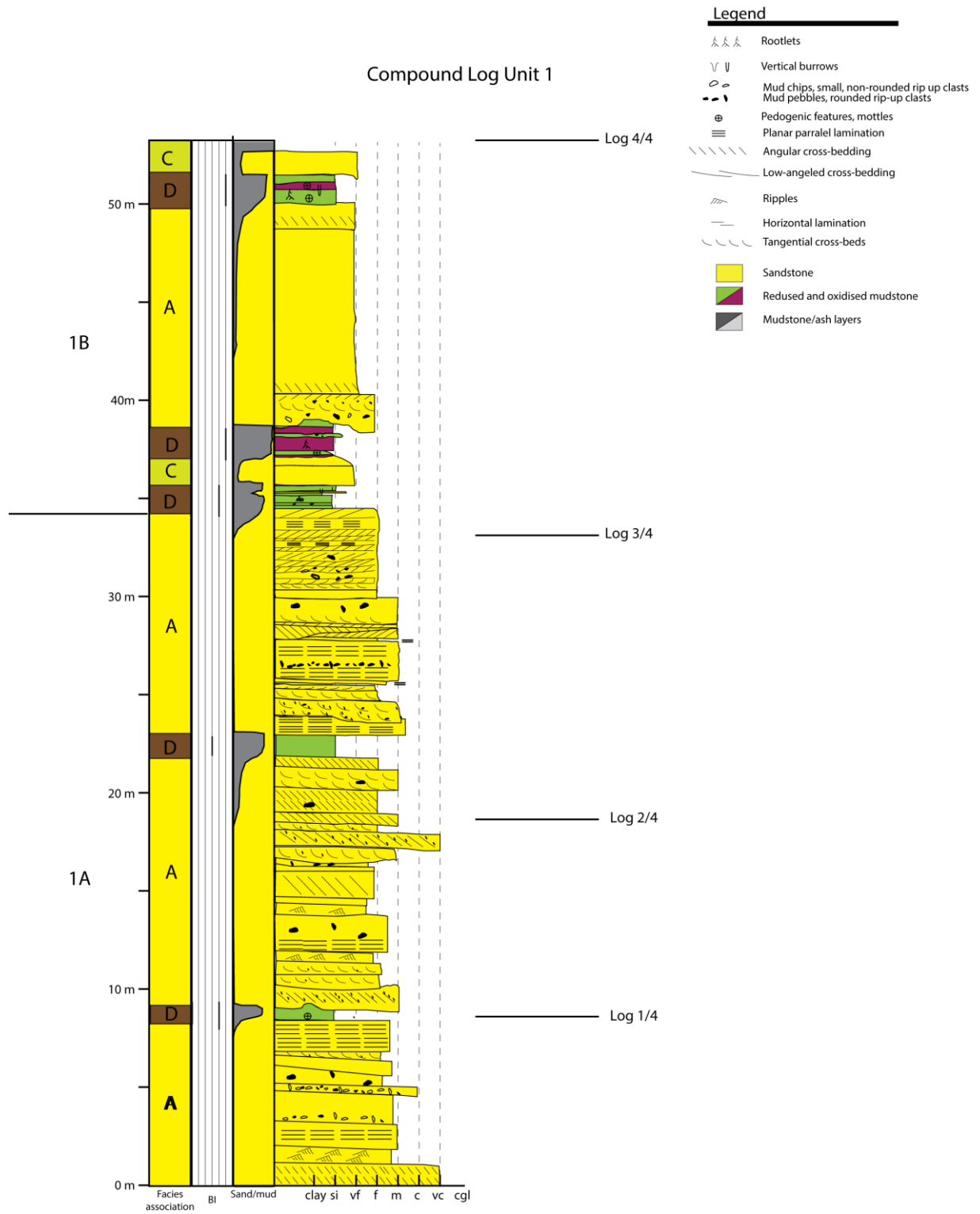
- Ronald C. Blakey., 2008. Chapter 7 Pennsylvanian–Jurassic Sedimentary Basins of the Colorado Plateau and Southern Rocky Mountains, *The Sedimentary Basins of the United States and Canada*, 10.1016/S1874-5997(08)00007-5, (245-296),
- Royse, F., 1993. Case of the phantom foredeep; Early Cretaceous in west-central Utah. *Geology* 21, 133– 136.
- Bridge, J. S., 2003. *Rivers and Floodplains: Forms, Processes and Sedimentary Record*, Malden. SERBIULA pp, 493
- Saleeby, J. B., and Busby-Spera, C., 1992, Early Mesozoic tectonic evolution of the western U. S. Cordillera, in Burchfiel, B. C., Lipman, P. W., and Zoback, M. L. eds., *The Cordilleran Orogen: conterminous U. S.: the geology of North America, Decade of North American Geology*, Geological Society of America, Boulder, v. G-3, pp. 107–168.
- Saleeby, J.B., Busby-Spera., 1992, Early Mesozoic tectonic evolution of the wester U.S Cordillera, in Burchfiled, B.C., Limpan P.W., and Zoback, M.L., eds., *The Codrilleran Orogen: Conerminous U.S.: Boulder, Coorado*, Geological Society of America, *The Geology of North America*, v. G-3
- Sandén, Axel & T. W. Boerboom, Herman & Donselaar, Marinus Eric & Storms, Joep & van Toorenenburg, Koen & van der Vegt, Helena & Weltje, Gert., 2016. Process-based modelling of sediment distribution in fluvial crevasse splays. 10.3997/2214-4609.201600929.
- SHANLEY, K.W. & MCCABE, P.J., 1994. Perspectives on the sequence stratigraphy of continental strata. *AAPG Bull.*, 78, 544–568.
- STANISTREET, I.G., ANDMCCARTHY, T.S., 1993, The Okavango Fan and the classification of subaerial fan systems: *Sedimentary Geology*, v. 85, p. 115–133
- Stokes, W.L, 1986, *Geology of Utah*, Utah Museum of Natural History: Utah Geological and Mineral Survey, xii, pp. 280.
- Stouthamer, E & Berendsen, H.J.A.. (2001). Avulsion frequency, avulsion duration, and interval period of holocene channel belts in the rhine-meuse delta, the Netherlands. *Nederlandse Geografische Studies*. 105-126.
- Stuart, J.Y., Mountney, N.P., McCaffrey, W.D., Lang, S., Collinson, J.D., 2014. Prediction of channel connectivity and fluvial style in the flood basin successions of the Upper Permian Rangal coal measures (Queensland). *AAPG Bulletin* 98, 191–212.
- Tabor, N. and Myers, T. (2015). Paleosols as Indicators of Paleoenvironment and Paleoclimate. *Annual Review of Earth and Planetary Sciences*, 43(1), pp.333-361.
- Tanner, L.H., Galli, K.G., Lucas, S.G. (2014). Pedogenic and lacustrine features of the BrushBasin Member of the Upper Jurassic Morrison Formation in western Colorado: Reassessing the paleoclimatic interpretations. *Volumina Jurassica*, XII (2): 115–130
- Thomson, J., 1876, On the windings of rivers in alluvial plains: *Royal Soc. London Proc.*, v.25, pp. 5-8.
- Turner, C. and Peterson, F., 2004. Reconstruction of the Upper Jurassic Morrison Formation extinct ecosystem—a synthesis. *Sedimentary Geology*, 167(3-4), pp.309-355.
- van Toorenenburg, K., Donselaar, M., Noordijk, N. and Weltje, G., 2016. On the origin of crevasse-splay amalgamation in the Huesca fluvial fan (Ebro Basin, Spain): Implications for connectivity in low net-to-gross fluvial deposits. *Sedimentary Geology*, 343, pp.156-164.
- van Toorenenburg, Koen & Donselaar, Marinus Eric & Weltje, Gert., 2017. The potential of fluvial crevasse splays as (secondary) reservoirs. *AAPG Annual Convention & Exhibition 2017*, At Houston, TX, USA

- Weissmann, G., Hartley, A., Nichols, G., Scuderi, L., Olson, M., Buehler, H. and Banteah, R., 2010. Fluvial form in modern continental sedimentary basins: Distributive fluvial systems. *Geology*, 38(1), pp.39-42.
- Weissmann, G.S., Hartley, A.J., Nichols, G.J., SCuderi, L.A., Olsen, M., Buehler, H., AND Banteah, R., 2010, Fluvial form in modern continental sedimentary basins: distributive fluvial systems: *Geology*, v. 38, p. 39–42.
- Weissmann, G.S., Hartley, A.J., Scuderi, L.A., Nichols, G.J., Davidson, S.K., Owen, A., Atchley, S.C., BHATTACHARYYA, P., CHAKRABORTY, T., GHOSH, P., NORDT, L.C., MICHEL, L. & TABOR, N.J., 2013. Prograding distributive fluvial systems geomorphic models and ancient examples. In: *New Frontiers in Paleopedology and Terrestrial Paleoclimatology* (Ed. by Dreise S.G., Nordt L.C. & McCarthy P.L.), SEPM Spec Pub., 104, 131–147.
- Williams, E.A., 2000. Flexural cantilever models of extensional subsidence in the Munster Basin (SE Ireland) and Old Red Sandstone fluvial dispersal systems. In: Friend, P.F., Williams, B.P.J. (Eds.), *New perspectives on the Old Red Sandstone*. Special Publications, vol. 180. Geological Society, London, pp. 239–268.
- Willis, B. and Tang, H., 2010. Three-Dimensional Connectivity of Point-Bar Deposits. *Journal of Sedimentary Research*, 80(5), pp.440-454.
- Wright, V.P. and Marriott, S.B., 1993. The sequence stratigraphy of fluvial depositional systems: the role of floodplain sediment storage. *Sed. Geol.*, 86, 203–210.

Appendix:



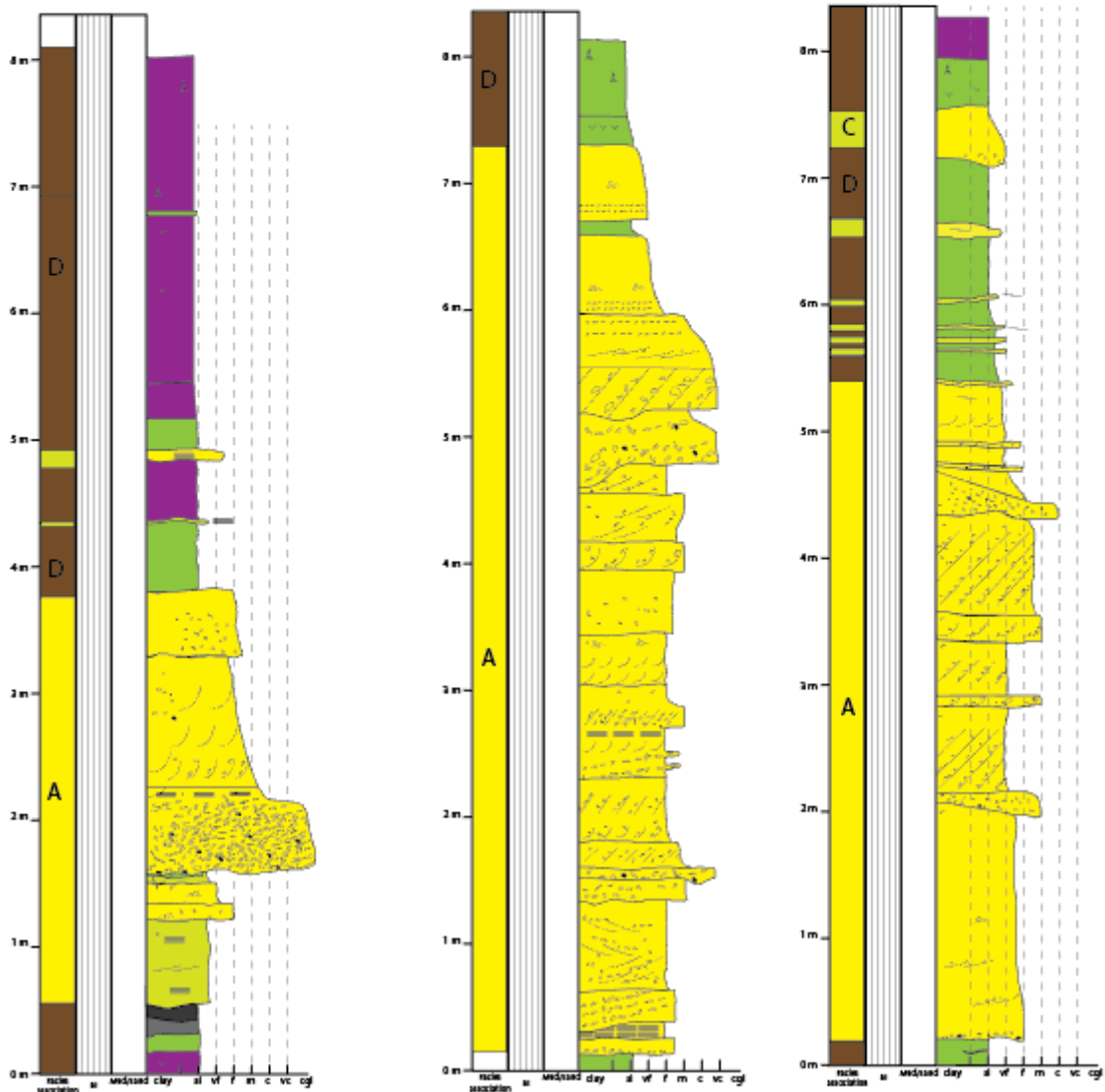
Detailed production results from flow simulating the reservoir model



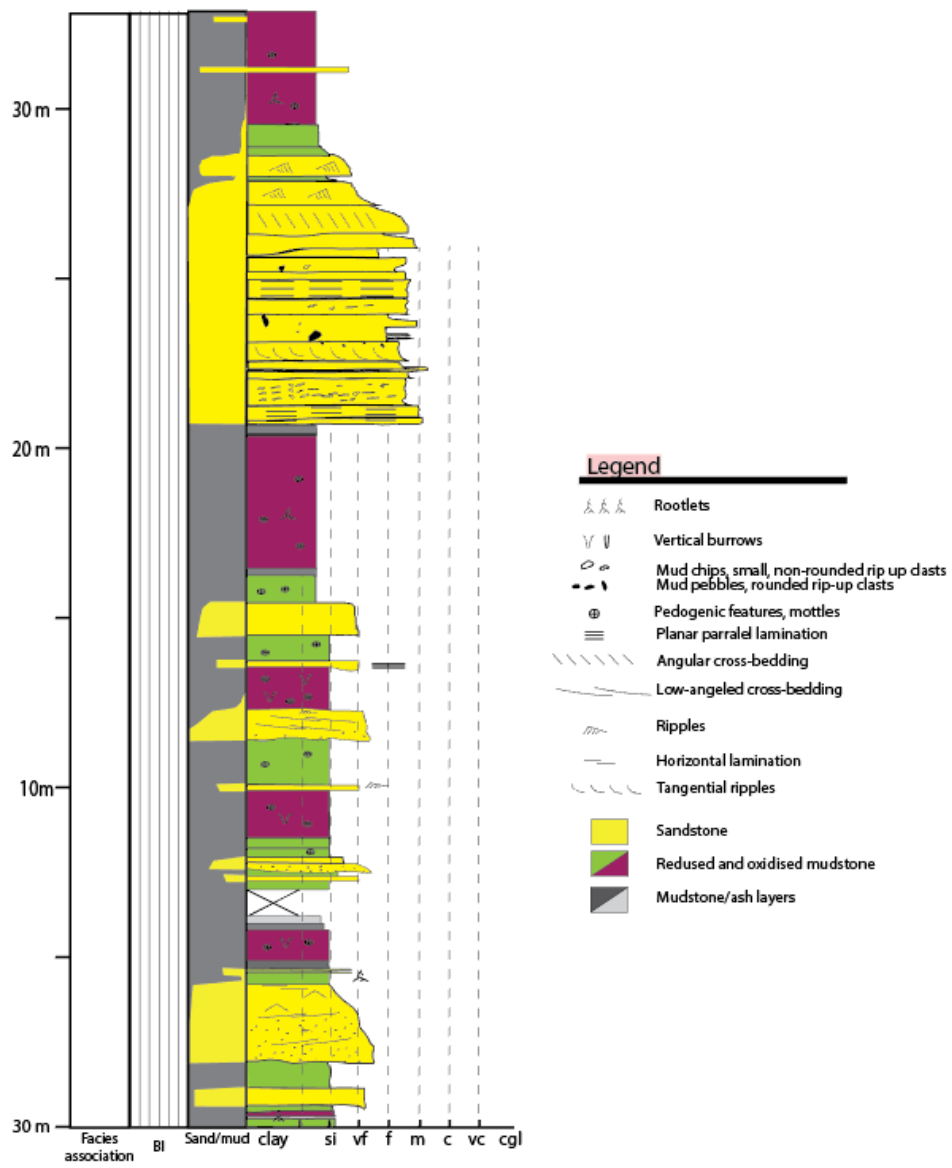
Legend

- ⋈⋈⋈ Rootlets
- V V Vertical burrows
- ○ Mud chips, small, non-rounded rip-up clasts
- ● Mud pebbles, rounded rip-up clasts
- ⊕ ⊕ Pedogenic features, mottles
- ▬ ▬ Planar parallel lamination
- ⧘ ⧘ Angular cross-bedding
- ⧚ ⧚ Low-angled cross-bedding
- 〰 〰 Ripples
- — Horizontal lamination
- 〰 〰 Tangential ripples
- Sandstone
- Reduced and oxidised mudstone
- Mudstone/ash layers

Channels Unit 3



Unit 2



Log Unit 3 and 4

